ELECTRICAL RESISTIVITY MEASUREMENTS OF LATTICE DEFECTS IN HEXAGONAL CLOSE PACKED METALS

Leonard D. Will

Ph.D.

University of Edinburgh

1973

CONTENTS

FIGURES AND TABLES

Tables, figures and equations are numbered with the number of the section or sub-section in which they appear, followed after a hyphen by a sequential table, figure or equation number. In the text references to tables and figures use the words "Table" or "Fig."; references to equations either use the word "equation" or the number is enclosed in parentheses.

Figures

Figures (cont.)

Figures (cont.)

Tables

ACKNOWLEDGEMENTS

The work described in this thesis was carried out under the supervision of Professor A. F. Brown in the Department of Natural Philosophy of the University of Edinburgh and latterly in the Department of Applied Physics of the City University, London.

Thanks are due to Professor Brown for his advice and encouragement; to Dr A. H. Seville for helpful discussions; to Professor N. Feather of the University of Edinburgh and Professor C. W. Miller of the City University, the heads of the departments in which I worked, for making research facilities available; to Mr P. R. Lewis, Librarian of the City University, and his successor, Mr S. J. Teague, for allowing me to spend time on this work while employed as a member of their staff; to the technical, workshop and library staffs of both universities for support facilities; and to the Science Research Council for financial support during the early part of the work.

DECLARATION

I declare that this thesis has been composed by me, and that, except where indicated, the work described in it is my own.

Leonard D. Will.

ABSTRACT

Lattice defects produced in zinc and cadmium by plastic deformation at 78 K have been investigated by means of electrical resistivity measurements at 78 K. Single crystals and polycrystalline samples of both metals have been used. The annealable increase in the resistivity of single crystals with deformation is generally less than 0.5% for deformations of up to 5% in zinc and 10% in cadmium. This is too small for annealing stages to be resolved satisfactorily, particularly since they are obscured by irregular changes in resistance during annealing, attributed to anisotropic thermal expansion of neighbouring sub-grains.

Polycrystalline zinc is too brittle to allow significant deformation at low temperature, but a measurable resistivity increase has been produced in polycrystalline cadmium. The increase is proportional to strain, with a coefficient (12.5 ± 0.7) nΩm per unit strain, half due to dislocations and half to point defects. This value is consistent with the point defect production mechanism being non-conservative movement of dislocation jogs, producing a defect concentration of 0.1% per unit strain, the resistivity of defects being 60 nΩm per 1% atomic concentration.

Isochronal and sequential isothermal annealing was performed, and the activation energy was determined by an improved version of the change-of-slope method which eliminates the necessity for subjective curve-fitting operations. The annealing spectrum was divided into three stages: stage III, at 80 to 130 K, activation energy 0.16 ± 0.03 eV; stage IV, at 130 to 180 K, activation energy increasing from ~0.2 eV to ~0.4 eV; and stage V, 180 to 220 K, 0.7 ± 0.1 eV. There was no unique

order of kinetics at any stage, and it appears that a number of overlapping processes took place. Stage III is attributed to the annealing of interstitials and stage IV to vacancies, but both these defects probably moved in groups of two or more and interacted with impurities. Stage V is attributed to dislocation rearrangement.

1. INTRODUCTION

1.1 Defects in metals

The properties of metals depend on their structure, and one of the major activities of research in metal physics has been the establishing of a relationship between structure and properties. In general, properties such as density, electrical conductivity, thermal conductivity and specific heat are characteristic of the chemical composition of the metal, and changes in physical structure give rise to relatively small variations in these properties.

The changes in physical structure which are of primary interest in the present work are those in which atoms are more or less permanently displaced from the sites which they would occupy in a perfect crystal. Lattice vibrations and other transient displacements will not be discussed in detail. The defects of interest may be broadly classified by their spatial dimensions:

Zero-dimensional (point defects): vacancies, interstitials, impurity atoms, and small clusters of one or more of these components.

One-dimensional (line defects): edge dislocations, screw dislocations.

Two-dimensional (surface defects): stacking faults, grain boundaries, surfaces.

Three-dimensional (volume defects): voids, large clusters of point defects or impurities.

All these defects are related because, for example, stacking faults are bounded by dislocations, and point defects can be produced by the intersection of moving dislocations.

The main aim of the present work is to obtain information about point defects in metals which have a hexagonal-close-packed structure (h.c.p.), particularly cadmium and zinc. Most previous

work has been done on face-centred-cubic (f.c.c.) metals, such as copper, but relatively little has been done on the h.c.p. metals, perhaps because they present a number of experimental difficulties; they are anisotropic, and they have low melting points so that very low temperatures are necessary to immobilise point defects. In addition, zinc is brittle at low temperatures, so that it is difficult to produce many point defects by mechanical deformation.

1.2 Background to the present work

Previous work by Anderson and Brown (1965) has shown that when zinc crystals are strained in tension at toom temperature deformation sometimes occurs in jumps, and that associated with each jump there is a pulse of resistivity which increases rapidly and then decays exponentially. They attributed these pulses to the creation and annealing of point defects, probably divacancies, and calculated an activation energy for movement of (0.32 ± 0.03) eV. The present work was initiated in the hope of relating these dynamic measurements at room temperature to static measurements of the properties of point defects obtained at low temperatures.

Because of its transition to brittle behavious below room temperature, however, the experimental difficulties of low temperature deformation and annealing of zinc precluded the obtaining of significant annealing data, although many attempts were made with both single crystals and polycrystals. It was therefore decided to carry out an investigation of the annealing behaviour of cadmium, because this metal is similar in many respects to zinc, having the same structure, but is more ductile at low temperatures.

Although some work on the annealing of cadmium has been carried out previously, only a few results have been obtained, compared with

the extensive investigations which have been made on the f.c.c. metals. The annealing curves show considerable variations, and the interpretation of some behaviour is still in doubt. In particular, it is not yet clear whether interstitial atoms anneal by long-range migration at very low temperatures (<26 K) or whether they remain present in some form to temperatures of about 100 K. An annealing stage found at about 80 to 120 K in the present work is compatible with the annealing of vacancies or their aggregates in that temperature range.

Results are presented on the resistivity increment due to point defects produced by low temperature deformation of zinc and cadmium, and on the behaviour during isochronal and isothermal anneals. In zinc and cadmium annealing stages overlap one another, and it is not possible to obtain an unambiguous description of each individual stage. The method usually used to obtain activation energies from annealing data, the change-of-slope method, involves subjective curve-fitting and estimation of slopes; this limits the confidence which can be placed on the values obtained. An improvement was therefore developed which enables activation energies to be calculated objectively from numerical annealing data and eliminates the subjective aspects.

2. THEORY AND REVIEW OF PREVIOUS WORK ON ZINC AND CADMIUM

There have been a number of reviews of theoretical and experimental work on point defects (e.g. Damask and Dienes 1963; Cotterill 1965; Seeger 1970), so the content of these will not be reproduced here. Most previous work has dealt with the face-centred-cubic (f.c.c.) metals, however, so this chapter will concentrate on what is known about defects in hexagonal-close-packed (h.c.p.) metals, zinc and cadmium in particular. A review on vacancies and interstitials in h.c.p. metals was presented to the 1968 Jülich conference (Schumacher 1970), so particular emphasis will be placed on more recent work. The various different methods by which point defects can be produced and studied will be considered in turn.

2.1 High temperature equilibrium methods

The concentration of point defects in equilibrium in a metal at any temperature is the value for which the free energy is a minimum, and is given by

$$C = \exp(S^f/k)\ \exp(-E^f/kT) \qquad (2.1\text{-}1)$$

where S^f $(\sim k)$ is the entropy contribution from the change in lattice vibration frequencies with and without the defect, E^f is the energy of formation of one defect, k is the Boltzmann constant and T is the temperature (Damask and Dienes 1963).

The value of S^f for interstitial atoms is less than for vacancies, and the value of E^f is calculated to be considerably more, so that only vacancies and their aggregates will be present in significant concentrations in thermal equilibrium. For example, if we take the formation entropies of vacancies and interstitials to be equal, and say that the

formation energy of an interstitial is 1 eV greater than that of a vacancy (c.f. values for noble metals quoted by March 1973; Damask and Dienes 1963, pp. 13-14; Van Bueren 1961, p. 33) the ratio of concentrations at 700 K, the melting point of zinc, is

$$\frac{C_{1v}}{C_{1i}} = \frac{\exp(-E^f_{1v}/kT)}{\exp(-E^f_{1i}/kT)}$$

$$= \exp[(E^f_{1i} - E^f_{1v})/kT]$$

$$= \exp 17$$

$$\sim 10^7$$

Here and subsequently we use the subscripts 1v and 1i to refer to mono-vacancies and mono-interstitials respectively; divacancies are denoted by the subscript 2v, and so on. The superscript f refers to formation of the particular defect; superscripts m and sd are used to indicate migration and self-diffusion.

The following techniques have been used to investigate defects in thermal equilibrium:

(i) Extrapolation of thermal expansion, electrical resistivity or specific heat data.

(ii) Measurements of dilatation and lattice parameter.

(iii) Positron annihilation measurements.

(iv) Diffusion measurements.

A summary of results from experiments of these types is given in Table 2.1-1.

2.11 Extrapolation measurements

In method (i) an equation, which may have some theoretical basis but which is often empirical, is fitted to data for the variation of a property with temperature at temperatures less than about two thirds of the melting point. Experimental data at high temperatures are

Metal	Property measured	E^f_{1v}/eV	S^f_{1v}/k	$C_v(T_m)$	Reference
Cd	$l(T)$	0.42	2.1	2.4×10^{-3}	Gertsriken and Slyusar (1958)
	$\rho(T)$	0.38		2.4×10^{-3}	Gertsriken and Slyusar (1958)
	$\rho(T)$	0.36 to 0.39		3×10^{-3}	Hillairet et al. (1969)
	$\frac{\Delta l}{l} - \frac{\Delta a}{a}$	0.42			Janot and George (1971)
	$\frac{\Delta l}{l} - \frac{\Delta a}{a}$	0.40 ± 0.02	0.3 ± 0.4	5.6×10^{-4}	Feder and Nowick (1972)
	Positron annihilation	0.41 ± 0.02	0.5		McKee, private comm., cited by Seeger (1973)
	Positron annihilation		3.3		Kuribayashi et al. (1973)
Zn	$\rho(T)$	0.31		3.3×10^{-3}	Gertsriken and Slyusar (1958)
	$l(T)$	0.44	1.65	3.3×10^{-3}	Gertsriken and Slyusar (1958)
	$l(T)$	0.50 ± 0.05	2.3 ± 0.5	2×10^{-3}	Gilder (1969)
	$l(T)$	0.50	1.9 ± 0.3		Svechkarev (1971) (recalculation of Gilder's data)
	Positron annihilation	0.54 ± 0.03			McKee et al. (1972) Seeger (1973)
	Positron annihilation		2.5		Kuribayashi et al. (1973)

Table 2.1-1. Properties of vacancies from high temperature equilibrium measurements

found to deviate from the extrapolation of this equation, and the deviation is said to be due to the formation of defects. The weakness of the method is that even if no defects appeared the high temperature data would still deviate from the extrapolated curve because of anharmonic terms in the lattice vibrations (Hoch 1970). As these terms cannot be calculated exactly, it is not known how much of the deviation is due to defects. As shown in Table 2.1-1, values obtained by this method for the concentration of defects at the melting point in zinc vary from 2×10^{-3} to 3.3×10^{-3}.

2.12 Dilatation and lattice parameter measurements

This method avoids the difficulty of extrapolation by measuring the temperature dependence of both length and lattice parameter at high temperatures. Since the creation of a vacancy is equivalent to removing an atom from the interior of the metal and placing it on the surface, this will increase the length, l, but will not directly affect the lattice parameter, a. If the vacancies are statistically distributed the relaxation of the adjacent atoms has equal effects on the lattice parameter as measured by X-rays and on the overall length of the specimen. The vacancy concentration is then given by

$$C_v = 2(\Delta l_a/l_a - \Delta a/a) + (\Delta l_c/l_c - \Delta c/c)$$

for a hexagonal crystal for which l_a, a and l_c, c are the lengths and lattice parameters parallel to the a- and c-axes respectively.

This method was applied to cadmium by Feder and Nowick (1972); their results are included in Table 2.1-1.

2.13 Positron annihilation

This is a recently developed sensitive technique for the detection of equilibrium concentrations of vacancies (Seeger 1973). It is not affected by the presence of interstitials, as the dilato-

metry/lattice parameter method would be, and its maximum sensitivity is in a temperature range where divacancies may be neglected, so that values of true vacancy formation energies may be measured rather than effective energies which are modified from the true values by the presence of these other defects. The method cannot be used to measure absolute values of concentrations, however.

The technique depends on the fact that positrons can be trapped at vacancies in a metal, and that properties such as their lifetimes and the momentum distribution of the electrons with which they annihilate will be different for trapped positrons from free ones. Lifetimes are measured by using a source which emits a γ-ray at the same time as a positron; the time between this γ-ray and one of the two annihilation γ-rays is measured electronically and recorded in a multichannel analyser. Information about the momentum distribution may be obtained either from the angular correlation of the two annihilation γ-rays or by measuring their Doppler broadening.

The best values obtained so far for cadmium and zinc are shown in Table 2.1-1. The value of E_{1v}^{f} for cadmium agrees well with the previous measurements by other techniques, although for zinc it is slightly higher than previously. Another value of E_{1v}^{f} =(0.52±0.05) eV has been reported for cadmium by Connors et al. (1971); this falls well outside the experimental error of other measurements, and Seeger (1973) thinks that it may be in error because of a large temperature extrapolation which was used in analysing the data.

2.14 Diffusion measurements

The predominant mechanism of self-diffusion in zinc and cadmium is thought, on the basis of isotope effect measurements, to be the movement of monovacancies (Seeger and Mehrer 1970, p. 50). The

activation energy for self-diffusion will then be the sum of the monovacancy formation and migration energies, i.e.

$$E^{sd} = E^{f}_{1v} + E^{m}_{1v}.$$

Since all three of these energies can be measured independently, this equation gives a check on the self-consistency of the values.

Measured values of the self-diffusion energy, E^{sd}, are given by Schumacher (1970) and have averages of 0.82 eV for cadmium and 1.0 eV for zinc. When taken together with the formation energies in Table 2.1-1 these imply monovacancy migration energies of about 0.4 eV for cadmium and 0.5 eV for zinc.

2.2 Quenching experiments

The difficulty of measuring equilibrium concentrations of defects at high temperatures by techniques such as electrical resistivity is that the defect resistivity is only a small fraction of the total resistivity due to thermal motion of the lattice atoms. An alternative approach is therefore to hold the specimen at a high temperature long enough for the equilibrium concentration of defects to be established, and then to cool it rapidly to a temperature low enough to immobilise the defects of interest. The supersaturated concentration of defects produced in this way may then be measured by static methods, and the temperature may be made very low so as to reduce the thermal component of resistivity. Various annealing treatments can be used to investigate the processes which occur as the defects are eliminated.

If the quench is done infinitely fast, the concentration of defects retained will be the equilibrium value at the high temperature, as given by (2.1-1). Measurements of electrical resistivity do not allow absolute concentrations to be measured unless the resistivity per defect is known, but relative concentrations for quenches from different temperatures allow calculation of the activation energy for vacancy formation, E^f_{1v}.

As discussed in section 2.1, the predominant defects present in equilibrium at high temperatures are vacancies and their aggregates, so it is almost entirely this type of defect which is present in quenched specimens. This simplifies the interpretation of annealing measurements, and by identifying effects due to vacancies helps to pick them out in the more complex annealing spectra which result from irradiation or plastic deformation.

For a quench to retain most of the vacancies present at high temperature the rate of cooling must be large, typically $\geqslant$ 1000 K s^{-1} (Vostrý et al. 1972), and the resulting thermoelastic stresses can produce plastic deformation. This effect is particularly troublesome in the h.c.p. metals because of their anisotropy, and is discussed in more detail in section 4.4.

The value of E_{1v}^{f} for cadmium has been measured by Vostrý et al. (1972) as (0.45 ± 0.04) eV, by quenching polycrystalline ribbons, 25 μm x 1 mm, to 4.2 K from temperatures in the range 273 K to 473 K. They consider that their improved experimental arrangements make this a better value than the previous estimate of about 0.4 eV (Sprušil et al. 1970).

Other estimates of E_{1v}^{f} are by Savitskiy et al. (1964), who obtained (0.37 ± 0.03) eV, and Zen et al. (1965), who obtained 0.31 eV, but these results were from quenching to about 273 K and measuring microhardness and density, and length, respectively. As vacancies are thought to be mobile below 273 K these measurements will relate to vacancy and vacancy-impurity aggregates.

The recovery stages found by Vostrý et al. (1972) and Sprušil et al. (1970) are shown in Fig. 2.2-1, which summarises the results of annealing experiments on quenched and irradiated zinc and cadmium and shows the labelling of annealing stages which we shall use in the subsequent discussion.

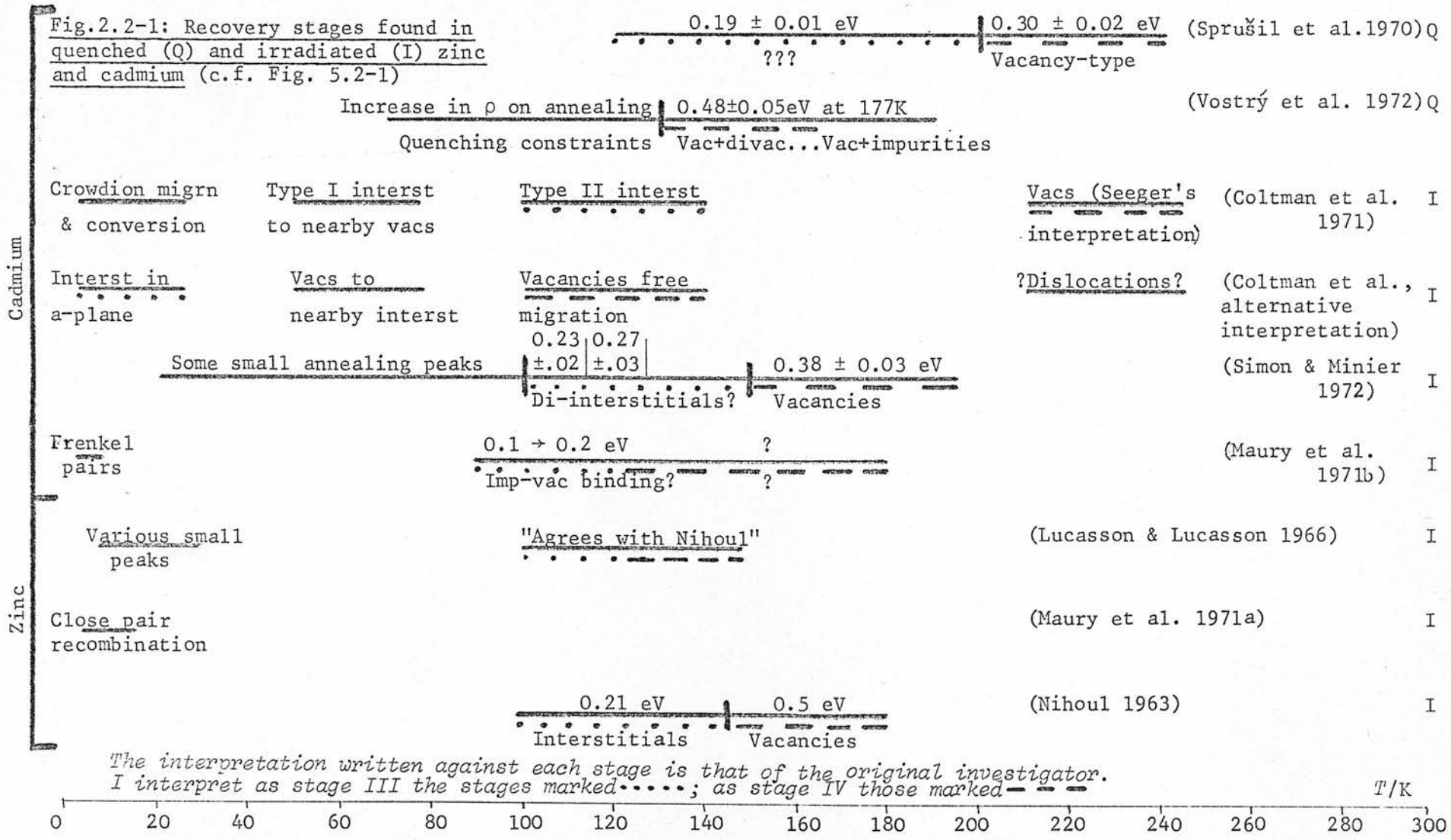

Fig.2.2-1: Recovery stages found in quenched (Q) and irradiated (I) zinc and cadmium (c.f. Fig. 5.2-1)

2.3 Irradiation experiments

Detailed isochronal annealing results on neutron irradiated cadmium have been published by Coltman et al. (1971). They observed a number of annealing peaks in the range 4.2 K to 300 K, but were unable to assign all of them to specific defects. They proposed two alternative models for the main annealing stages.

In the first model metastable interstitials, probably crowdions, migrate at temperatures below 26 K and can annihilate with vacancies. They can also be converted to a more stable form which combines with nearby vacancies in a peak at 60 K, and which migrates freely in the range 100 K to 140 K.

The second model postulates a single type of interstitial, which lies between the basal planes. The peaks below 26 K are due to movement of these interstitials on their own planes, with no movement in the direction of the c-axis. Some will annihilate with vacancies on the adjacent planes, but others will be trapped in the stress fields of vacancies or interstitials on near but non-adjacent planes. At 60 K the vacancies are able to move and annihilate the nearby interstitials which they have been trapping. The peak at 100 to 140 K is attributed to long-range migration of free vacancies.

Coltman et al. do not consider that their data enables them to make a choice between these two possible models. They found that the stage III peak at 100 - 140 K did not fit a single order of kinetics, and therefore thought it inappropriate to try to calculate an activation energy. The number of jumps which one defect would have to make to reach another defect at the estimated concentration of 3×10^{-6} was, however, compatible with the number 5×10^{4} derived from Peiffer and Stevenson's (1963) energy value of 0.35 eV, which

had been attributed to vacancy migration.

Seeger (1970) calculated that for a vacancy migration energy of 0.36 eV the number of jumps for Coltman's 225 K peak would be 10^7 to 10^8 in a pulse of 5 minutes, and he considered that this order of magnitude was what would be expected, so that the 225 K should be attributed to vacancies. The position of Coltman's stage III peak depends on defect concentration; Seeger finds that at large doses, when it occurs at 105 K, vacancies with E_m = 0.36 eV would have a number of jumps of only 10^{-2} or 10^{-1} in each five-minute pulse. Thus although Coltman's calculation of the number of jumps for small doses seems reasonable, Seeger's value for the same peak at higher doses is not compatible with vacancy migration. He therefore attributes it to free migration of interstitials, explaining all the peaks at lower temperatures by the recombination of Frenkel pairs of varying initial separations. He agrees with Coltman that vacancy-interstitial pairs may exist in two configurations (a-pairs and c-pairs), the relative concentration of which depends on dose. The type which predominates at small doses must anneal at low temperatures and the other type requires energies up to that of free interstitial migration.

Simon and Minier (1972) irradiated polycrystalline cadmium with 3 MeV electrons at 20 K. This temperature was too high for them to investigate Coltman's stage I annealing (below 26 K), although they saw some evidence for its existence. They say that they did not observe the stage II peak at 60 K, and assumed that the displacement energy required to create c-pairs was too great for many to be produced by their irradiation. There is a peak at about 60 K on most of their graphs, however, particularly on one obtained from less pure (5N) material. They agreed with Seeger on ruling out the vacancy for stage III because

of the small number of jumps it would make, and concluded that the stage was due to interstitials and multi-interstitials. Finally they allocated vacancy migration to stage IV, at 150 - 160 K, for which they found an activation energy of (0.38 ± 0.03) eV. This is said to agree with their results on quenched cadmium samples which showed a peak at 170 K, the higher temperature being because there were less dislocation sinks in the quenched than in the irradiated cadmium. The published report of the quenching work, however, (Vostrý et al. 1972), shows that a peak isolated at 177 K had too high an energy ((0.48 ± 0.05) eV) and too few jumps ("a few hundred") to be free monovacancy migration, and was thought to be due to the freeing of vacancies from impurity traps. The remainder of the quenching results showed a broad stage extending from 130 K to 190 K, which was thought to be due to mono- and di-vacancies.

The remaining irradiation work on cadmium was done by Maury et al. (1969, 1971b). They were mainly interested in mechanisms of damage rather than recovery, but did some isochronal annealing, finding recovery stages at 5.5 K and 90 - 180 K. The 5.5 K stage was said to be recombination of close Frenkel pairs, but the other broad stage was not analysed in detail. An assignment of 0.1 to 0.2 eV as the activation energy for recovery at ~120 K was however compatible with their model for the production of defects by the displacement of small numbers of dissolved hydrogen impurity atoms, initially held in shallow traps such as vacancies, with a binding energy of ~0.1 eV.

Maury et al. also irradiated zinc with electrons at 10 K and annealed isochronally up to 150 K (Lucasson and Lucasson 1966; Maury et al. 1971a). Despite some trouble with poor reproducibility they identified annealing in a number of substages up to 32 K, at least those

below 15 K being attributed to recombination of Frenkel pairs. They also found a major stage at 100 to 150 K which agrees with the previous findings of Blewitt (1957) and Nihoul (1963).

Nihoul, who irradiated zinc with neutrons at 77 K, found continuous annealing between 100 and 180 K. There were two main peaks centred at 105 K and 155 K, with activation energies (0.21 ± 0.02) eV and (0.50 ± 0.03) eV respectively. Interstitials or divacancies were thought responsible for the first peak, which had second order kinetics, and vacancies were tentatively suggested for the second, although as the order of kinetics found was greater than 2 the process is probably complex and the 0.50 eV found may be an effective activation energy which should not be firmly associated with any particular defect.

2.4 Plastic deformation experiments

A number of experiments have previously been carried out on point defects produced by plastic deformation in cadmium, but discussion of these will be postponed to section 5.2 where they can be considered in conjunction with the results of the present work.

2.5 Theoretical calculations

Although many theoretical calculations of the properties of point defects in cubic metals have been carried out (reviewed by March 1973; Johnson 1973) very little work has been done on hexagonal metals. In 1963 Harrison calculated E^f_{1v} for zinc, obtaining 1.8 eV. "This", he says, "would appear to be an over-estimate" since it is incompatible with an experimental self-diffusion energy of ~1 eV. He obtained 6.5 nΩm for the electrical resistivity due to 1% of vacancies in zinc, compared with Reale's (1962) calculated values of 14 nΩm for zinc and 15 nΩm for cadmium.

Most other theoretical work has been concerned with comparisons between energies for the production and migration of defects and other properties of metals, such as melting point (Neumann 1967; Osipov 1971), sublimation energy (Sprušil 1963) and Debye temperature (Tewary 1973; Neumann 1967). These calculations rely on establishing a relationship between pairs of properties which have been measured experimentally in a number of metals and then assuming that the same relationship holds for metals of which only one of the properties has been measured.

Neumann obtains the following relationships between the melting temperature, T_m, and defect energies for f.c.c. and h.c.p. metals:

$$\begin{aligned} E_{1v}^{f} &= (0.816 \times 10^{-3}\ \text{eV K}^{-1})\ T_m \\ E_{1v}^{m} &= (0.684 \times 10^{-3}\ \text{eV K}^{-1})\ T_m \\ E^{sd} &= (1.55 \times 10^{-3}\ \text{eV K}^{-1})\ T_m \end{aligned} \qquad (2.5\text{-}1)$$

These expressions agree with experimental data to within 10% to 20%. He derives Mukherjee's (1965) relation between the Debye temperature and defect energies

$$E = (\Theta_D^2 / c^2)\ M\ V^{\frac{2}{3}} \qquad (2.5\text{-}2)$$

where E is a defect energy, Θ_D is the Debye temperature, M and V are the atomic mass and volume respectively, and c is a constant which is the same, within 10%, for many f.c.c. and h.c.p. metals. The value of c^2 depends on the particular energy being considered; the values found by Neumann (converted from molar to atomic units) are shown in Table 2.5-1.

E	c^2/(eV kg m^2 K^2)
E_{1v}^{f}	6.5×10^{-40}
E_{1v}^{m}	7.15×10^{-40}
E^{sd}	3.34×10^{-40}

Table 2.5-1

From these equations we can calculate energies for zinc and cadmium as shown in Table 2.5-2.

		Zinc	Cadmium
T_m/K		693	594
Θ/K		224	142
$MV^{\frac{2}{3}}$/kg m^2		0.625×10^{-44}	1.33×10^{-44}
E^f_{lv}/eV	*	0.58	0.49
	†	0.48	0.41
E^m_{lv}/eV	*	0.48	0.41
	†	0.44	0.38
E^{sd}/eV	*	1.08	0.92
	†	0.92	0.81

Table 2.5-2. Values of defect energies for zinc and cadmium calculated from Neumann's relationships. Values calculated from (2.5-1) are marked *; values calculated from (2.5-2) are marked †.

3. EXPERIMENTAL

A general view of the experimental arrangements is shown in Fig. 3.1

3.1 Specimen materials and preparation

3.11 Materials

Both zinc and cadmium were obtained from each of three different suppliers:

i) Supplier: Metallurgical Services Ltd.

Purity: Stated to be "pure" but no analysis available.

Form: Zinc: 2mm diameter wire.

Cadmium: 4mm diameter wire. When drawn down to 2mm diameter, this cadmium wire was found to have a resistance ratio, $R_{273}/R_{4.2}$ = 1400.

ii) Supplier: Johnson Matthey Chemicals Ltd.

Purity: Zinc: 99.999%. The supplier's spectrographic analysis was as follows:

Element	Estimate of quantity present parts per million
Iron	5
Silicon	1
Bismuth, Cadmium, Calcium, Magnesium	less than 1

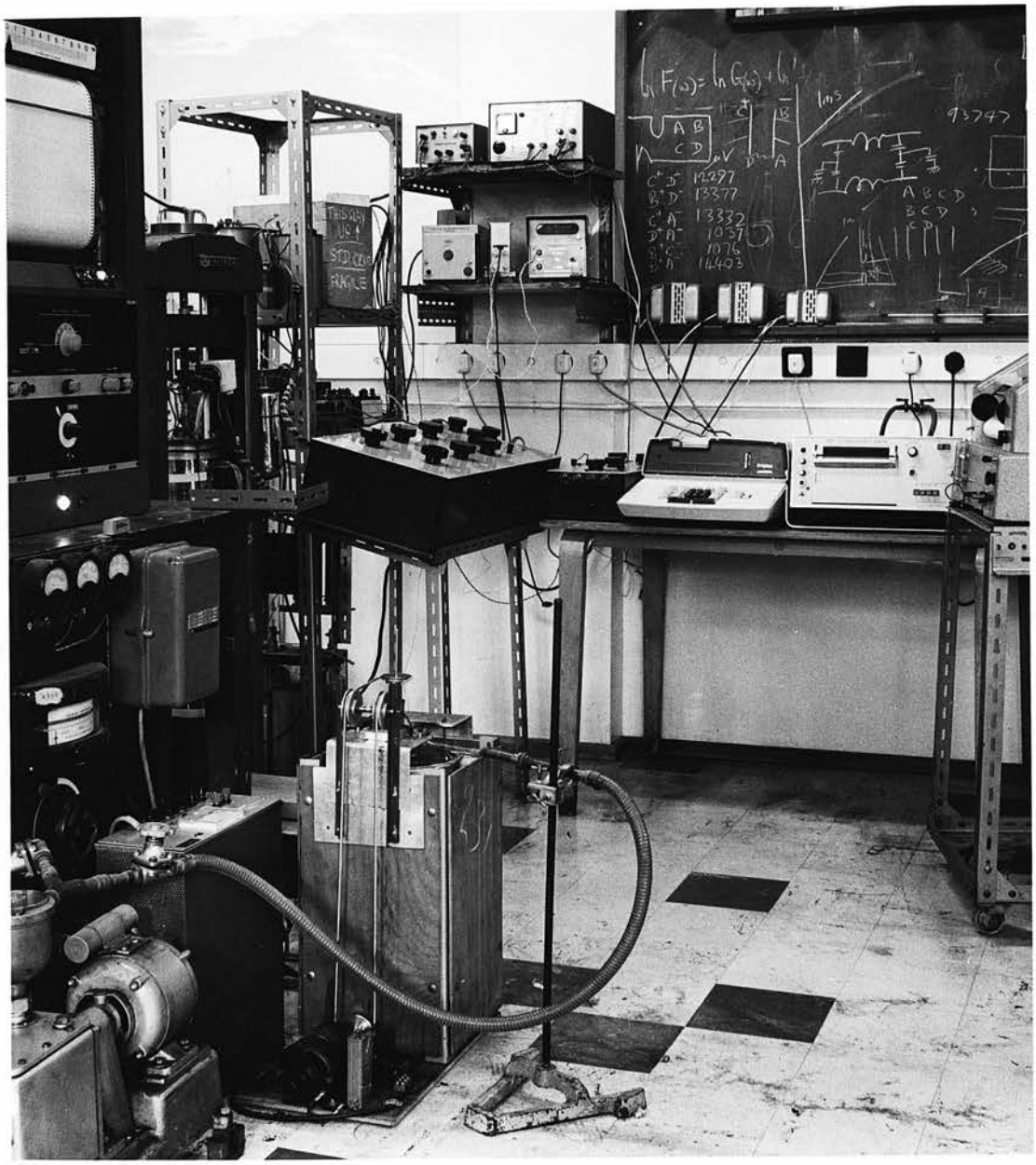

Fig. 3-1: General view of the experimental arrangements

Cadmium: 99.996%. The supplier's spectrographic analysis was as follows:

Element	Estimate of quantity present parts per million
Indium	30
Lead	2
Iron	1
Silver	1
Bismuth, Copper, Magnesium	each element less than 1

Form: 2mm wire. The zinc wire was drawn by Johnson Matthey from 7mm rods, and the spectrographic analysis applies to the material before drawing.

iii) Supplier: Koch-Light Laboratories Ltd.

Purity: Zinc: 99.999%, catalogue no. 8109H.

Cadmium: 99.9999%, catalogue no. 8839H.

Form: 1mm wire.

The Metallurgical Services material was used for preliminary experiments, but most of the results were obtained from Johnson Matthey materials. Only a few runs were done with the metal obtained from Koch-Light.

3.12 Polycrystalline specimens

Polycrystalline specimens were cut to the required length, washed in a solvent such as carbon tetrachloride or trichloroethylene to remove any greasy contamination, and chemically polished with an etch developed by J. J. Gilman (1956), viz:

CrO_3, 160g

Hydrated Na_2SO_4, 20g

H_2O, 500cm^3

They were then sealed in glass tubes under a low pressure of helium, annealed at 417K (0.7 T_m) for about two hours and allowed to cool slowly inside the oven. After another light etch the specimen and dummy, which were annealed simultaneously to make them as similar as possible, were mounted in the deformation apparatus as described in section 3.21. After being mounted, and when all electrical leads had been attached, the specimen and dummy were left for at least a day at room temperature to recover from mounting strains. Sometimes separate short potential leads were attached to the specimen and subsequently joined to the main leads inside the cryostat (see 3.32); in this case it was possible to anneal the specimen in an oven after the grips and leads had been attached, but the temperature could not exceed the melting point of the solder, 343K.

3.13 Single crystal specimens

These were grown in a Metallurgical Services single crystal unit, illustrated in Fig. 3.13-1. The travelling furnace, which moved along the fixed glass tube at a speed of 1.6mm/min, was wound so as to give a steep temperature gradient at its lower end. The furnace temperature distribution has been measured by Anderson (1965). The tube could be evacuated or filled with an inert atmosphere. Oxygen-free nitrogen or helium were usually used to avoid evaporation which occurred when the metal was melted under vacuum. Various different types of crucible were used to contain the crystals during growth:

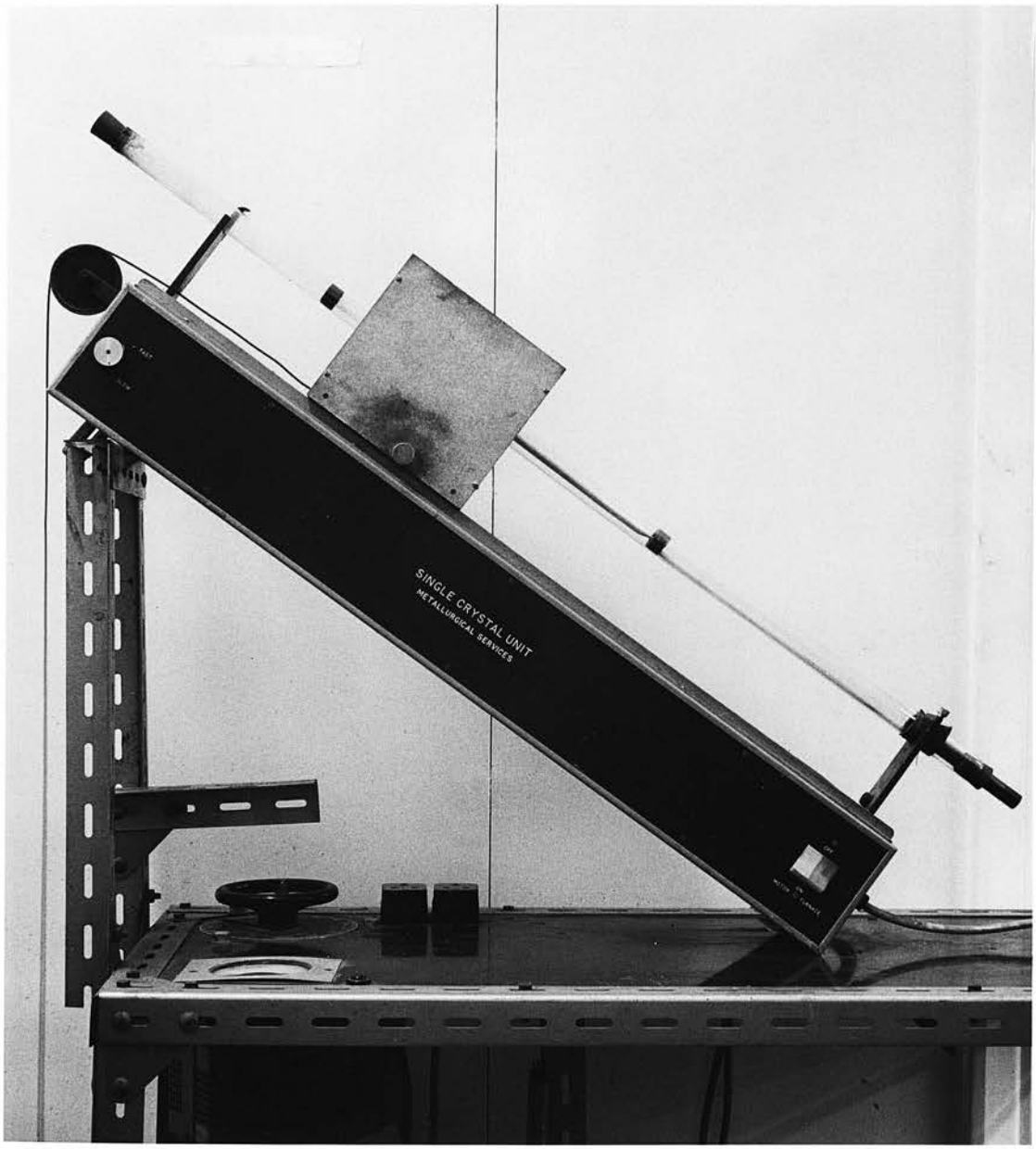

Fig. 3.13-1: Single crystal unit

a) Glass tubes with a 2mm precision bore (Chance Bros. Ltd. - "Veridia") were used, held on carbon spacers at the centre of the furnace tube. Crystals grew successfully in these, but were difficult to extract without damage. An internal graphite coating did not make extraction much easier, but drawing down the wire so that it was a fairly loose fit in the tube was sometimes helpful.

b) Two of these 250mm long precision bore tubes were ground down for half their thickness, to a plane through the axis, so that when fitted together they formed a split mould. The wire was put between the halves and they were then slid into a larger glass tube which just fitted their outside diameter and held them together. This assembly was then mounted in the furnace on carbon supports as before. Crystals grown in this mould were rather easier to extract, but unwanted grains were present more often, presumably being nucleated at the joint between the two parts of the mould. The increased amount of glass between the specimen and the furnace would also have detracted from the quality by decreasing the steepness of the temperature gradient at the growing face.

c) A split graphite crucible with three longitudinal slots of 2mm square section cut in one side was fairly successful but there was still some difficulty in extracting the crystals without damage.

d) The method which was best for avoiding damage to the crystals was the "soft-mold" technique (Noggle 1953). They were grown in a glass tube of 7mm internal diameter, packed with a fine powder of pure alumina or silica. After growth the powder could be loosened and shaken out and the crystal slid out without strain.

This method led to some slight surface roughness, but most of this was removed by the chemical polishing.

Single crystals were etched lightly in dilute hydrochloric acid to check for unwanted grains, and were given the same polishing, mounting and annealing treatment as polycrystalline specimens. They were cut to length by spark cutting or, in the case of cadmium, with a pair of fine wire cutters, and in the case of zinc, by low temperature cleavage. Since about 6mm at each end of the crystal was embedded in solder when mounted, and since the potential lead was attached at least 5mm away from the grips, strains produced at the point of cutting should not have affected the measurements.

3.14 Orientation measurements

Until it had been shown that defects were in fact produced in measurable quantities by low temperature deformation, it was not thought worth making detailed measurements of crystal orientation in order to investigate the production mechanisms. Thus although some cadmium crystals were orientated by Laué back-reflection x-ray techniques for another purpose, most orientation measurements were optical ones. In particular, the orientation of the basal plane of zinc single crystals was determined by low temperature cleavage, the angle between the cleavage plane and the crystal axis being measured by optical goniometry, using an arrangement similar to that of Goss (1953).

Before x-ray crystallographic equipment became conveniently available, some experiments were carried out with the "light figure" method of Yamamoto and Watanabe (1950, 1955) who used a technique which Chalmers (1935) had developed earlier for the study of twinning in tin. For this an arrangement similar to that of the Laué method was

used, but with a narrow collimated beam of light from a high pressure mercury lamp instead of a beam of x-rays. The crystal surface was etched in Yamamoto's solution, and the reflections from the etch pits then showed the crystallographic directions. A typical "light figure" or back-reflection photograph from the basal plane of a zinc crystal is shown in Fig. 3.14-1.

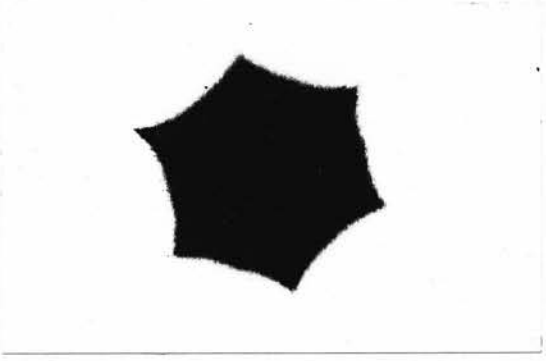

Fig. 3.14-1: Light figure obtained by reflection from etch pits on the (0001) plane of zinc single crystal. The points of the figure point in the $<11\bar{2}0>$ directions.

3.2 Deformation apparatus

First experiments were carried out using a small Polyani-type tensile testing machine similar to the one used by Anderson (1965). This had not been designed for low-temperature work, however, and did not have sufficient space for a cryostat to be fitted. An Instron tensile testing machine, model TM-M-L, became available later, and all subsequent work was done on this. The Instron machine had two modifications which made it particularly suitable for this work: an extra length of crosshead travel to provide space for a cryostat, and two decade speed reducers allowing deformation rates down to 5×10^{-6} m s^{-1}. A deformation rate of 0.05 mm min^{-1} (8.3×10^{-7} m s^{-1}) was usually used for zinc, but with cadmium, in which brittleness is not such a problem, rates of up to 20 mm min^{-1} (3.3×10^{-4} m s^{-1}) could be used. Fig. 3.2-1 shows load vs. extension for polycrystalline Cd.

Strain was determined either by measuring from the Instron chart or by measuring the distance between the potential leads with a travelling microscope before and after deformation. Because it was necessary to take the differences between two sets of readings this gave an accuracy of ±0.1 mm in the extension, which is ±10% in extensions of 1 mm ($\varepsilon \simeq 2\%$) or ±2% in extensions of 5 mm ($\varepsilon \simeq 10\%$).

Two glass dewar vessels were manufactured to size by T. W. Wingent Ltd., to form a cryostat suitable for use with liquid nitrogen or liquid helium. The outer vessel was evacuated and sealed, and the inner one was fitted with a pumping connection. The dewars were mounted on a sliding platform which allowed them to be moved in and out of the space under the moving crosshead of the Instron (Fig. 3.2-2). The jig which held the specimen could be detached by removing the six Allen screws A and B (Fig. 3.2-3) so that it was possible to move it clear of the

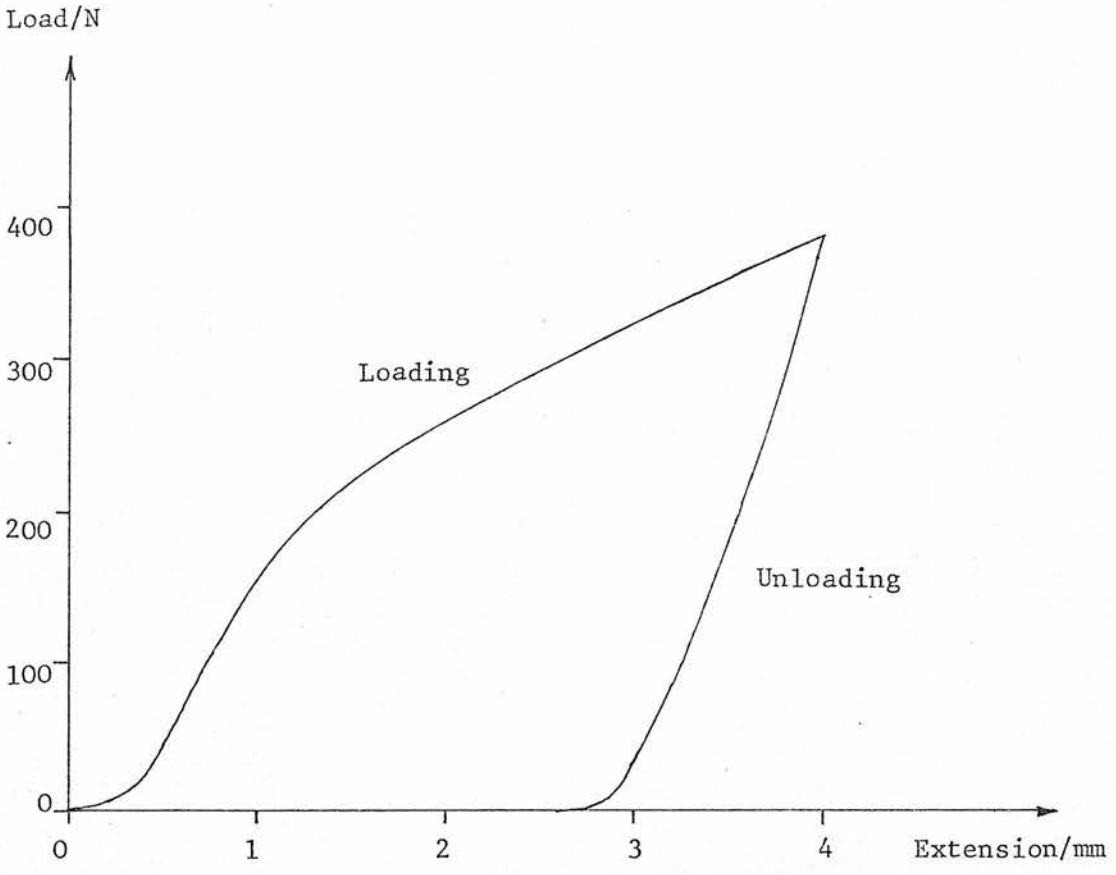

Fig. 3.2-1: Load-extension curve for a specimen of polycrystalline cadmium at 78 K.

Before deformation, diameter = 2 mm

length = 50 mm

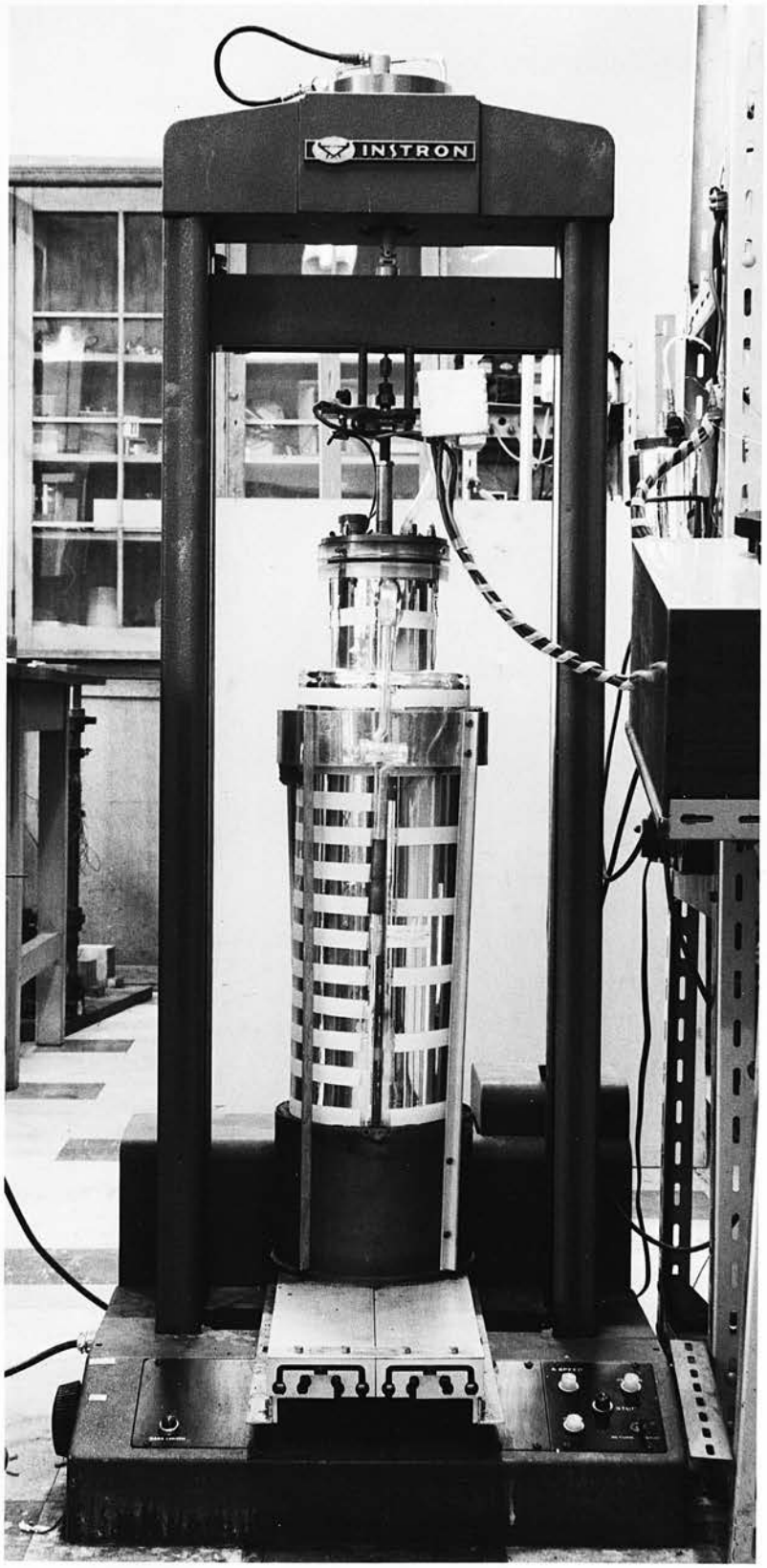

Fig. 3.2-2: Cryostat mounted in Instron

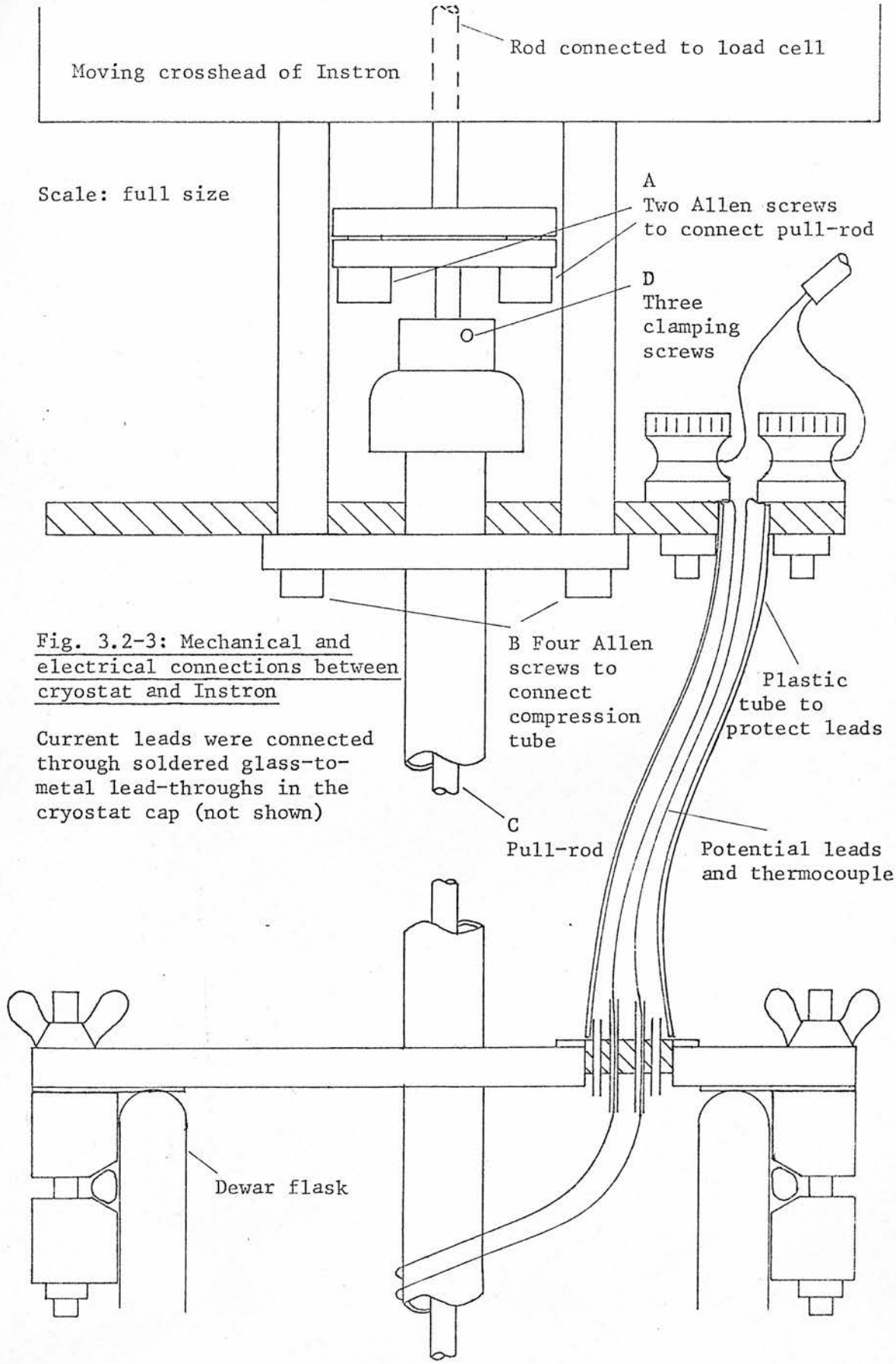

Fig. 3.2-3: Mechanical and electrical connections between cryostat and Instron

Current leads were connected through soldered glass-to-metal lead-throughs in the cryostat cap (not shown)

machine for the annealing stage of the experiment after deformation had been carried out. After deformation pull-rod C was clamped by the three screws D before it was disconnected from the load-cell.

3.21 Specimen grips and mounting procedure

Various forms of grip and mounting techniques were used, including mechanical clamps, specimens grown in a dumbell shape, specimens with dumbell ends moulded on in solder or electrically conducting epoxy resin, and specimens soldered directly into the grips. In all cases precautions had to be taken to avoid introducing unintentional deformation into the specimen while mounting; this was generally done by clamping the two grips in a jig which was not removed until the specimen was mounted in the machine. One successful form is shown in Figs. 3.21-1 and 3.21-2; this was developed from a design by Kuhlmann-Wilsdorf and Raghavan (1962), and incorporates the clamping jig in the testing assembly itself. Two screws A project from each side of each grip, and these are held firmly against the frame during mounting by a clamping bar B. When the specimen is mounted the clamping screws C are released and the grips are free to move vertically. Strips of polytetrafluoroethylene (p.t.f.e.) insulate the grips from the frame to allow resistance measurements to be made.

This assembly did not provide for a dummy specimen, however, which was found necessary for accurate resistance measurements, so a new jig was designed as shown in Figs. 3.21-3 and 3.21-4. The specimen was soldered directly into two brass end pieces shown in Fig. 3.21-5 which were clamped in a jig (Fig. 3.21-6) so that the length of the specimen between the grips was 50 mm. The jig also supported the whole length of the specimen during mounting.

Soldering was done using a small gas flame applied to the brass grips until their temperature was sufficiently high to allow low-

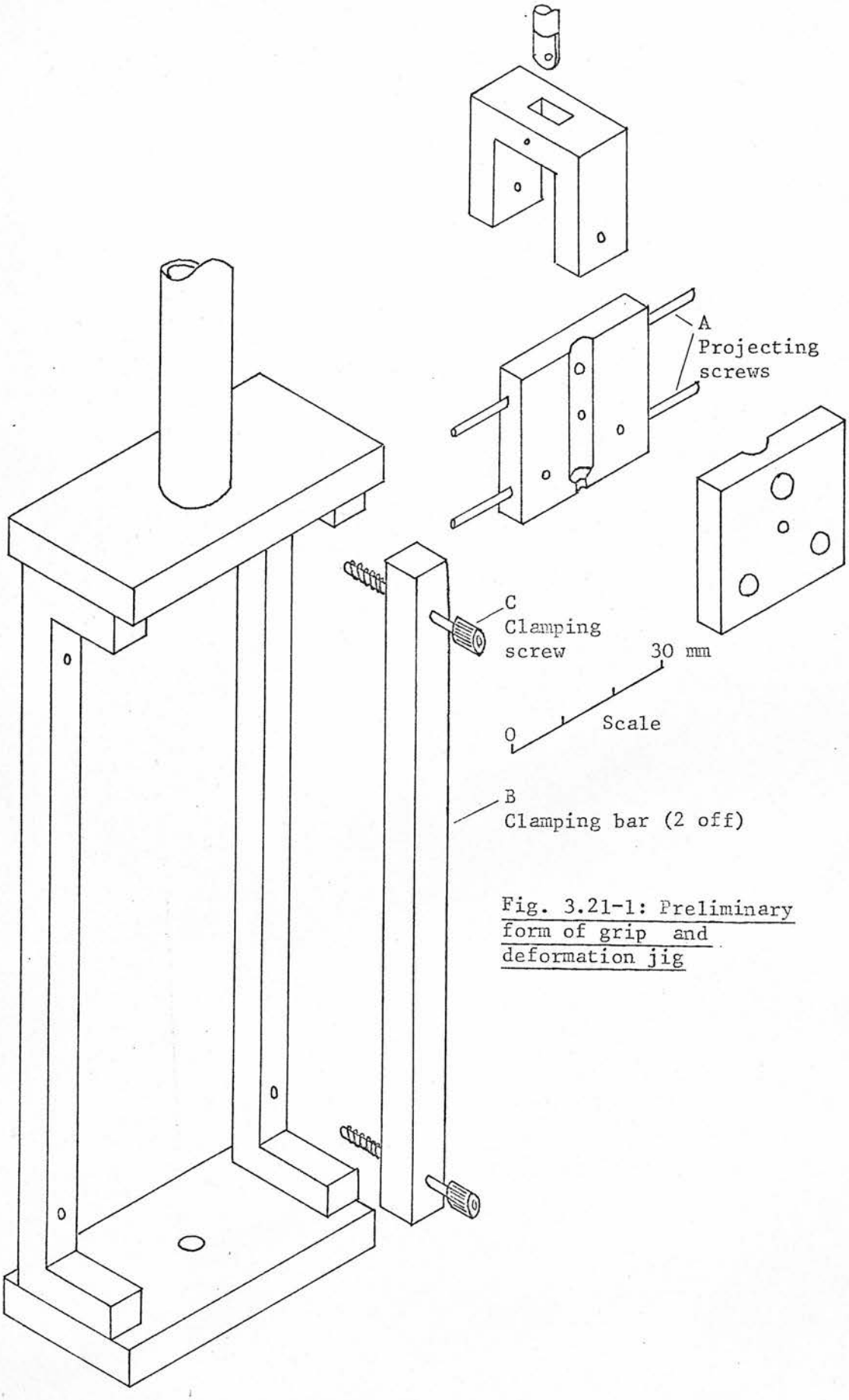

Fig. 3.21-1: Preliminary form of grip and deformation jig

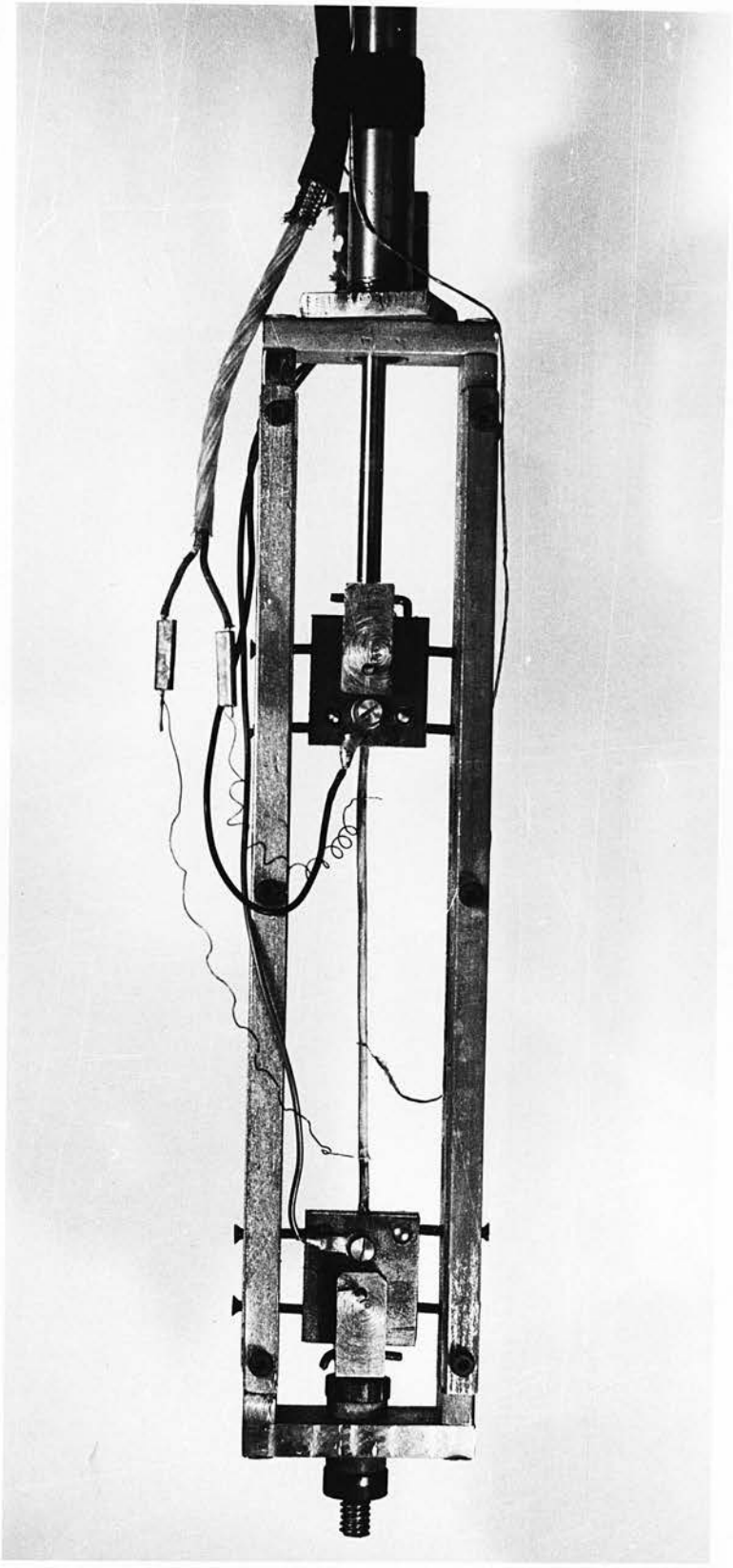

Fig. 3.21-2: Specimen mounted in a longer version of the jig shown in Fig. 3.21-1

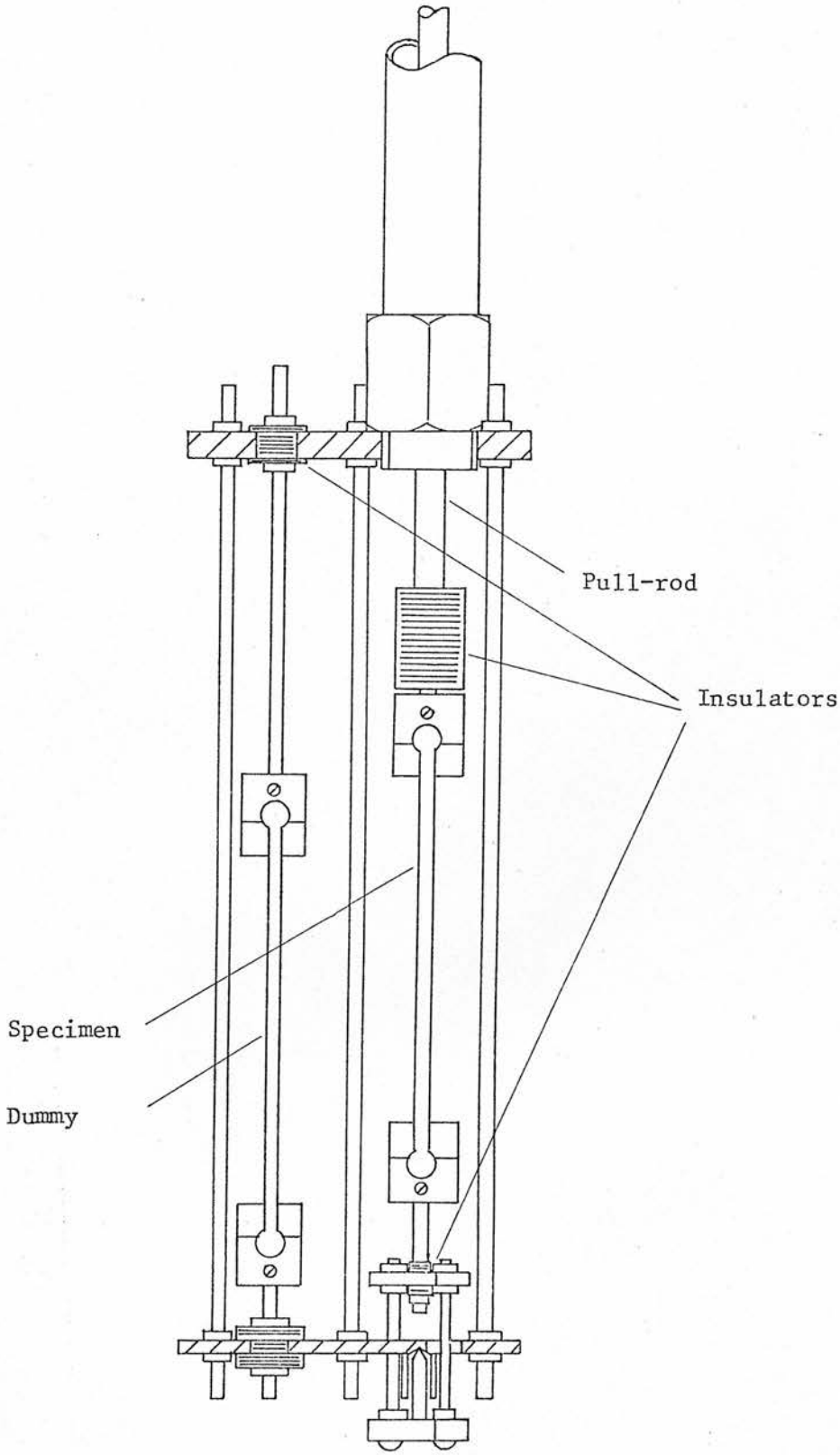

Fig. 3.21-3: Deformation jig

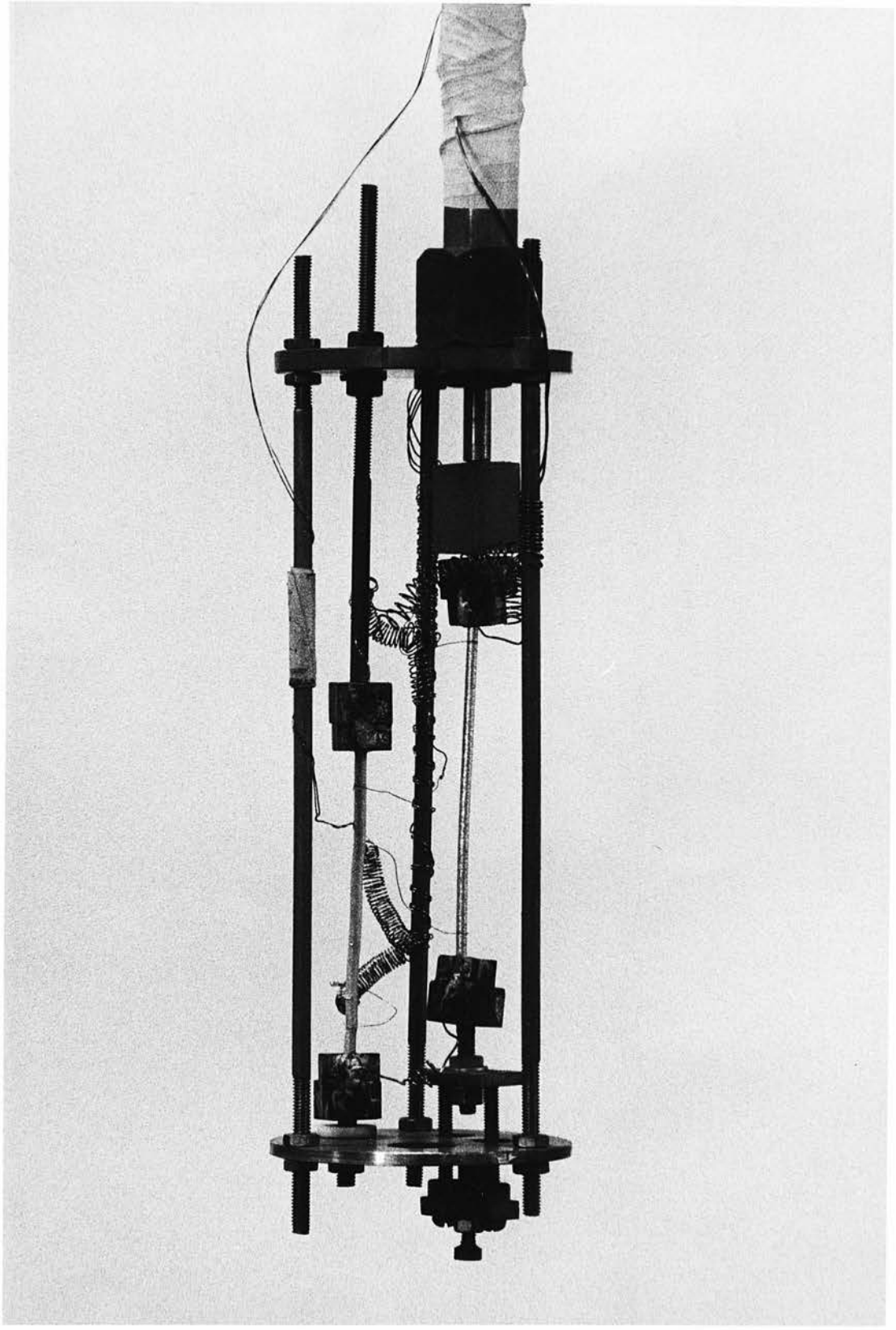

Fig. 3.21-4: Specimen and dummy mounted in deformation jig

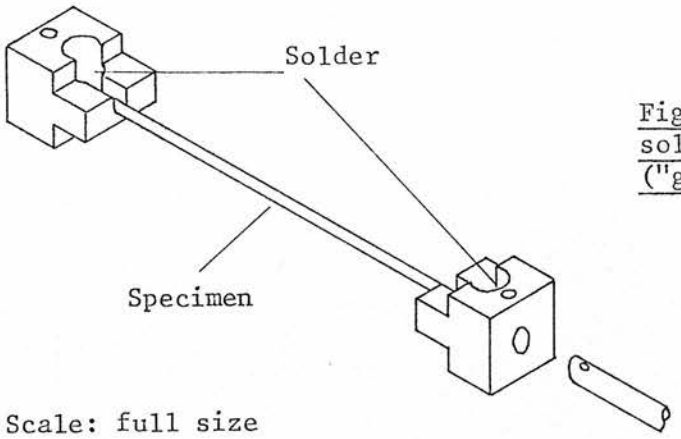

Scale: full size

Fig. 3.21-5: Specimen soldered into end pieces ("grips")

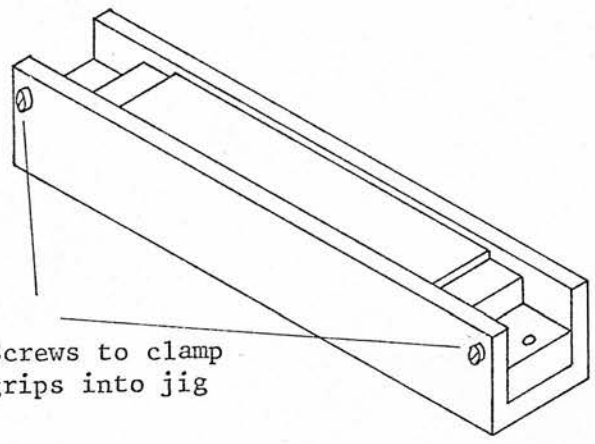

Fig. 3.21-6: Mounting jig to hold specimen during soldering and mounting

melting-point solder to flow into the recess provided around the end of the specimen. The grips were attached to the pull-rod and the bottom mounting by means of small steel screws or pins which were a loose fit in holes drilled transversely through the ends of the rods; this allowed a small amount of rotation to take place as an aid to alignment.

The bottom grips of both specimen and dummy were not clamped rigidly to the lower plate of the deformation jig, but were left loose so that stresses would not be set up due either to misalignment in mounting or to thermal changes in overall length during deformation or annealing. The bottom grip attachment of the specimen was designed to be self-aligning, as shown in Fig. 3.21-3, to avoid bending stresses on the specimen. The mounted specimen and dummy are shown in Fig. 3.21-4. (The slight curvature to be seen in the specimen is due to accidental deformation during photography and did not arise during the experiment.)

3.22 Torsional deformation apparatus

A modification the the tension apparatus was made to allow some tests to be carried out with torsional deformation. (Fig. 3.22-1). It was hoped that by removing the component of tensile stress it might be possible to produce more strain in zinc specimens before fracture occurred, but no significant increase in the strain at fracture was found. The torsion apparatus probably introduced some errors into the stress-strain curve recorded by the Instron - the cord may have stretched slightly and there would have been some friction at the p.t.f.e. guides and at the plain bearing at the bottom of the compression spring - but this was not a primary consideration as the main purpose of the apparatus was to produce a slow and steady twist of the specimen, which it did quite adequately.

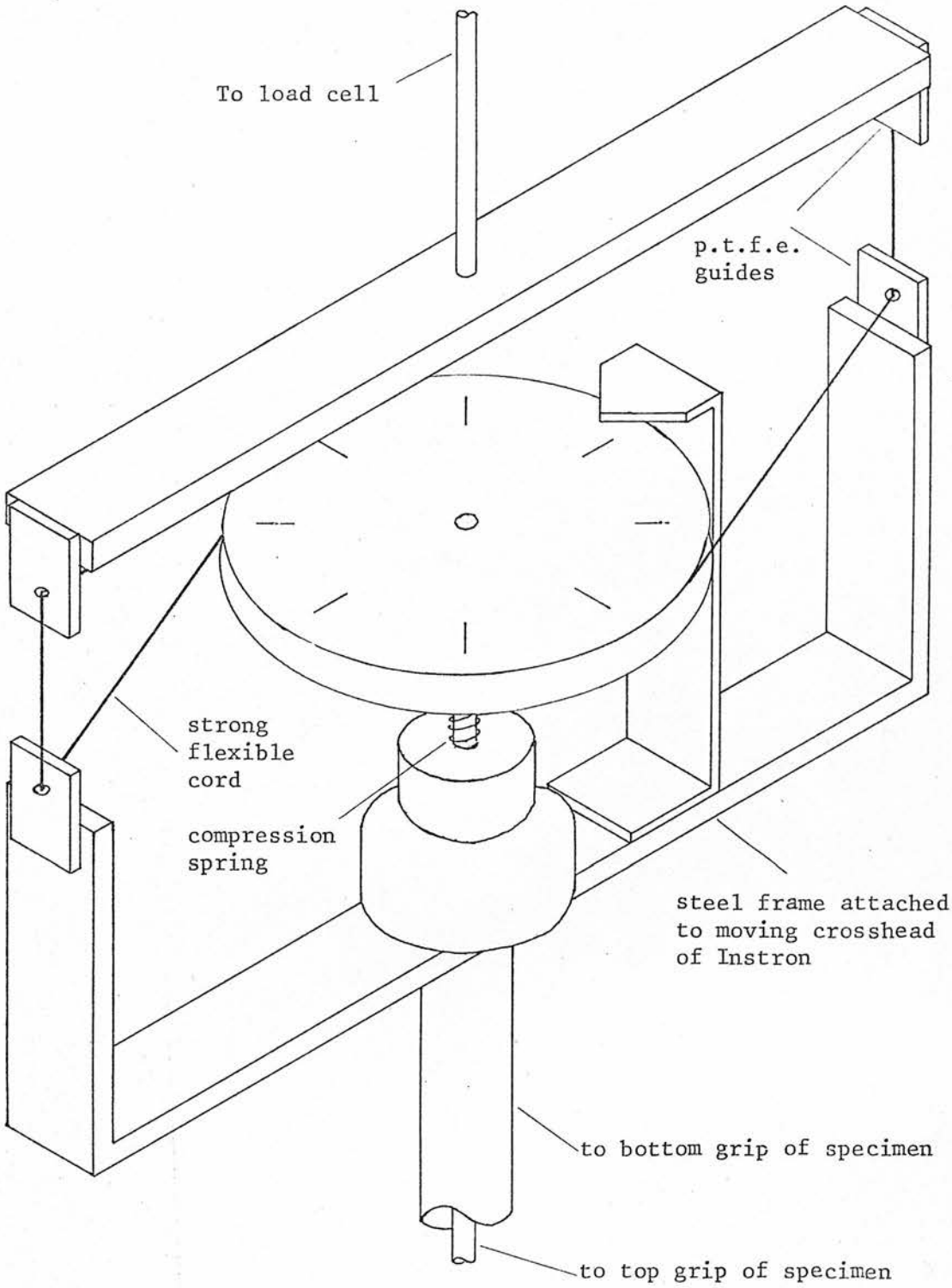

Fig. 3.22-1: Modification of apparatus to allow deformation in torsion

3.3 Resistivity measurement

3.31 Apparatus (Fig. 3.31-2)

Resistivity measurements were made by a potentiometric method using a Tinsley Diesselhorst pattern thermoelectric-free potentiometer, type 3589-R/AUTO serial number 174734. The circuit used is shown in Fig. 3.31-1. All leads in the room temperature part of the specimen current circuit were of large diameter copper cable (7/.0029") ($3mm^2$) so that their resistance would be small enough for variations to have little effect on the current. The size of those within the cryostat was 28swg ($0.1mm^2$).

All leads inside the cryostat were wrapped round the compression tube of the deformation jig, and insulated and protected by a thin wrapping of polytetrafluoroethylene tape.

3.32 Potential leads

All connections at room temperature in the potential circuit were made with well-insulated, screened, untinned, twin twisted copper cables, joints being clamped in bare copper terminal posts to avoid thermal or contact e.m.f 's. The potential leads have to make good electrical contact with the specimen at a well-defined position, have to stay firmly attached during the stretching and annealing operations, must not produce excessive stress concentrations which could lead to fracture or interfere with the uniform deformation of the specimens, and must not produce spurious contact e.m.f 's. Various methods of attachement were tried, such as solder, electrically conducting epoxy resin, small copper clamps and copper contacts inserted at the grips. None of these proved satisfactory, and it was decided that spot-welding should be used. "Ewald" miniature welding equipment, model P10-10S2, was acquired by the laboratory; this

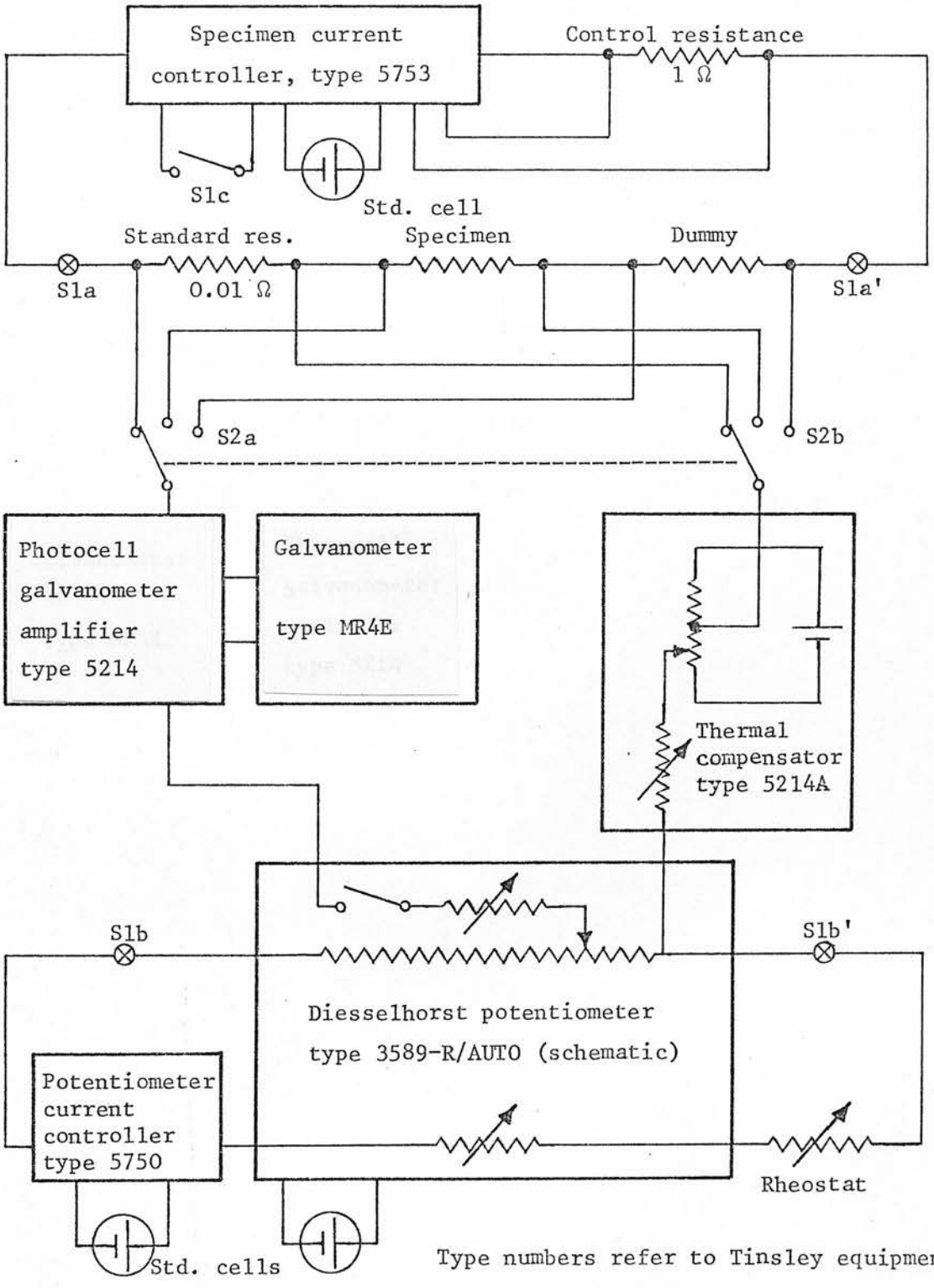

Switch contacts S1a and S1a' are interchanged when current is reversed, simultaneously with contact S1b and S1b'; S1c is opened during reversal.

Fig. 3.31-1: Resistance measuring circuit

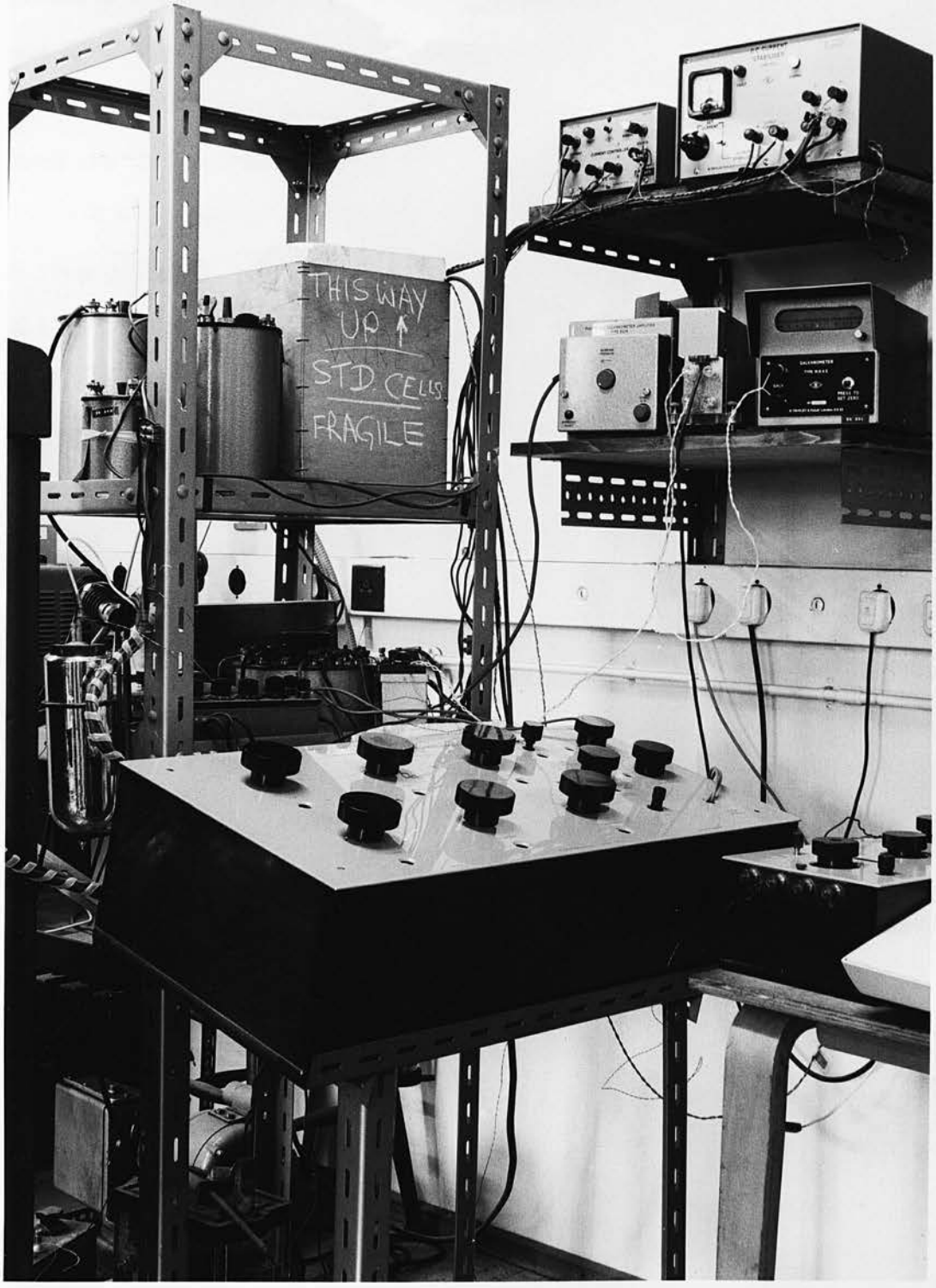

Fig. 3.31-2: Apparatus for resistance measurement

provided a bench-mounted welding head with controlled welding pressure, and also a pair of hand-held welding tweezers which were very convenient for attaching leads after the specimen had been mounted into the deformation apparatus.

A weld energy of 25J was found satisfactory for attaching 0.15mm diameter (38swg) copper wire to 2mm diameter zinc crystals. A formula for the optimum ratio of diameters for satisfactory spot welds between wires of two different metals is given by Strong (1938), but this gives a diameter of 1.08mm copper for attachment to 2mm diameter zinc, and such a thick copper lead would cause too much damage. The copper wire did not appear to fuse with the zinc in most cases, but microscopic observation showed it to be firmly embedded in the surface. The diameter of copper wire used was chosen as small enough not to damage the specimen too much and large enough not to have too high a resistance and thus reduce measurement sensitivity. The wires were continuous from the specimen to clamped copper connections at room temperature at the top of the stretching jig, passing through a multiple tubular glass to metal seal in the cryostat cap. For tests with 1mm diameter specimens short lengths of thinner wire were attached to the specimen and then connected to the main potential leads with spot welds or solder. The use of potential leads of the same material as the specimen was considered but was decided unnecessary; all the connections between zinc or cadmium and the copper leads would have to be kept at the same temperature to avoid thermal e.m.f 's, and since the specimen was at a uniform temperature it was more convenient to make the connections there. Fracture did not usually occur at the point of lead attachment.

3.33 Sensitivity of resistance measurement

Because scatter in the experimental points is an important factor in limiting the analysis which can usefully be done on the final results, it is probably worth describing here, in rather more detail than would otherwise be appropriate, possible causes of this scatter and the steps taken to remove it.

The sensitivity of the galvanometer amplifier and secondary galvanometer was usually adjusted to give a deflection of 50mm for a potential change of 100nV. By interpolation on the galvanometer to the nearest 5mm, readings were taken to 10nV. This was about 0.003% of the potential across the specimen. The resistance of the Diesselhorst potentiometer is not affected by the setting of its dials, so this sensitivity was constant at all settings. Greater sensitivity was possible, but was not justified by the stability of the voltages being measured. This instability could have arisen from

(i) Variation in current in the specimen or the potentiometer.

(ii) Variations in thermal e.m.f's in the potential circuit.

(iii) Induced e.m.f's from external electromagnetic fields.

3.34 Current stability

The potentiometer current stability was checked against a standard cell, and the specimen current was checked against the potentiometer by monitoring the voltage across the standard resistance in the specimen circuit. Before the 1A current controller was acquired, the specimen current stability was the limiting factor in the accuracy of the measurements, and various attempts were made to improve it. The major steps were

(i) The use of a large capacity lead-acid accumulator (Chloride Batteries type YCG33, 400 ampere-hour capacity).

(ii) The use of a resistance network based on the arrangement suggested by Gerritsen (1956). This is shown in Fig.3.34-1. The best stability obtainable from arrangements (i) or (ii) was 1 in 10^4, and this performance was rather unpredictable.

(iii) The use of a feedback arrangement based on a Sefram "Graphispot" recording galvanometer (Fig.3.34-2). This instrument consists of a sensitive light-spot galvanometer and a separate chart recorder built into the same case. The pen carriage of the recorder is fitted with a photocell assembly which controls a servo motor to move the pen to follow movements of the light spot from the galvanometer. A slider on the pen carriage is in contact with a linear resistor which extends across the whole width of the scale, so that a voltage proportional to the spot deflection can be obtained. This voltage was fed into the base circuit of a power transistor in series with the specimen and thus controlled the specimen current. The galvanometer was connected as shown to respond to any differences in voltage between a standard resistance in the specimen circuit and a standard cell.

This arrangement proved fairly satisfactory and could give a stability of 5 in 10^5 when working at its best, but it was difficult to adjust to maintain this sensitivity. It was also rather susceptible to drift due to changes in the 120V battery used across the linear resistor.

(iv) A current controller designed for the job was eventually purchased. This is a Tinsley type 5753, and works on the same principle as the Sefram arrangement described in 3, except that the photocell voltage is fed back electrically without the need for moving parts. A similar instrument (Tinsley type 5750) was purchased to control the potentiometer current. To avoid vibration, the two current controllers were installed, with the galvanometer amplifier and indicating galvanometer, on shelves fixed to a main wall of the building. This apparatus gave an overall current stability of ± 2 in 10^6, as measured by making a continuous measurement of

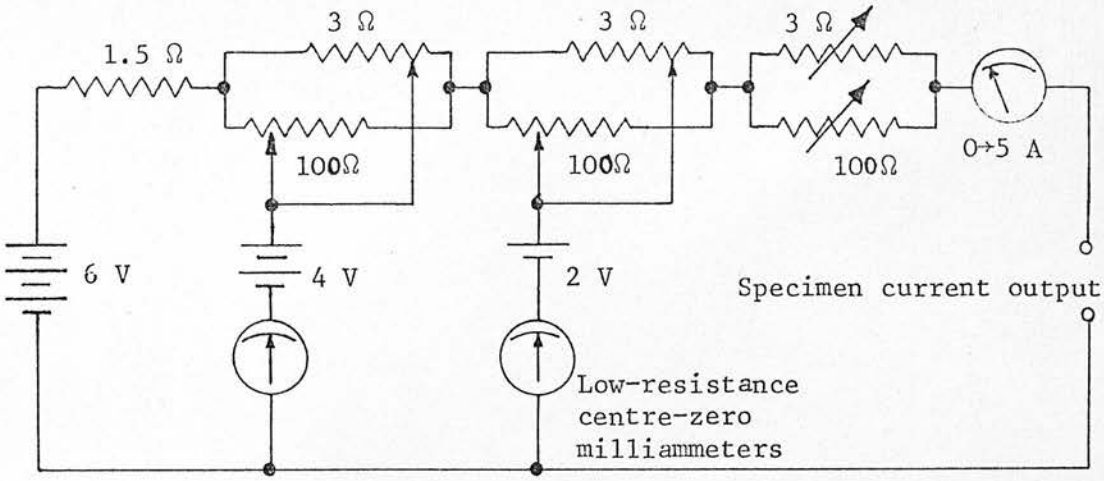

Fig. 3.34-1: Current stabilising circuit after Gerritsen (1956).

The tappings on the variable resistances are adjusted so that when the correct specimen current is flowing it is supplied entirely by the 6 V cell. The 4 V and 2 V cells counteract any variations in the current.

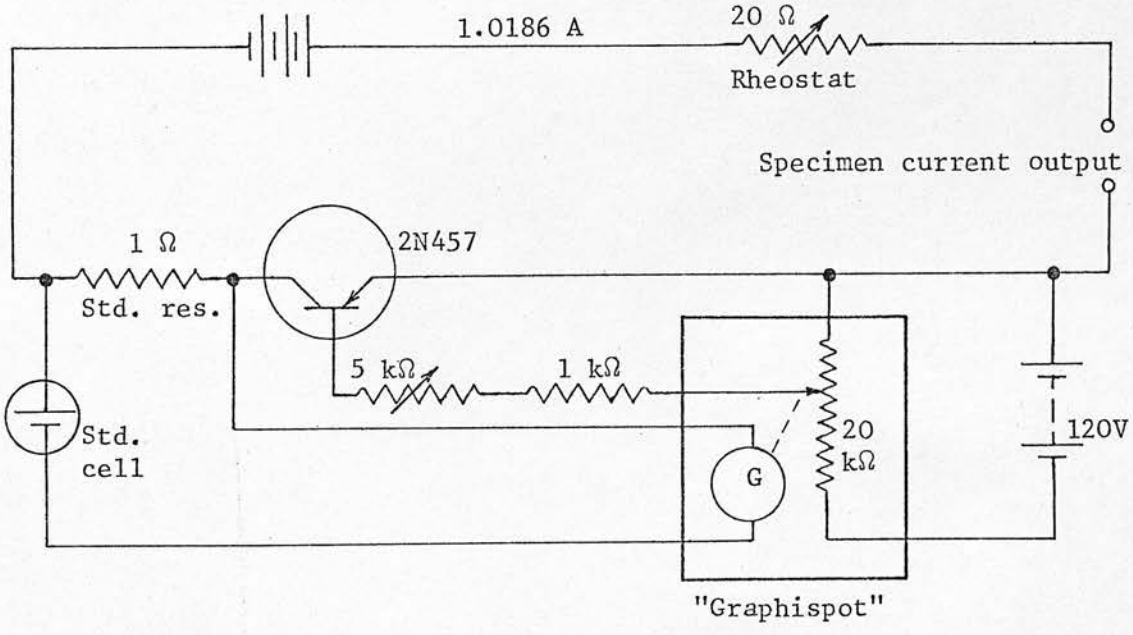

Fig. 3.34-2: Current stabilising circuit using Sefram "Graphispot" spot-follower recording galvanometer. The position of the tapping on the 20 kΩ potentiometer is controlled by the light beam from the galvanometer, G.

the voltage across the standard resistance for times of at least 20 minutes (Fig.3.34-3a).

3.35 Thermal e.m.f's

The remaining fluctuations may have been caused by varying thermal e.m.f's or by variations in temperature. Thermal e.m.f's in the galvanometer circuit were balanced out by injecting a small voltage from a Tinsley thermal compensator, type 5214A. Those in the specimen circuit were generally about 0.1 to 0.2 μV, and were allowed for by repeating each measurement with the current reversed.

The difference in thermal e.m.f. between the two pairs of specimen voltages in each set of readings (see Section 3.38) averaged 0.035 μV over 16 sets. With a specimen voltage of about 350 μV this represents a fluctuation of ±0.005%, which is half of the total fluctuation. To check whether the variation arose at the specimen or at the switches and connections in the circuit outside the cryostat, the thermal e.m.f. across the specimen was monitored with no current flowing. It was found to vary within ±0.01 μV, or 0.003% of the voltage produced across the specimen by the measuring current. Manipulating some of the switches produced additional fluctuations of about the same size. Expanded polystyrene was used to protect the apparatus from draughts; the switches were cleaned and lubricated, and were rotated several times at the beginning of each day's measurements and subsequently, but it was not possible to reduce the spurious voltages below the figures quoted above. The reversing switch was fitted with a contact intended for wiring in series with the galvanometer to open its circuit just before and close it just after the current

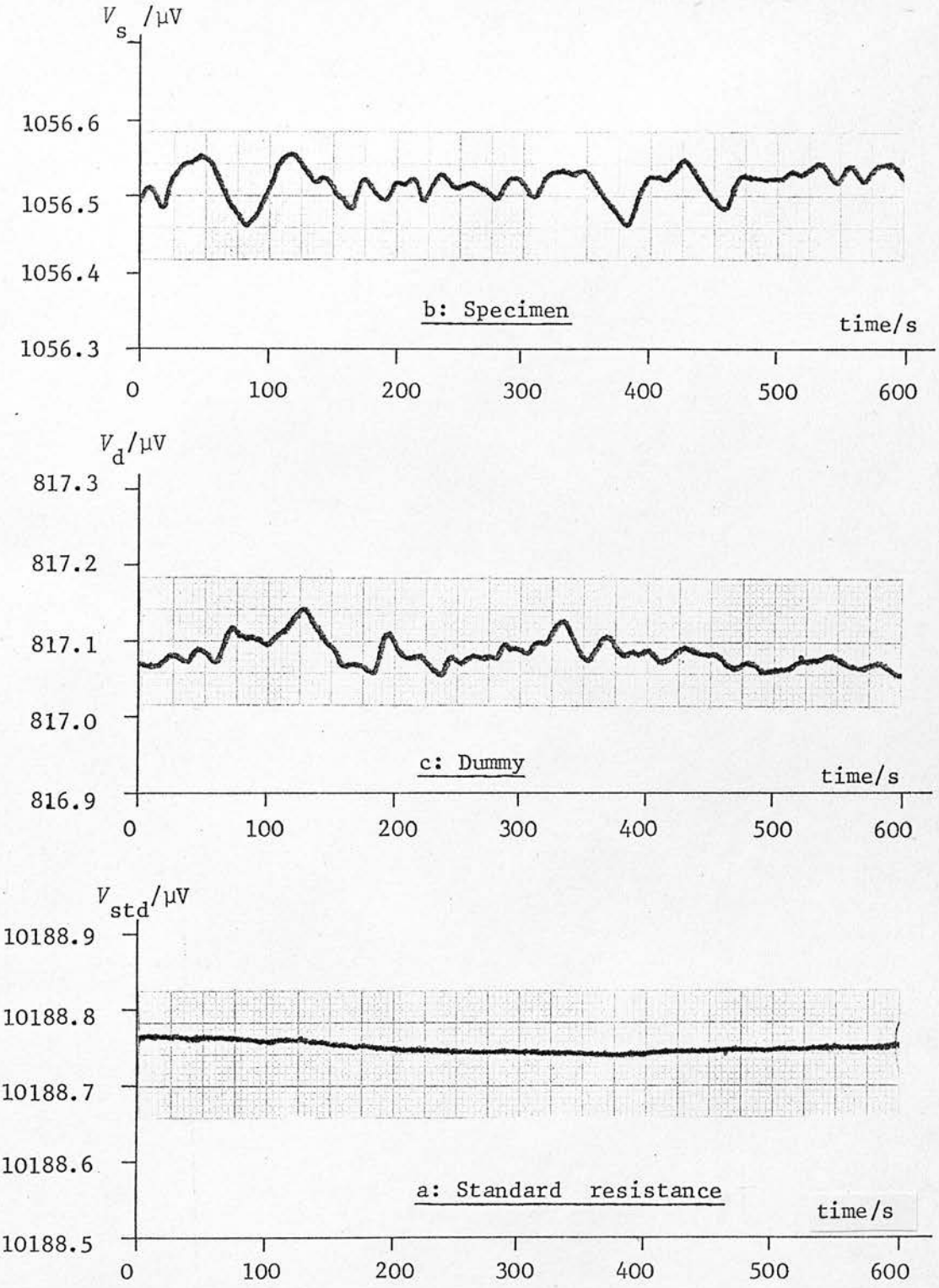

Fig. 3.34-3: Stability of voltage measurements

was reversed, thus avoiding large deflections due to surges. This contact (S1c in Fig. 3.31-1) was instead wired so as to interrupt the feedback circuit of the specimen current controller, thus avoiding it being sent out of balance when the current was reversed.

The possibility was considered that the current supplied by the controller might be slightly different after being reversed, but this can be ruled out because the fluctuations in the potential across the standard resistance were the same size as those across the specimen, although the actual potential itself was thirty times greater.

3.36 Induced e.m.f's

It is difficult to separate the effect of these from the effect of thermal e.m.f's, and both are included in the size of the fluctuations quoted above. Precautions were taken to reduce them as far as possible by using screened connections, twisting pairs of wires together to avoid loops, and connecting metal cases of apparatus to a common earth

3.37 Variations in specimen temperature during resistance measurements

Fluctuations in the temperature of specimen and dummy would show as fluctuations in voltage across them when the specimen current is flowing. Such fluctuations are shown in Fig. 3.34-3, b and c, and are about ±0.005%. Most of this is due to the thermal e.m.f fluctuations discussed above, but up to about ±0.003% may be due to short-term fluctuations in specimen and dummy temperature. The temperature coefficient of resistivity of cadmium is 1.6% K^{-1} at 80 K (Meaden 1965), so fluctuations of this size correspond to temperature variations of about 2 mK.

The long-term drift in temperature is negligible over the time

required to take a set of readings, about four minutes. Since the ratio, r, of specimen voltage to dummy voltage is required, fluctuations in these two measurements can add; a set of ten measurements of r was distributed about its mean with a standard deviation of 0.006%. In experimental runs time did not permit each resistance measurement to be repeated ten times, although it was usually repeated three times. The mean of a sample of three was calculated, using Student's t, to lie within ±0.015% of the mean of the population, at a 95% confidence level. (Brinkworth 1968, pp. 36-40).

Steady drift or constant deviation from the nominal temperature is taken account of in the method of analysing the readings (section 3.38).

3.38 Procedure for taking resistance readings

In order to allow for slight drifts in temperature or current, each measurement of resistance was made from a set of ten readings, taken at uniform time intervals in the following order:

1	V_{std}	D
2	V_{std}	R
3	V_s	D
4	V_s	R
5	V_d	D
6	V_d	R
7	V_s	D
8	V_s	R
9	V_{std}	D
10	V_{std}	R

V and R represent potentials and resistances, with suffixes "std", "s"

and "d" standing for "standard", "specimen" and "dummy" respectively. The symbols R and D in the third column show whether the current was flowing in the reversed or direct direction.

This symmetrical sequence ensures that if there is any uniform drift the means of the readings of V_{std} and of V_s will be the values these quantities would have had at the time of measurement of V_d. After this method had been in use for some time a lengthy justification of it by Spružil (1965) was found. The readings were entered at the time of taking into an electronic printing calculator (Friden model 1151) which was programmed to accept them in the above order and to print out the three ratios

$$R_s = \frac{(3) + (4) + (7) + (8)}{(1) + (2) + (9) + (10)}$$

$$R_d = \frac{2 \times [(5) + (6)]}{(1) + (2) + (9) + (10)}$$

$$r = R_s/R_d$$

where the numbers in parentheses are the sequence numbers of the readings in the table on the preceding page. It was thus possible to check, and to plot a graph of, the values of the ratio r as the readings were taken, so that any doubtful or interesting values could be confirmed by a repeated reading if necessary.

The potential across the standard resistance, V_{std}, was constant by at least an order of magnitude better than V_s and V_d, and it was therefore omitted from some sets of readings when time was limited. It was still checked regularly, however, and the temperature of the standard resistance was noted so that corrections could be applied. The temperature coefficient of resistance of the standard resistance was $1.7 \times 10^{-5} K^{-1}$.

3.39 Calculation of resistivity changes from resistance measurements

The resistivity due to defects has to be calculated from measured values of the resistances of the specimen and the dummy before and after annealing. This may be done as follows:

Let the resistances before annealing be

specimen: $R_s = R''_s + \Delta R_s$

dummy: R_d

ratio: $r = R_s/R_d$

and after annealing

specimen: R'_s

dummy: R'_d

ratio: $r' = R'_s/R'_d$

ΔR_s is the part of the specimen resistance which is due to defects and R''_s is the resistance the specimen would have if the defects could be removed without causing any other changes, so that

$$\Delta R_s = R_s - R''_s \qquad (3.39\text{-}1)$$

We do not know the value of R''_s, but we suppose that during the annealing process it underwent the same changes as R_d, so that

$$\frac{R''_s}{R'_s} = \frac{R_d}{R'_d}, \text{ giving } R''_s = R'_s \cdot \frac{R_d}{R'_d} \qquad (3.39\text{-}2)$$

The dummy was chosed to be as similar as possible to the specimen and underwent the same treatment, so that they would be affected equally by changes due to thermal strain or differences in measuring temperature before and after annealing. (See section 4.41).

Now substituting R''_s from (3.39-1) into (3.39-2), we get

$$\frac{\Delta R_s}{R'_s} = \frac{R_s}{R'_s} - \frac{R_d}{R'_d} = \left(\frac{r}{r'} - 1\right) \frac{R_d}{R'_d}$$

If we assume that the shape of the specimen does not alter during annealing, we can put $\Delta R/R'_s = \Delta\rho/\rho$, where $\Delta\rho$ is the resistivity due to defects and ρ is the resistivity of the annealed specimen. Thus finally

$$\frac{\Delta\rho}{\rho} = \left(\frac{r}{r'} - 1\right) \frac{R_d}{R'_d}$$

This is similar to the expression derived after much detailed analysis by Sprušil (1965). Other workers have published alternative procedures for the analysis of resistivity changes (Rider and Foxon 1966; Míšek 1970, 1971) but these depend on measurements of resistance at two different temperatures and assume that the resistivity due to defects is the same at both, i.e. that Matthiessen's rule holds and that the defects do not anneal out (Dimitrov 1968). To avoid annealing of defects in cadmium and zinc deformed at 78 K, the two temperatures would have to be at 78 K and below. These alternative methods do not appear to have any great advantages over the one outlined above, for the present work.

An analysis of changes in $\Delta\rho$ does not require an accurate determination of ρ, since $\Delta\rho$ is always measured relative to the same value of ρ. An approximate value is most conveniently found by measuring the resistances of the annealed specimen at 293 K and 78 K and assuming that the room temperature resistivity is that given in the literature. In this way ρ at 78 K was found to be 16.3 nΩm for cadmium and 11.6 nΩm for zinc.

Changes in $\Delta\rho$ are required in analysing annealing stages rather than $\Delta\rho$ itself, and ρ, r' and R'_d are treated as constants throughout an annealing run. The uncertainty of $\Delta\rho$ is then mainly determined by the uncertainty of $\left(\frac{r}{r'} - 1\right)$, i.e. of $(r - r')/r'$. Since $r' \sim 1$,

and $R_d/R'_d \sim 1$, the absolute error in $\Delta\rho/\rho$ is about the same as the absolute error in r, ±0.00015 (0.015%) for 95% confidence (section 3.37) or an absolute standard deviation of 3.5×10^{-5}. The standard deviation of the difference between two values of $\Delta\rho/\rho$ will then be $\sim 5 \times 10^{-5}$. The differences between values of $\Delta\rho/\rho$ vary between 2×10^{-3} and zero, so the fractional standard deviation is 2.5% upwards.

If the value of ρ for cadmium is taken as 16.3 nΩm, an error of ±0.015% in $\Delta\rho/\rho$ corresponds to an absolute error in $\Delta\rho$ of 2.4 pΩm.

3.4 Temperature measurement and annealing

3.41 Temperature measurement

The temperature of the specimen and dummy was measured with a copper-constantan thermocouple spot-welded to the dummy at a point about one third of its length from one grip. If there was any variation in temperature along the length of the dummy (or the specimen) due to heat transfer to or from the grips, a point of attachment lying between the middle of the specimen and one grip would give an approximate mean value.

The thermocouple wires used were 36 s.w.g. copper and constantan, supplied by The Saxonia Electrical Wire Co. Ltd. E.m.f.-temperature tables used were those given in BS 1828:1961 (1961). The thermocouples were calibrated at the boiling point of liquid oxygen, as recommended in BS 1828, and an appropriate correction was applied to the tables. Repeated measurements of thermocouple e.m.f. in the calibration bath were reproducible to within ±1 μV, corresponding to an uncertainty in temperature measurement of ±0.05 K. Additional calibration points used as a check were the sublimation point of CO_2 (Scott 1941) at 194.64 K, and the boiling point of Freon 13 (191.8 K). The reference junctions of thermocouples were kept in a flask of crushed melting ice.

For temperatures above 273 K a mercury-in-glass thermometer was used in the liquid bath as well as a thermocouple, and a low temperature liquid-in-glass thermometer was used in the range 200 K to 273 K as an additional check.

3.42 Choice of type of cryostat for annealing

Two types of annealing experiment were to be carried out; isothermal and isochronal pulse annealing. In order that the results

might be easily interpretable, it was desirable that the following sequence of events should be followed as closely as possible:

a) After deformation, the specimen should be maintained at a temperature T_0 low enough to prevent migration of the defects of interest, and constant enough for there to be no significant fluctuation in temperature between the times of measuring the resistance of the specimen and measuring the resistance of the dummy. The sequence of resistance measurements allows for any small constant drift in temperature.

b) The temperature of specimen and dummy should be raised instantaneously to the required annealing temperature, T_a, maintained there for a predetermined time, and then returned instantaneously to the measuring temperature T_0.

c) It should be possible to repeat steps a) and b) as often as required, the temperature T_a either being the same on each repetition (isothermal pulse annealing) or set to a different predetermined value each time (isochronal pulse annealing).

Two main types of cryostat have been used in the temperature range between the boiling point of liquid nitrogen and room temperature; both types were investigated in order to choose the most appropriate one for the present work.

"Pool" type cryostats. (e.g. Scott 1941; Peiffer and Stevenson 1963)

In this type the specimen is isolated from a pool or reservoir of cryogenic fluid, usually liquid nitrogen, by a space filled with a gas. The pressure of the gas may be varied so as to adjust the rate of heat exchange between the specimen and the fluid. A specimen heater is usually provided, and in equilibrium this balances the heat lost through the exchange gas. A temperature sensor is connected to a

controller which adjusts the heater supply to maintain the required temperature. Sometimes a current is passed through the specimen to make it act as its own heater.

"Continuous flow" cryostats. (e.g. Wessel 1957; Huber 1969)

In this type there is no reservoir of liquid inside the cryostat, but instead the specimen is held in a continuous stream of cold liquid or gas, supplied from an outside reservoir. The temperature of the stream is controlled externally to maintain the correct specimen temperature.

Some preliminary experiments were done using the continuous flow principle, but it was not found possible to produce rapid changes in temperature because of the low heat capacity of the nitrogen liquid or gas used as a fluid. The rate of heating found on blowing nitrogen or air at room temperature on to the cold specimen from a perforated spiral tube surrounding it was only 1.2 K s^{-1}. The rate of cooling, on pumping liquid nitrogen through the tube, was about 4 K s^{-1}. While these rates could undoubtedly have been improved if the apparatus had been developed further, it was thought unlikely that they could be made large enough to avoid unacceptable uncertainty in the times of annealing pulses lasting a few minutes and involving temperature changes of 100 K or more. Another drawback of the continuous flow cryostats was that they cannot usually hold temperatures constant to better than about ±0.5 K (Huber 1969). While this would have sufficed for the annealing pulses, random fluctuations of this magnitude would have introduced errors of 0.8% in measurements of resistance, which is too great (see section 3.37). It would therefore have been necessary to use a liquid bath for resistance measurements, and the combination

of the two types of cryostat would have complicated the apparatus considerably.

3.43 Annealing apparatus

The cryostat constructed for an annealing bath was therefore of the pool type, and is shown in Fig. 3.43-1. It consists of two concentric double-walled vessels, the inner one fitted with a pumping connection, the outer one evacuated and sealed. The space between the two vessels was filled with liquid nitrogen, and the inner vessel held the temperature bath fluid. For the temperature range 92 K to 192 K Freon 13 was used; from 185 K to room temperature methylated spirits was used. Section 3.44 below deals with the choice of a bath fluid.

The inner bath was fitted with a stirrer, consisting of a stainless steel tube, 27 mm diameter, inside which was fitted a stainless steel shaft bearing two propellers (Fig. 3.43-2). The shaft rotated in three Glacier "DU" bearings (made of porous bronze impregnated with a mixture of p.t.f.e. and lead) mounted at each end and at the centre of the tube, and it was driven at 1400 r.p.m. by a belt from an external electric motor. The action of the propellers was to pump fluid up the tube, sucking it in at the bottom and discharging it through three ports just above the surface. In this way thorough circulation was effected. This design of circulation system is similar to one used at the National Bureau of Standards (Scott 1941). On the outside of the tube a heating element of Nichrome tape was wound non-inductively; its resistance was 10 Ω at room temperature.

Current for the heater was provided from a Kingshill power

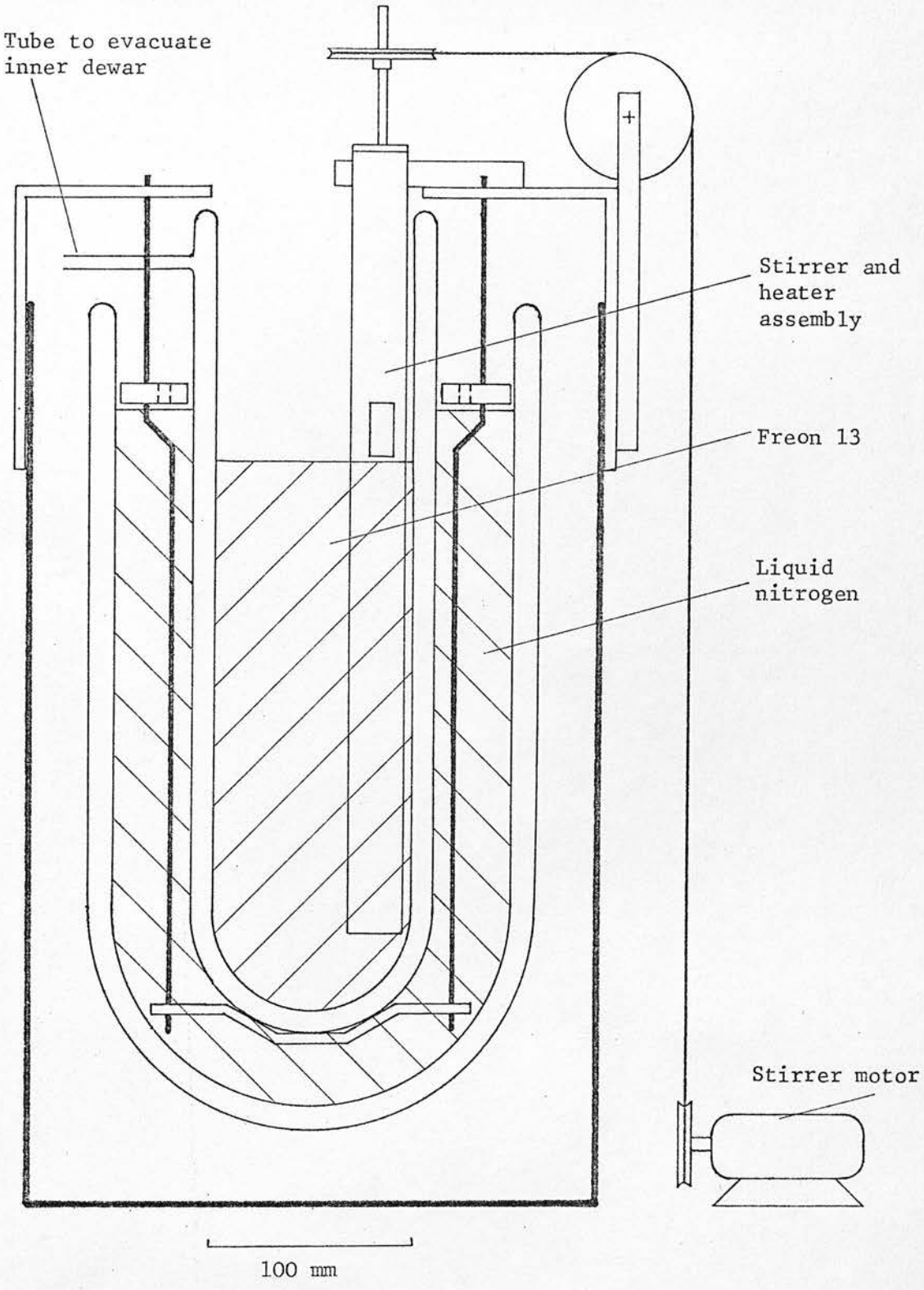

Fig. 3.43-1: Annealing bath cryostat

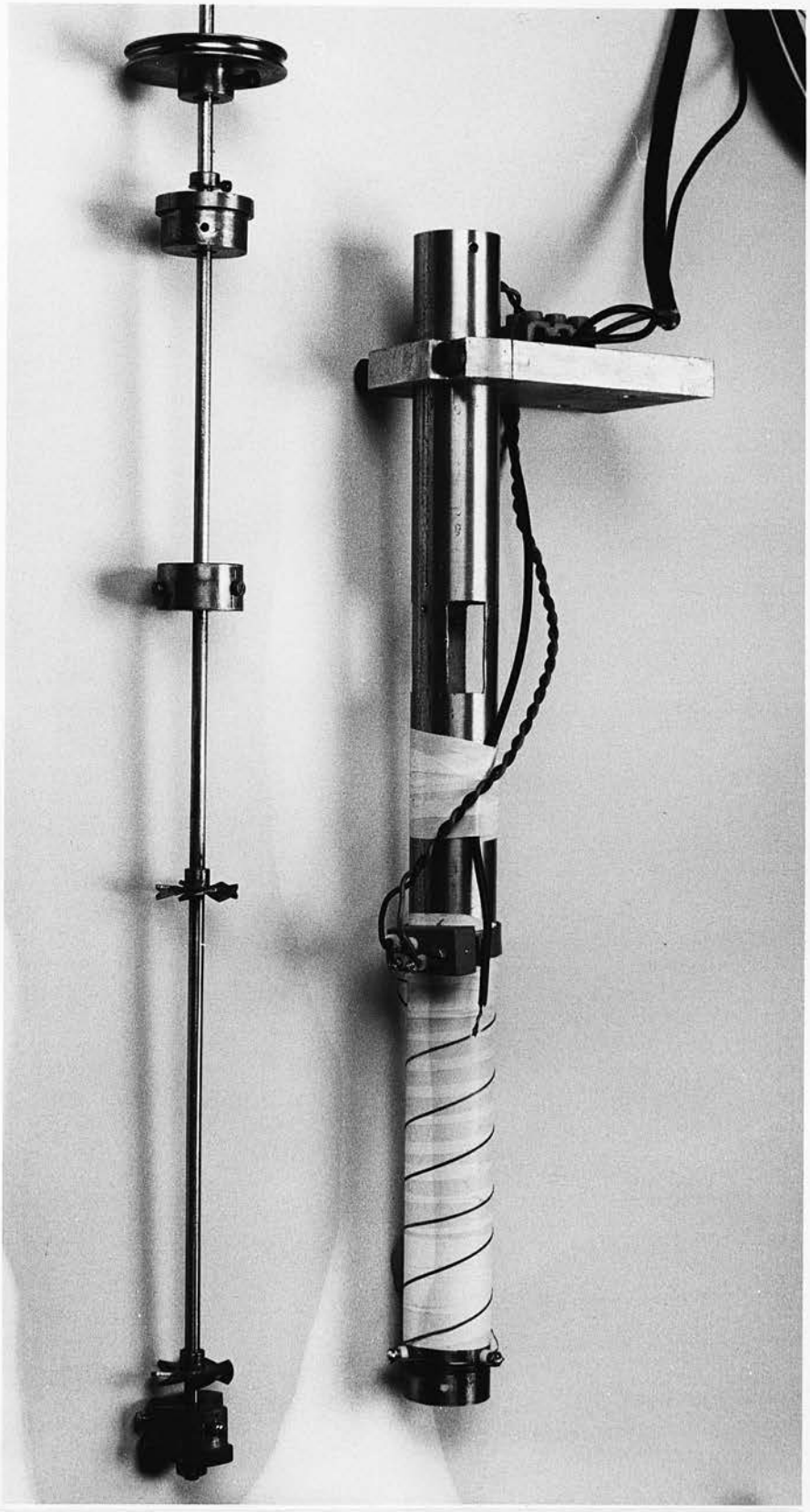

Fig. 3.43-2: Stirrer and heater assembly for annealing bath

supply, type S505, which gave up to 250 W (50 V at 5 A). The heat capacity of the bath when containing 2 litres of fluid was about 5000 J K^{-1}, so the maximum heater input gave a rate of temperature rise of 0.05 K s^{-1}. It thus took about 200 s to change the temperature by 10 K from one annealing temperature to the next. The heat capacity of the specimen, dummy and the jig which held them was estimated from their cooling effect on the bath liquid to be about 67 J K^{-1}, so it was necessary to set the bath temperature about 1 K to 2 K above the desired annealing temperature.

The temperature of the bath was controlled by a Transitrol type 991F controller, using a copper-constantan thermocouple as a sensing element. This controller could switch a bypass rheostat into parallel with the heater if the temperature was too high. As the controller was designed to control temperatures above 300 K, it was necessary to reverse the polarity of the thermocouple connections; the calibrated temperature scale of the controller could not then be used, so the actual controlled temperature was measured and set using another calibrated copper-constantan thermocouple. The temperature uniformity throughout the bath depended on the temperature being controlled; at worst, near the freezing point of alcohol where the increased viscosity reduced the effectiveness of the stirring, variations in temperature from one part of the bath to another did not exceed 0.25 K. The temperature was constant with time to within ±0.4 K.

The pressure of gas in the space between the walls of the inner dewar was varied according to the desired temperature: for temperatures above about 150 K the space was evacuated, but when more cooling was needed a little air was admitted.

3.44 Choice of temperature bath fluid

The requirements for a suitable fluid or set of fluids are

a) At least one of the fluids used must be liquid at the lowest annealing temperature to be used, and at least one must be liquid at the highest temperature.

b) The liquid range should be as large as possible, to avoid having to use several different fluids.

c) The liquid and any vapour given off should be, if possible, non-inflammable and non-toxic.

d) The liquid and its vapour should not react adversely with any of the materials with which it might come into contact.

e) The specific heat capacity of the liquid should be as large as possible.

f) It should be fairly readily available at reasonable cost.

The first of these requirements is the most important, and Fig. 3.44-1 shows the liquid ranges of various possible fluids. From this it can be seen that no one fluid can cover the whole range from 78 K to 293 K, the nearest possibility being Freon E1, with a liquid range of 118 K to 313 K. This has the great advantage of being a liquid at room temperature, and therefore easily handled, but it was thought necessary to obtain some annealing points at temperatures below 118 K, so another fluid would have to be used with it for these points. In any case, Freon E1 is expensive, costing £28.40 per litre.

The fluids chosen were therefore Freon 13 for the range 95 K to 190 K and ethanol (in the form of industrial methylated spirits, which is >90% ethanol) for temperatures above 190 K. The main alternatives to ethanol were Freon 114B2, which is expensive and has a higher freezing point, and the NBS mixtures, which produce corrosive substances

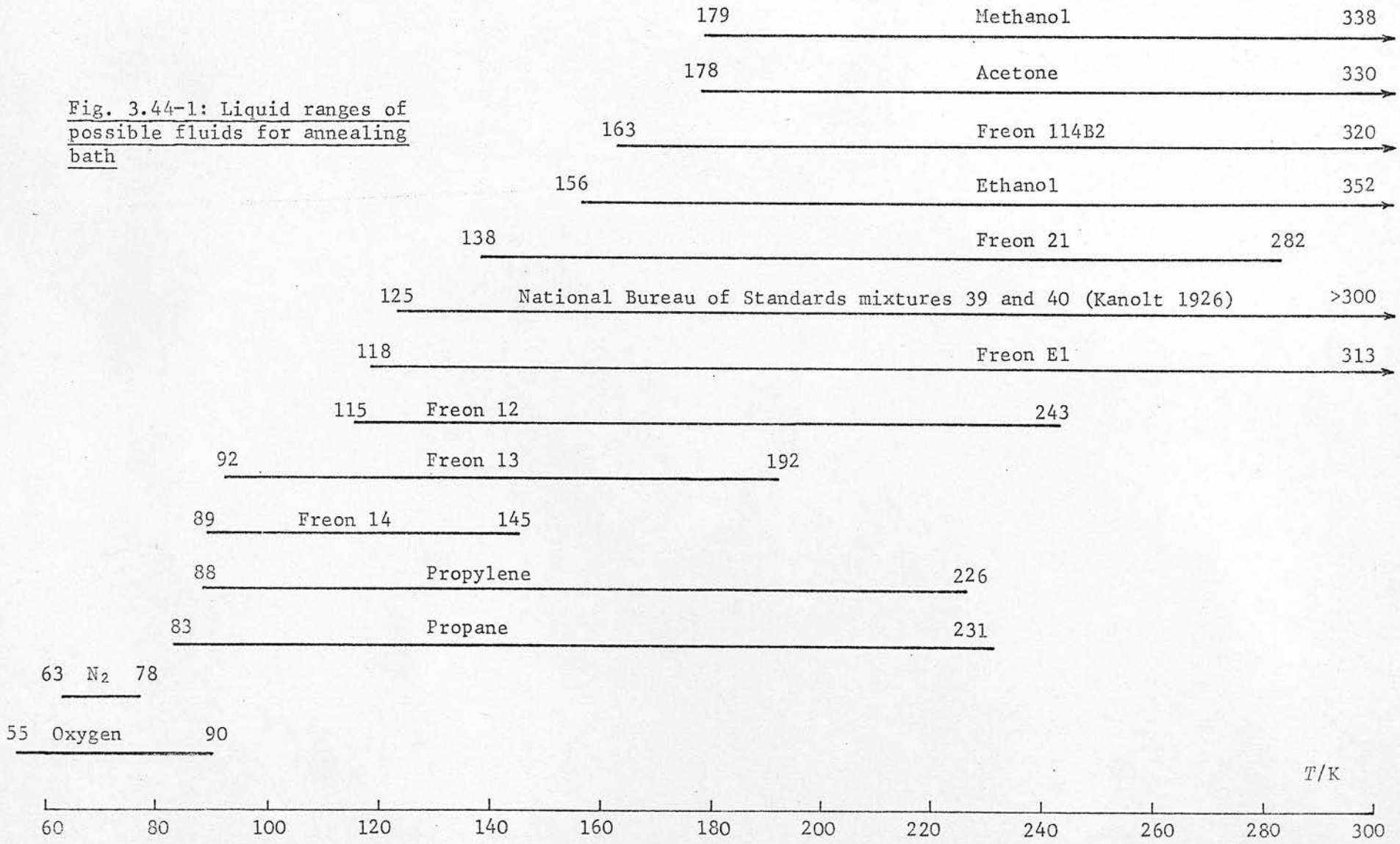

Fig. 3.44-1: Liquid ranges of possible fluids for annealing bath

by oxidation when exposed to air. Propane and propylene were rejected because of the danger associated with their volatility and inflammability. The viscosity of ethanol became rather large at the lower end of its temperature range, and in addition to making it more difficult to stir this made a greater quantity remain on the specimen jig when it was transferred back to the liquid nitrogen bath, possibly creating strains when it froze. Replacing ethanol by Freon E1 would have been an improvement; the kinematic viscosity of Freon E1 is about a tenth of that of ethanol at 200 K.

Freon 13 has a vapour pressure of about 3.4 MPa (500 lbf in^{-2}) at room temperature and was condensed into the cryostat by making it flow through a copper coil immersed in liquid nitrogen. It was found possible to return it to a storage cylinder after use by cooling an empty cylinder in liquid nitrogen and pouring the Freon in through a funnel attached to the valve outlet.

3.45 Temperature pulses

The temperature of the specimen was monitored throughout each pulse by recording on an ultraviolet chart recorder either the output from the thermocouple welded to the dummy specimen or the potential across the potential leads of the specimen itself, thus making it act as its own resistance thermometer. Typical pulses are shown in Fig. 3.45-1.

The pulses departed from the ideal rectangular shape in two respects: the rise and fall times were not negligible, and in the case of low temperature anneal using Freon 13 a spike appeared on the end of the pulse as the specimen was transferred back into the liquid nitrogen bath. To correct for these effects, each pulse was divided into a number of sections (about six in most cases) which could be

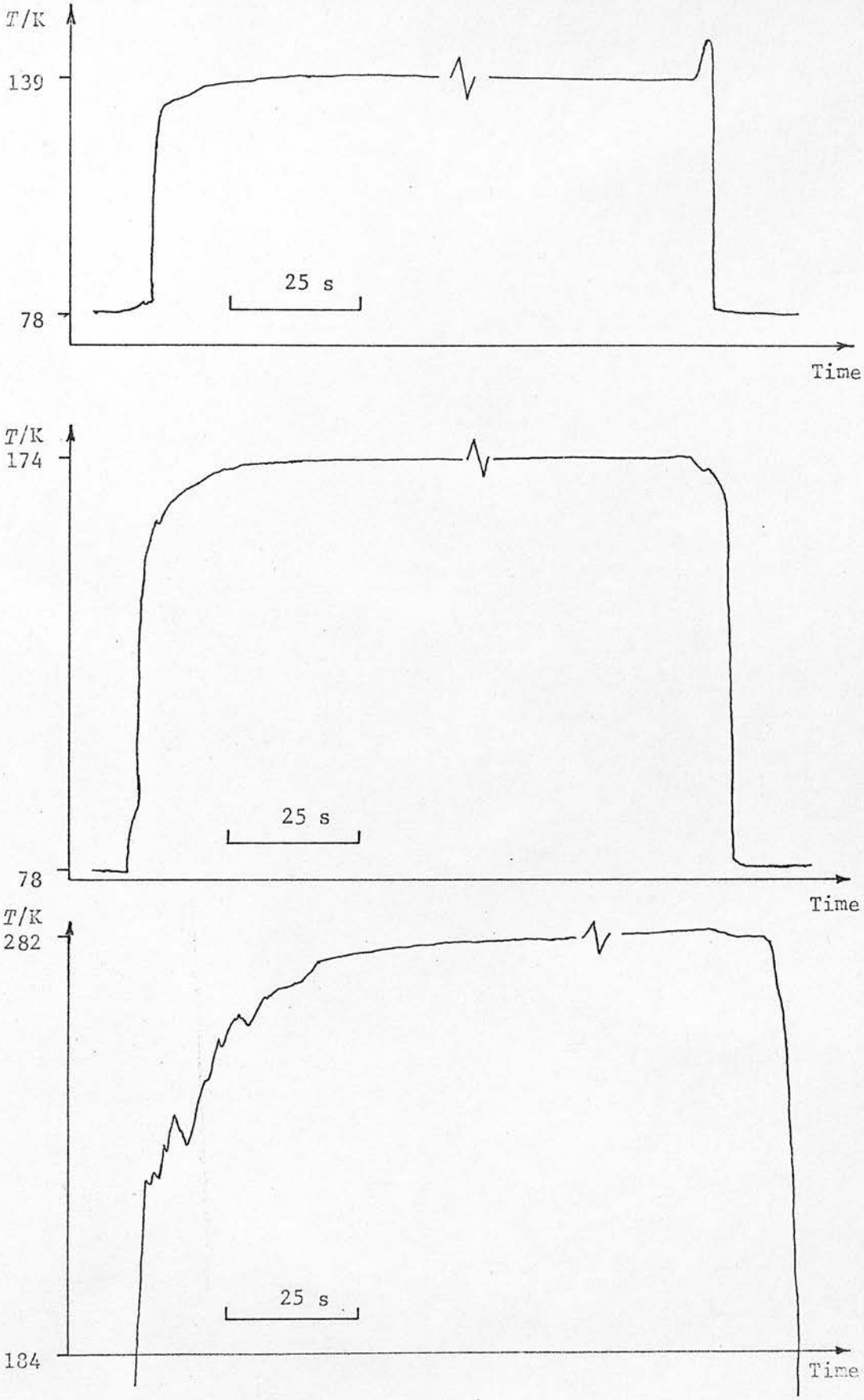

Fig. 3.45-1: Annealing pulses

approximated by straight lines, and a computer calculation was then carried out to find the length of the equivalent rectangular annealing pulse at the required temperature. The calculation assumed that a time t_1 at a temperature T_1 was equivalent to a shorter time t_2 at a higher temperature T_2, and vice versa, using the relationship

$$\frac{t_1}{t_2} = \exp \frac{E^m}{k} \left(\frac{1}{T_1} - \frac{1}{T_2}\right) \qquad (3.45\text{-}1)$$

This involves the assumption that a single annealing process occurs at both temperatures with the same activation energy E^m - an assumption which is valid only, if at all, for small temperature differences. Efforts were made, therefore, to keep the pulses as square as possible by rapid transfers of the jig between baths. It would have been an improvement to use larger annealing baths; not only would this make transfer easier, but also the larger heat capacity would reduce the temperature change produced by inserting the cold specimen.

A preliminary analysis of the results was carried out using an estimated value of E^m and the energy values obtained from this were used in a subsequent analysis. Further iterations did not produce significant changes in the values of E^m obtained.

At low temperatures, where the correction for the spike was predominant, the time correction was up to +20s; at higher temperatures, where the correction for the finite rise and fall times was more important, the correction was about -10s.

The accuracy of the values of corrected annealing time depends on the accuracy with which time and temperature could be read off the recorded pulse. Time could be read to ±0.5 s, and could have been made more accurate by increasing the speed of the recorder chart. A potentiometer was used to back off part of the potential and allow greater sensitivity in the measurement of temperature, which could be read to ±0.1 K; if

E^m is taken as 0.2 eV this leads to an uncertainty of 2% in the corrected value of t at 100 K calculated from (3.45-1). A corrected pulse time of 90 s was therefore uncertain to ±(0.5 +(0.02 x 90))s ~2.5 s. The absolue accuracy was determined by the thermocouple calibration, discussed in 3.41, and the speed of the recorder chart, which was derived from the mains frequency.

3.5 Measurements at liquid helium temperature

To try to improve the accuracy with which the resistivity due to defects could be measured, liquid helium was used on some occasions rather than liquid nitrogen as a temperature bath for resistance measurements.

The resistance of a typical monocrystalline specimen of Metallurgical Services' cadmium was 1500 μΩ at 293 K, 340 μΩ at 78 K and 1.04 μΩ at 4.2 K. Although the temperature-dependent part of the resistance was greatly reduced, it was found that the fluctuations in measured voltage mentioned in sections 3.35 and 3.36 were still present at about the same value as at 78 K. At liquid helium temperature they led to an uncertainty of ±0.5% in the ratio r. These fluctuations presumably arose in the measuring circuit and were not due to changes in the temperature of the specimen. Their effect would have been reduced if it had been possible to make a large increase in the current through the specimen, but the specimen current controller had a maximum output of 2 A. It would have been possible, however, to use the current controller in parallel with another source of current; an increase to at least 10 A would have been needed to be worthwhile. This was not done, because it was decided that the annealing procedure should first be developed using measurements at 78 K. For the reasons stated in

section 3.42, a pool type cryostat was used, and making resistance measurements at liquid helium temperature after each annealing pulse would have meant transferring the specimen twice for each measurement - first from the annealing bath to a liquid nitrogen bath, and then to the liquid helium bath. This would have been possible, and the temperature-time records show that the temperature would not have risen appreciably above 78 K during the second transfer, but the risk of mechanical or thermo-mechanical damage to the specimen would have been increased, and the consumption of liquid helium would have been fairly high: about 300 cm^3 were evaporated each time the specimen was put into the bath, and this was done about 60 times in an annealing run, so that over 20 litres of helium would have been required per run.

The use of measurements at liquid helium temperatures has, nevertheless, been shown to be practical, and the apparatus has been developed, so that a more extensive programme of measurements at that temperature would form a worthwhile project for future work. Other workers who have made measurements at 4.2 K in conjunction with annealing pulses in the range 78 K to 300 K (e.g. Vostrý et al. 1972; Coltman et al. 1971) have usually used a cryostat in which the annealing was performed in situ without removing the specimen. In these cases the specimen had to be heated by a heater, and the error due to the finite rise time of the annealing pulse could have been more serious. This error is not discussed by either Vostrý or Coltman.

4. RESULTS AND ANALYSIS

4.1 Defects produced by plastic deformation

The main purpose of the experiment was to look at annealing processes rather than production processes, so the production of defects was not analysed in detail. Initial measurements were made of the total defect production for a given strain, to check whether a sufficient change in resistivity had been produced for an analysis of its annealing behaviour to be carried out. Fig. 4.1-1 shows, as a function of strain, the amount of resistivity introduced by low temperature plastic deformation which anneals out at room temperature in polycrystalline cadmium. Also shown are the values of annealable resistivity obtained by Peiffer and Stevenson (1963), Stevenson and Peiffer (1964) and Simon and Delaplace (1972). Simon and Delaplace say that the resistivity increment was linear with strain up to 7% strain, and that in a specimen deformed 8%, 30% of the resistivity increment annealed out at room temperature. There is no direct evidence, then, for the line which has been drawn through their point and the origin, although they assume that the resistivity due to point defects and the resistivity due to dislocations are each separately proportional to strain.

The points from the present experiment on Fig. 4.1-1 are scattered within a range greater than the experimental error in each point. Most of the points were obtained from different specimens, and Schumacher (1970), referring to plastic deformation of cadmium, has said that "even numerically equal amounts of cold work on several specimens may involve a rather pronounced scatter in the electrical resistivity increase in certain temperature ranges and, more important, dissimilar

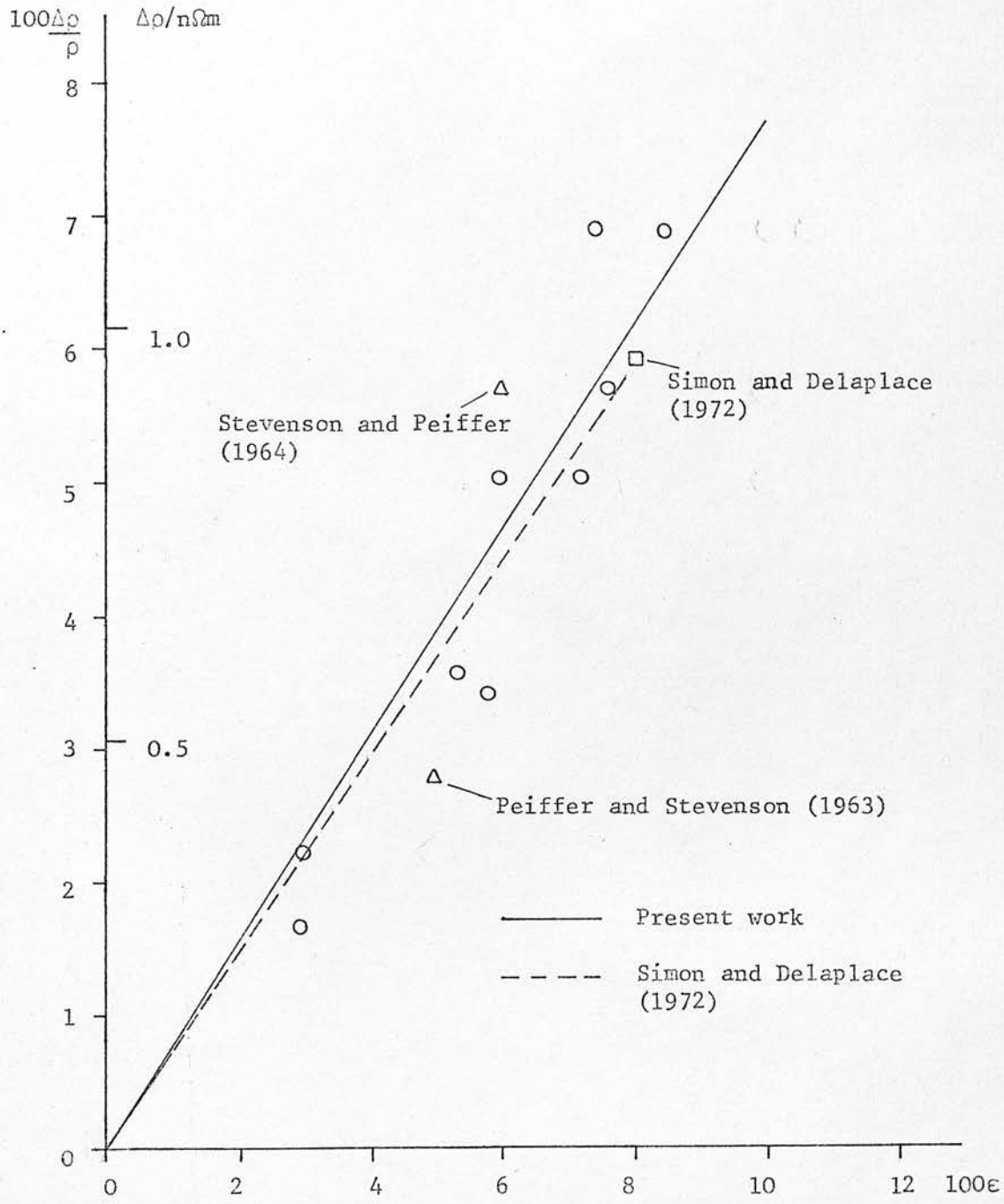

Fig. 4.1-1: Annealable resistivity increment in polycrystalline cadmium as a function of strain

Errors in the strain, ε, are about the same as the diameter of the circles drawn at each point; errors in $\Delta\rho/\rho$ are negligible on the scale of this graph.

defect distributions". A test was carried out to see whether the points obeyed a relation of the form

$$\frac{\Delta\rho}{\rho} = c\varepsilon^m$$

where c and m are constants. A graph was plotted of $\log_{10}(\Delta\rho/\rho)$ against $\log_{10}(\varepsilon)$, and a best straight line fit to the points gave the gradient $m = 1.1 \pm 0.3$ (Fig. 4.1-2). The increase of annealable resistivity with deformation is compatible with a linear relationship, and not with a $\frac{3}{2}$ power or quadratic law as is found in f.c.c. metals. The best straight line through the origin to fit the points on the graph of $\Delta\rho/\rho$ against ε had a gradient 0.77 ± 0.04, which gives the relationship

$$\Delta\rho/\rho = (0.77 \pm 0.04)\varepsilon$$

for strains up to 10%.

Since ρ was found to be 16.3 nΩm for cadmium at 78 K, the increment in resistivity can be expressed as (12.6 ± 0.7) nΩm per unit strain for strains up to 10%.

For the case of single crystals, the resistivity increments were much smaller than for polycrystals. Values obtained for zinc and cadmium are shown in Fig. 4.1-3. Most of the deformations shown for zinc crystals are around 1% to 2%; many attempts were made to obtain values from larger strains, but in most cases the specimen fractured during deformation. No conclusions can reasonably be drawn about the law of resistivity increase with strain, though it can be said that in most cases a deformation of 1 to 2% produces an annealable resistivity change of 0.1 to 0.2%, and that even for cadmium strained 15% the annealable resistivity was only 0.3%. One point for zinc gave a larger resistivity change, but the reason for its occurrence is not known - it may have been due to some imperfections in the crystal acting as sources for a greater number of defects.

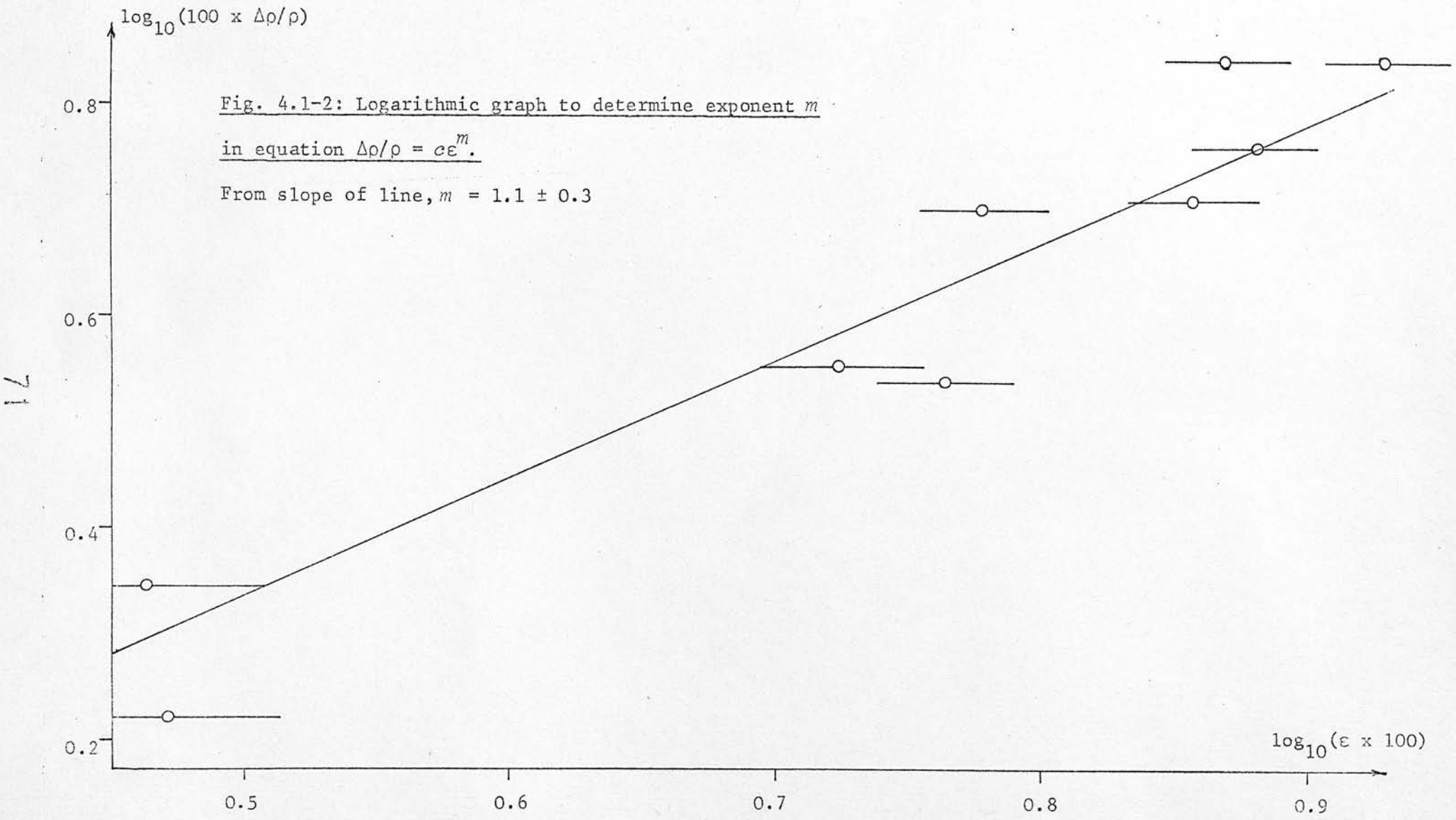

Fig. 4.1-2: Logarithmic graph to determine exponent m in equation $\Delta\rho/\rho = c\varepsilon^m$.

From slope of line, m = 1.1 ± 0.3

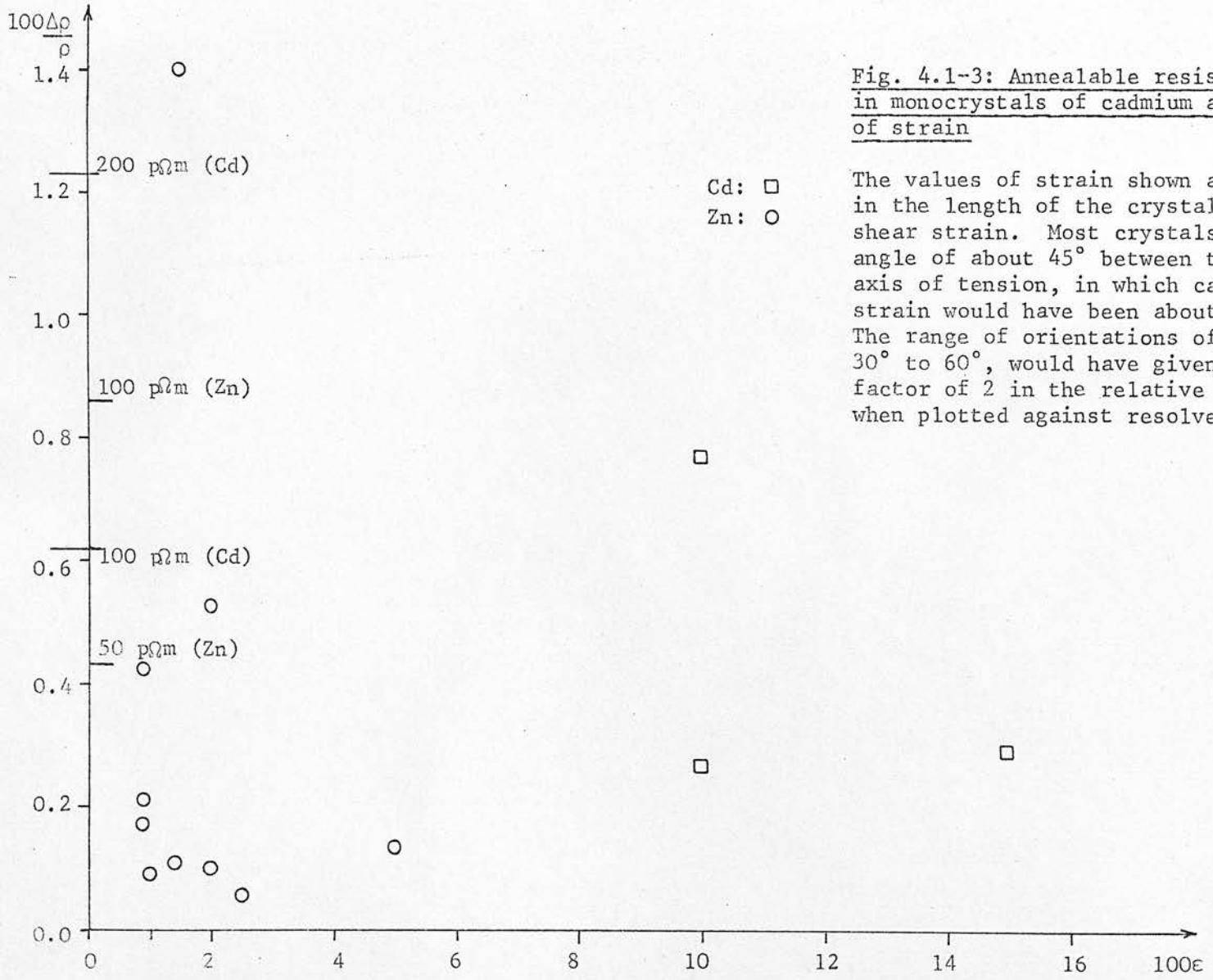

Fig. 4.1-3: Annealable resistivity increment in monocrystals of cadmium and zinc as a function of strain

The values of strain shown are macroscopic strain in the length of the crystal, and not resolved shear strain. Most crystals were oriented with an angle of about 45° between the glide plane and the axis of tension, in which case the resolved shear strain would have been about twice the linear strain. The range of orientations of the crystals used, about 30° to 60°, would have given variations of up to a factor of 2 in the relative positions of the points when plotted against resolved shear strain.

Since the accuracy of measurements of $\Delta\rho/\rho$ was ~0.015% (section 3.39), changes of 0.1% to 0.2% were not large enough for any significant analysis of annealing stages to be possible.

4.2 Annealing of defects

4.21 Isochronal annealing

Fig. 4.21-1 shows an isochronal annealing curve obtained from a polycrystalline cadmium specimen (Cd 20) deformed 7.4% and annealed in pulses of $3\frac{1}{2}$ min. from 105.6 K to 281.8 K. The differential annealing curve is also shown. The main characteristics are two peaks at 138 K and 192 K, with a broad region of annealing extending from 90 K to 180 K.

In Fig. 4.21-2 the same curve is shown together with isochronal curves derived from the values of resistivity at the end of each stage of sequential isothermal annealing for specimens Cd 22 and Cd 29. The total time at each temperature for these specimens was longer than for Cd 20, so the resistivity shows a more rapid decrease with temperature on the isochronal curve, but the main features are still present. The normalised differential annealing curves are shown in Fig. 4.21-3. The longer annealing times have resulted in the loss of some of the sub-structure (this will be discussed further in section 5.2) and have moved the peak at about 140 K to a slightly lower temperature.

4.22 Isothermal annealing

Fig. 4.22-1 shows the changes in resistivity during a series of sequential isothermal anneals at temperature increments of 10% up to 207 K. Above this temperature the resistivity increased and changed in an irregular manner, probably because of strains produced by temperature changes, as discussed in section 4.4. Another series of anneals on a different specimen is shown in Fig. 4.22-2.

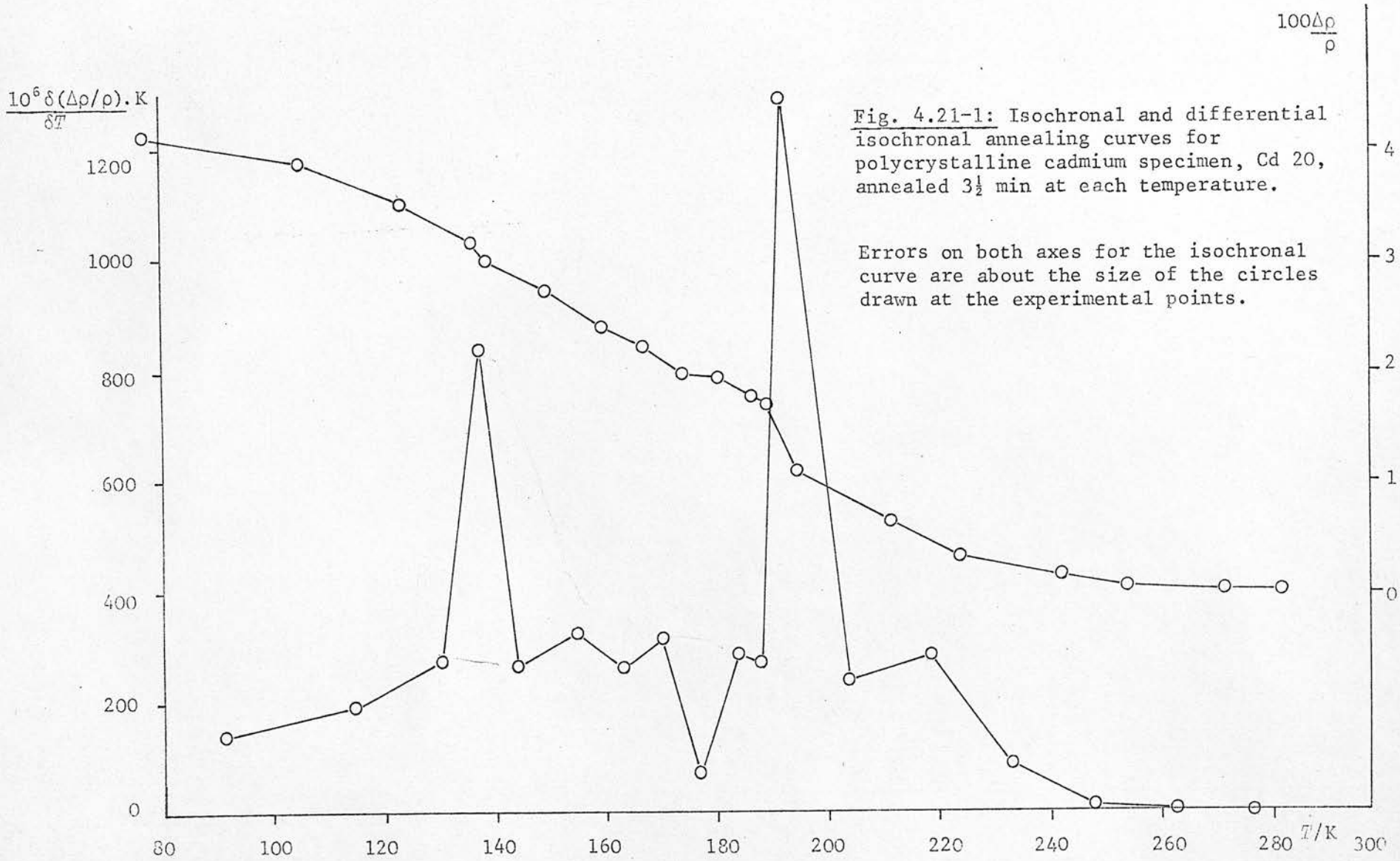

Fig. 4.21-1: Isochronal and differential isochronal annealing curves for polycrystalline cadmium specimen, Cd 20, annealed 3½ min at each temperature.

Errors on both axes for the isochronal curve are about the size of the circles drawn at the experimental points.

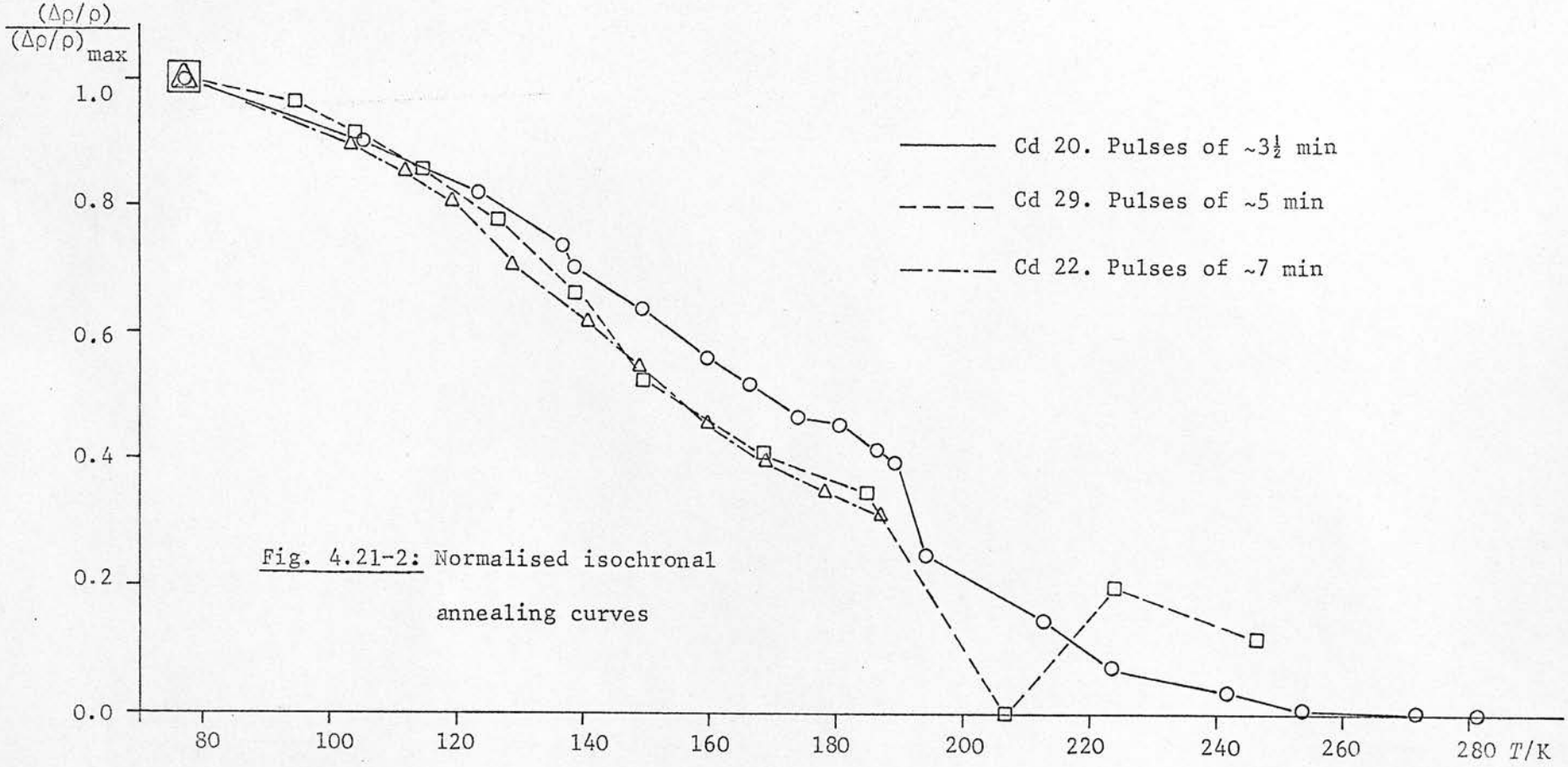

Fig. 4.21-2: Normalised isochronal annealing curves

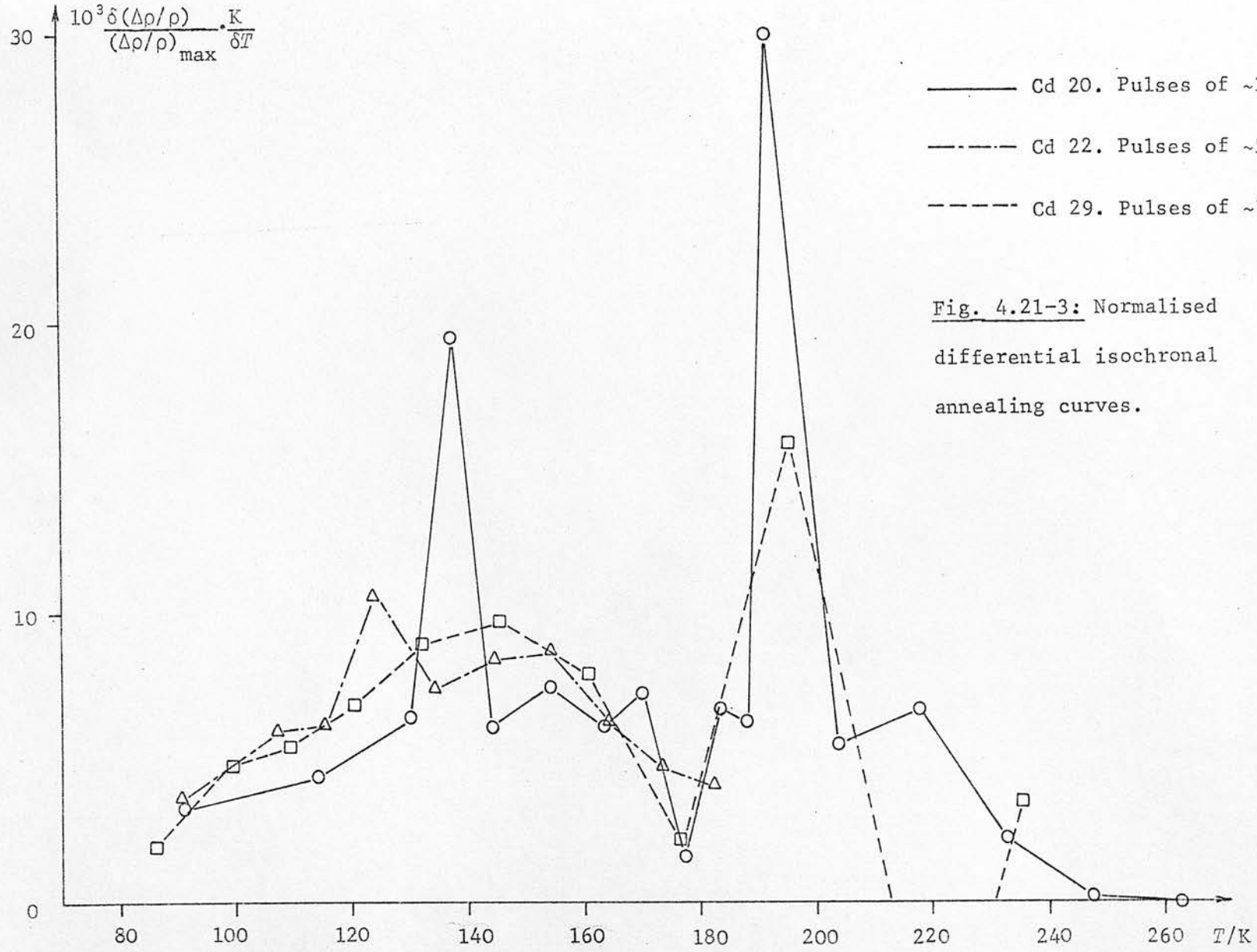

Fig. 4.21-3: Normalised differential isochronal annealing curves.

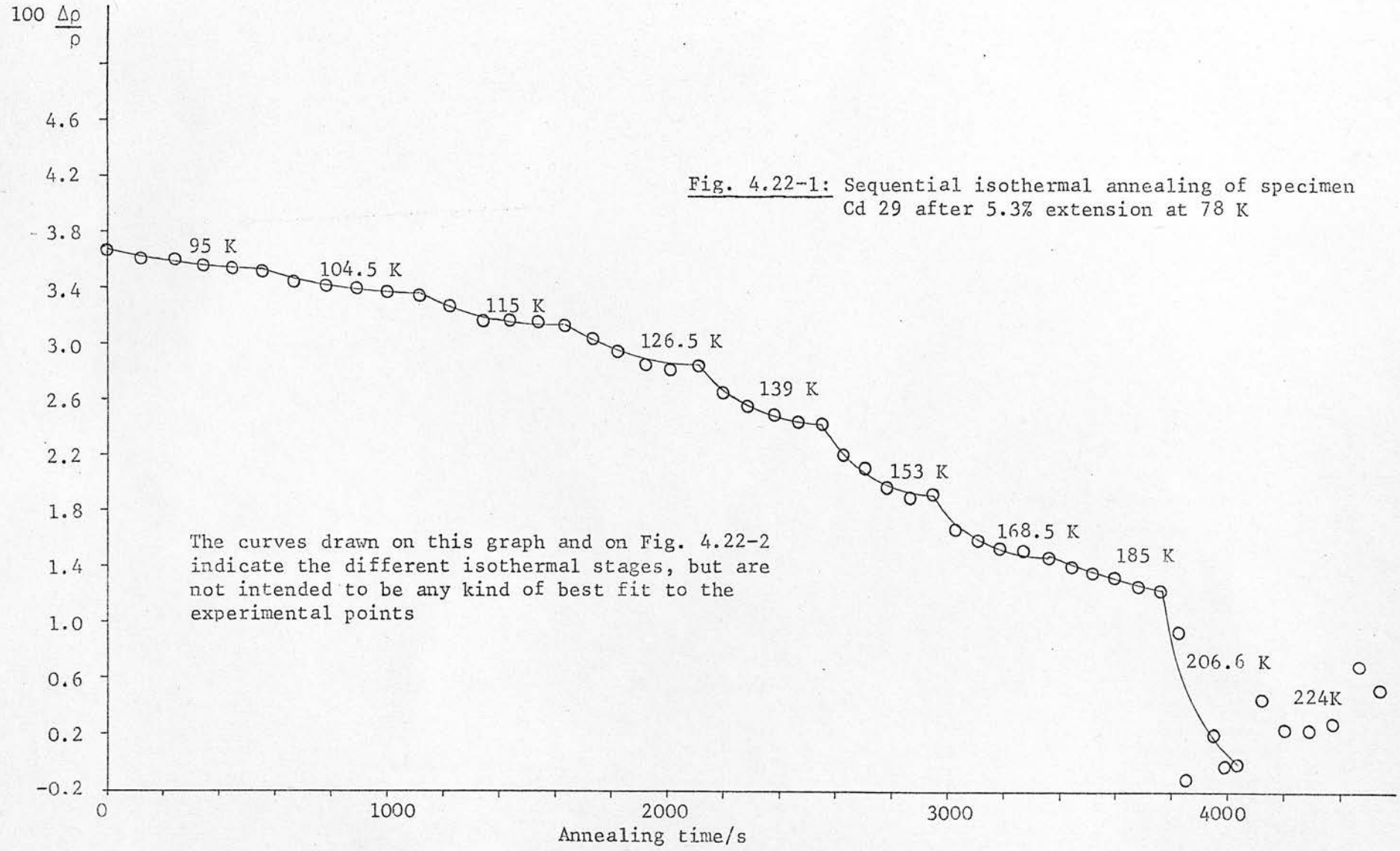

Fig. 4.22-1: Sequential isothermal annealing of specimen Cd 29 after 5.3% extension at 78 K

The curves drawn on this graph and on Fig. 4.22-2 indicate the different isothermal stages, but are not intended to be any kind of best fit to the experimental points

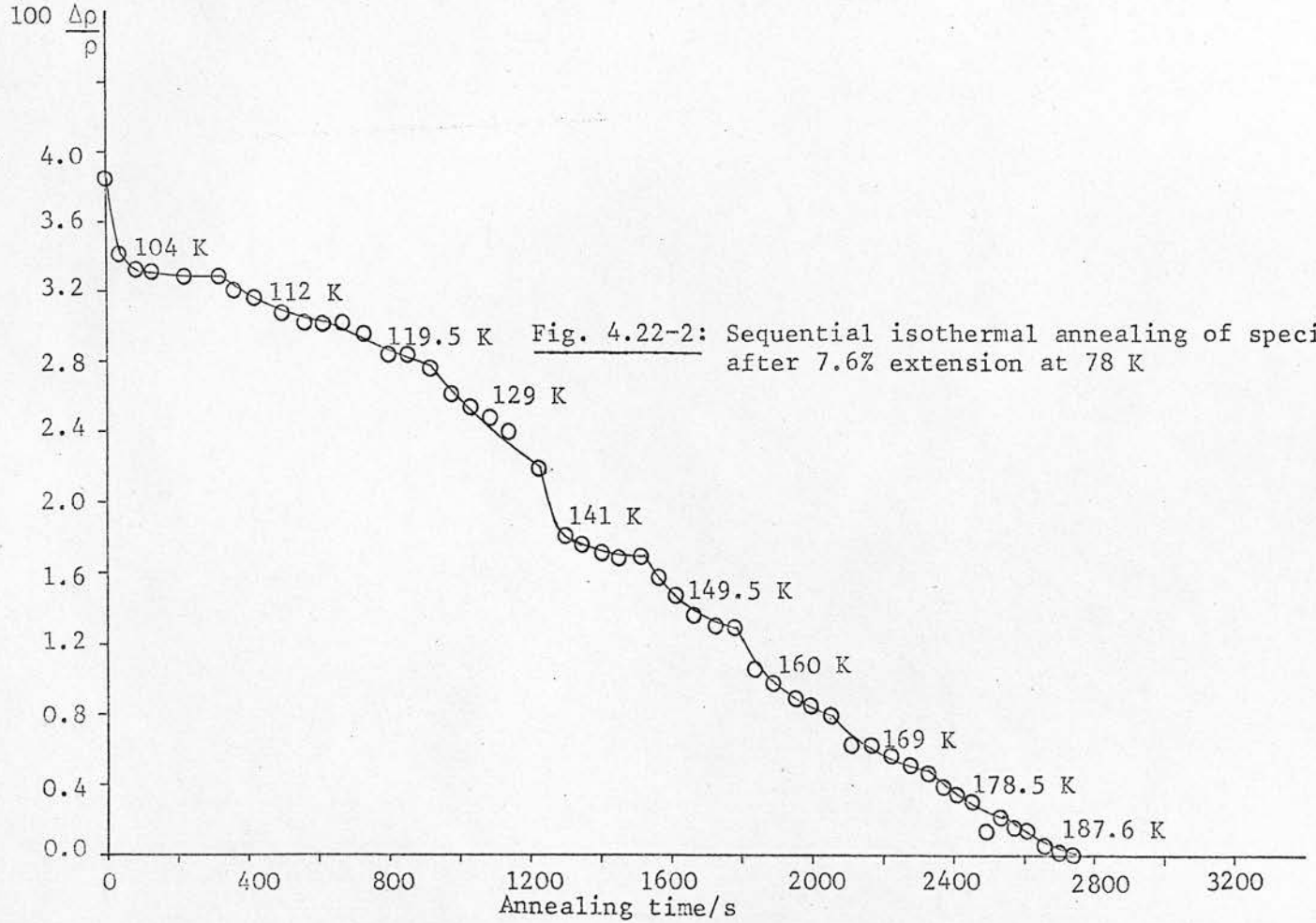

Fig. 4.22-2: Sequential isothermal annealing of specimen Cd 22 after 7.6% extension at 78 K

4.3 Analysis of annealing data

The annealing processes which occur in cold-worked metals are more complicated than those in quenched or irradiated materials because of the large number of different types of defect which may be present. In addition to point defects there is necessarily a significant density of dislocations, which not only act as traps and sinks for point defects but also themselves contribute to resistivity changes, in processes such as polygonization and recrystallization. It is therefore not surprising that the annealing spectra observed will be complex and not usually describable in terms of a few discrete processes. An analysis for activation energies. orders of kinetics and numbers of jumps was nevertheless carried out as described below in order to extract as much information as possible from the results to assist their interpretation.

4.31 Methods of measuring the activation energy of annealing, E^m

The theoretical expression which is usually assumed for the thermally activated annealing of defects in a metal is (Damask and Dienes 1963, p.146)

$$dn/dt = -F(n)K_0\exp(-E^m/kT) \qquad (4.31\text{-}1)$$

where n is the fractional concentration of the defect, $F(n)$ is some continuous function of n, K_0 is a constant made up of a vibration frequency, a geometrical factor and an entropy term, and E^m is the activation energy of the process, independent of n.

It is usually assumed that n is proportional to some observable property such as an increment in resistivity ρ', so that (4.31-1) can be replaced by

$$d\rho'/dt = -F(\rho')K_0\exp(-E^m/kT) \qquad (4.31\text{-}2)$$

Damask and Dienes give details of four methods by which the value of

the activation energy may be determined from the results of annealing experiments, and other methods have been published by Afman (1971), Bell and Sizmann (1966), Gevers et al. (1966), Balarin et al. (1967) and Balluffi and Siegel (1965) ("Palmer method"). Of these methods the change-of-slope method of Overhauser (1953), or variations of it, is most widely used, because it has the advantage that the activation energy can be determined from a single specimen. Other methods, such as that of cross-cuts, require a set of identical samples which have to be annealed at different temperatures; it is difficult to ensure that two cold-worked samples are identical. Schumacher (1970) has criticised the use of the cross-cut method by Stevenson and Peiffer (1963) on these grounds. He also refers to the limitations of the change-of-slope methods, and these are dealt with further in the present work.

4.32 Change-of-slope method

In the change-of-slope method a specimen is annealed isothermally at a temperature T_1 for a certain time, and then the temperature is changed to T_2 and isothermal annealing continued at that temperature. This gives a variation of resistivity with time of the form shown in Fig. 4.32-1.

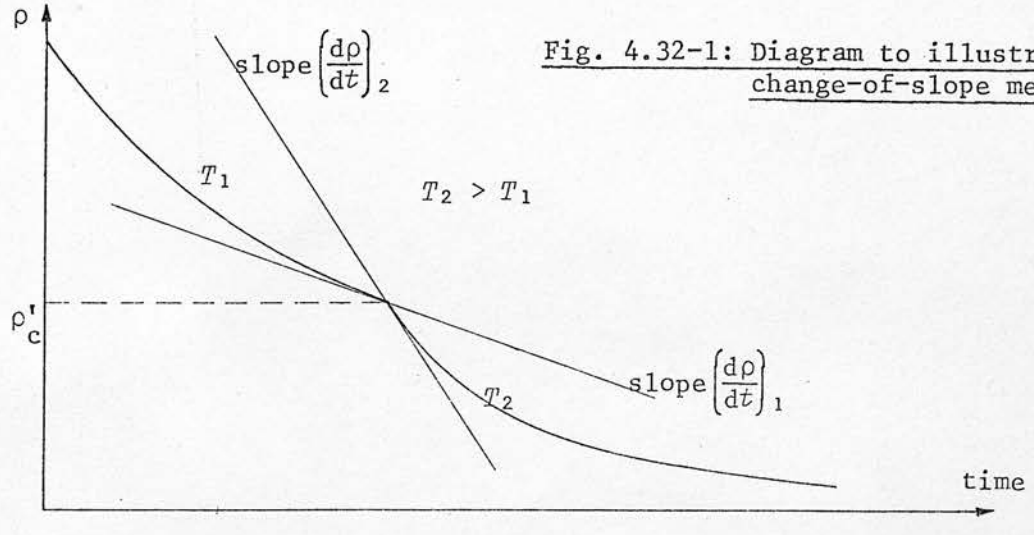

Fig. 4.32-1: Diagram to illustrate change-of-slope method

The rate of change of resistivity with time on either side of the point ρ'_c is given by equation (4.31-2) with appropriate values of temperature, thus:

$$(d\rho'/dt)_1 = -F(\rho'_c)K_0\exp(-E^m/kT_1)$$

$$(d\rho'/dt)_2 = -F(\rho'_c)K_0\exp(-E^m/kT_2)$$

Dividing these two equations and taking logarithms gives

$$E^m = k\left(\frac{1}{T_2} - \frac{1}{T_1}\right)^{-1}\ln\left(\frac{(d\rho'/dt)_1}{(d\rho'/dt)_2}\right)$$

from which E^m can be calculated if values of the slopes and temperatures are known.

The main drawback of this method is the difficulty of deciding on the values of the slopes, which are very dependent on the few experimental points on either side of ρ'_c. The usual procedure is to draw a smooth curve by eye through the experimental points and measure its slope at ρ'_c, but it is more satisfactory to use an analytical method. In some of the earliest work of this type Dugdale (1952) fitted the empirical expression

$$\rho' = A - B\log_{10}(t + \gamma)$$

to the curve, A, B and γ being arbitrary constants. He then used the slope at ρ'_c given by the equation.

In the present work both the "by-eye" method and a curve-fitting method were used. The equation which was fitted had a theoretical basis rather than being an empirical one like Dugdale's, although the values found for the constants implied that the situation was more complex than is assumed by the straightforward theory.

The theoretical expression for the curve is equation (4.31-2), in which the function $F(\rho')$ has to be determined. If it can be assumed that the annealing process obeys a chemical rate equation, $F(\rho')$ will be some power of ρ', say ρ'^{γ}, where γ is the order of the reaction. If

the value of γ can be found, and if it is a small integer such as 1 or 2, this gives a useful clue to the type of annealing process which is taking place. For example, point defects migrating without mutual interaction to inexhaustible sinks gives $\gamma = 1$; mutual annihilation of two species of point defect with equal initial concentrations gives $\gamma = 2$ (Damask and Dienes 1963).

The annealing equation (4.31-2) then becomes

$$d\rho'/dt = -\rho'^{\gamma} K_0 \exp(-E^m/kT) \qquad (4.32\text{-}1)$$

This may be integrated to give

$$\rho'/\rho'_0 = \exp[-K_0 t \exp(-E^m/kT)] \quad \text{for } \gamma = 1 \qquad (4.32\text{-}2)$$

and

$$\frac{1}{(\rho')^{\gamma-1}} - \frac{1}{(\rho'_0)^{\gamma-1}} = (1-\gamma) K_0 t \exp(-E^m/kT) \text{ for } \gamma \neq 1 \qquad (4.32\text{-}3)$$

where ρ'_0 is the value of ρ' before annealing, i.e. at $t = 0$. These equations cannot be used to find γ if it is unknown, except by trying various values of γ to find one which fits the data.

4.33 Logarithmic curve-fitting improvement of change-of-slope method

A method of obtaining γ and E^m from equation (4.32-1) is mentioned by Damask and Dienes (1963), but does not seem to have been developed, although Fujita and Damask (1964) used a modified version of it to find γ. After it had been used for some time in the present work Spružil and Vostrý mentioned in a private communication that Nihoul was also suggesting its revival.

The method is to take logarithms of (4.32-1), giving

$$\ln(-d\rho'/dt) = \ln K_0 - E^m/kT + \gamma \ln \rho'$$

Thus a graph of $\ln(-d\rho/dt)$ against $\ln\rho'$ will have a gradient γ and an intercept $A = \ln K_0 - E^m/kT$. If two such graphs are plotted for different values of T, T_1 and T_2, giving intercepts A_1 and A_2, then

$A_1 - A_2 = -\frac{E^m}{k}\left(\frac{1}{T_1} - \frac{1}{T_2}\right)$, from which E^m can be found.

The type of graph obtained from two sequential anneals of the kind shown in Fig. 4.32-1 is shown schematically in Fig. 4.33-1.

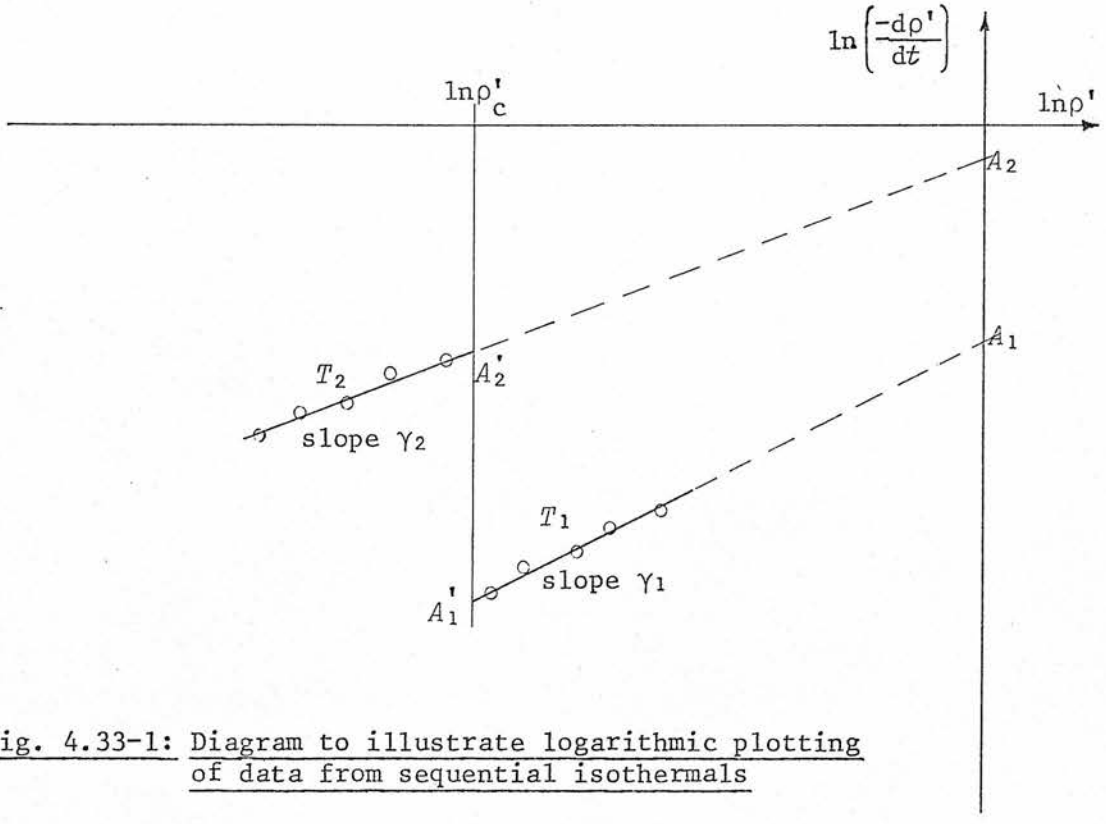

Fig. 4.33-1: Diagram to illustrate logarithmic plotting of data from sequential isothermals

The graph falls in the negative region of both axes because in practice it is convenient to measure ρ' as a fraction of the total resistivity of the annealed specimen. Thus ρ' and $d\rho'/dt$ are both less than 1 and the logarithms are negative.

In using this method it is found that uncertainties in the values of the intercepts A_1 and A_2 may be large, because they are found by extrapolation over a long distance to the line $\ln\rho' = 0$. Intercepts were therefore taken at A'_1 and A'_2 instead, on the line $\ln\rho' = \ln\rho'_c$, where ρ'_c is the value of ρ' at the time the temperature was changed. $A'_1 - A'_2$ then gives directly the logarithm of the ratio of slopes at that point.

To plot the graph of Fig. 4.33-1 it is still necessary to measure slopes on the graph of ρ' vs. t, but now several slopes can be used from points along the whole length of each isothermal curve, and they will all contribute to establishing the position of the straight line. In order to remove subjective effects as far as possible, slopes were found numerically in two ways:

a) The slopes of lines joining adjacent experimental points (ρ'_i, t_i) and (ρ'_j, t_j) on the ρ' vs. t graph were taken as the values of the slope of that graph at the mean point $((\rho'_i+\rho'_j)/2,\ (t_i+t_j)/2)$.

b) A parabola was fitted to each set of three adjacent experimental points and the slope of the parabola at the middle point of the three was taken as the slope of the graph at that point.

In each case the uncertainty in the gradient was determined by combining the uncertainty in each of the points to give the uncertainty in the coefficients of the straight line or parabola.

There were usually six points on each isothermal segment, so these procedures provided a total of nine values of $(d\rho'/dt)$ to which the straight line logarithmic graph could be fitted. There was no apparent systematic difference between the values obtained using method (a) and those obtained using method (b). The nine points are not all independent, so only the number of independently measured points was used in calculating the number of degrees of freedom, which is required in finding the standard deviations of the slope and intercept. A weighted least squares fit was used, as described by Fischer (1969), with the correction of an error in Fischer's formula for the standard deviation of the intercept. (x_i in the numerator instead of x_i^2.)

Values of $(t_j - t_i)$ were fairly constant, as were their uncertainties, so were not taken into account in determining the weights. The

appropriate weighting factors w_{ij} are inversely proportional to the squares of the standard deviations in $\ln(-d\rho'/dt)$, i.e. if Δ indicates the standard deviation of a quantity which it precedes,

$$\sqrt{w}_{ij} \propto \frac{1}{\Delta \ln(-d\rho'/dt)}$$

$$= \frac{(d\rho'/dt)_{ij}}{\Delta(d\rho'/dt)_{ij}}$$

$$\propto \frac{(\rho'_j - \rho'_i)}{\Delta(\rho'_j - \rho'_i)}$$

$$\propto (\rho'_j - \rho'_i) \quad \text{since} \quad \Delta(\rho'_j - \rho'_i) \text{ is constant.}$$

The actual values of the uncertainties are not involved at this stage. They are discussed in section 3.3.

The logarithmic graphs obtained are shown in Fig. 4.33-2. These were drawn by a computer-controlled graph plotter from the sequential isothermal annealing curves of Fig. 4.22-1. The error bars on the points correspond to three times the standard deviation in ρ', calculated as discussed in section 3.39. Here ρ' has been identified with the measured quantity which in that section was called $\Delta\rho/\rho$. The validity of this identification will be discussed later.

There appears to be a deviation of the points from a straight line at the lower end of some isothermal segments in Fig. 4.33-2; the amount of the deviation is about -1 in the logarithm of the gradient. These points have the largest uncertainty, because the changes in ρ' are small and are therefore given a smaller weight in computing the best straight line. Nevertheless, the points do appear to fall consistently below the line rather than being randomly scattered, so some systematic error must be having effect. Two possibilities suggest themselves: the curve-fitting process used to determine gradients may

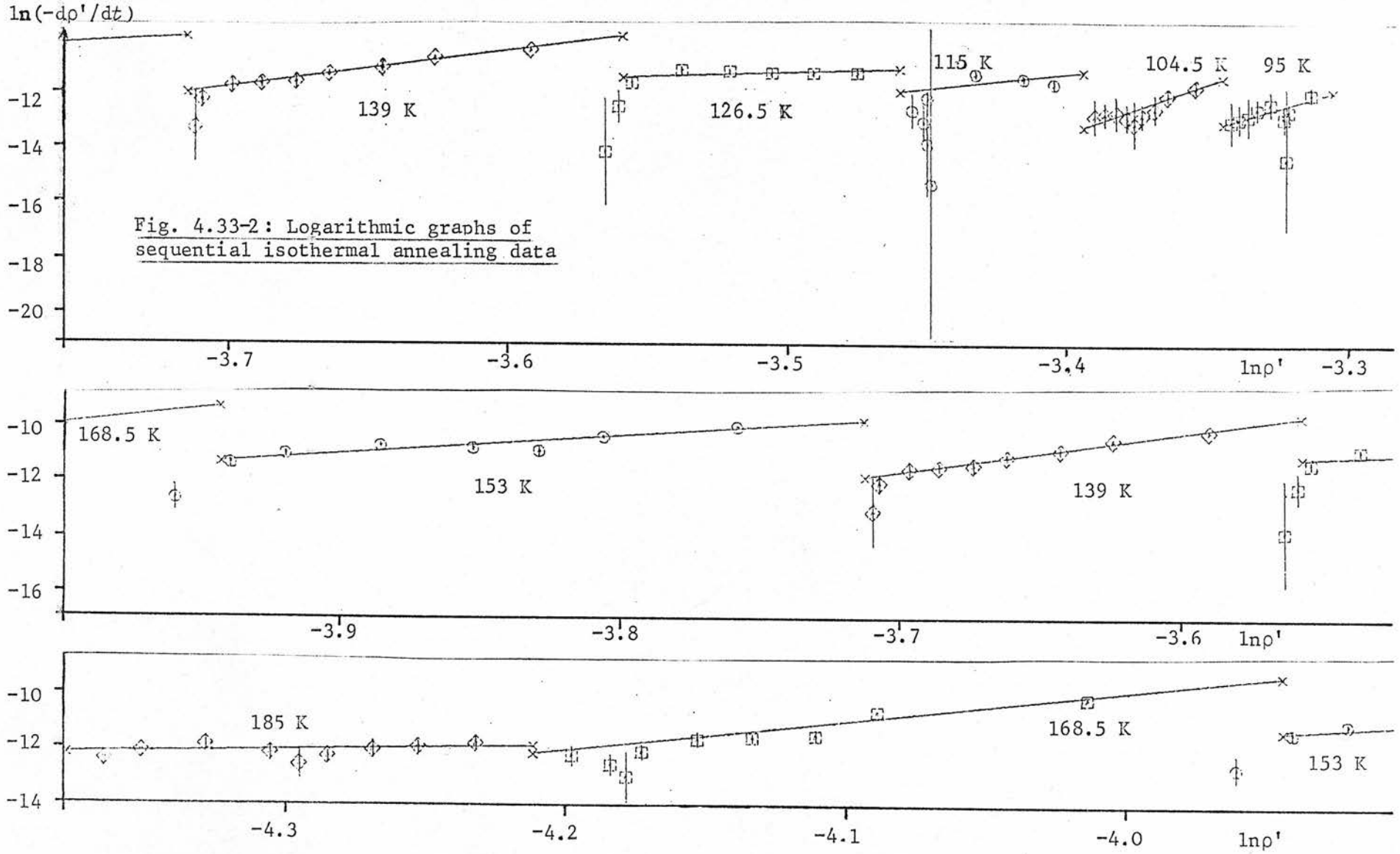

Fig. 4.33-2: Logarithmic graphs of sequential isothermal annealing data

be inadequate or the value of γ or E^m may not be constant. These possibilities will now be considered.

Systematic errors in determination of gradient

A systematic error is introduced when a segment of the curve is approximated by a straight line, because the value of ρ' at the mid-point of the line (D in Fig. 4.33-3) is greater than the value of ρ' at the point C, where the tangent to the curve has the same slope as the line AB.

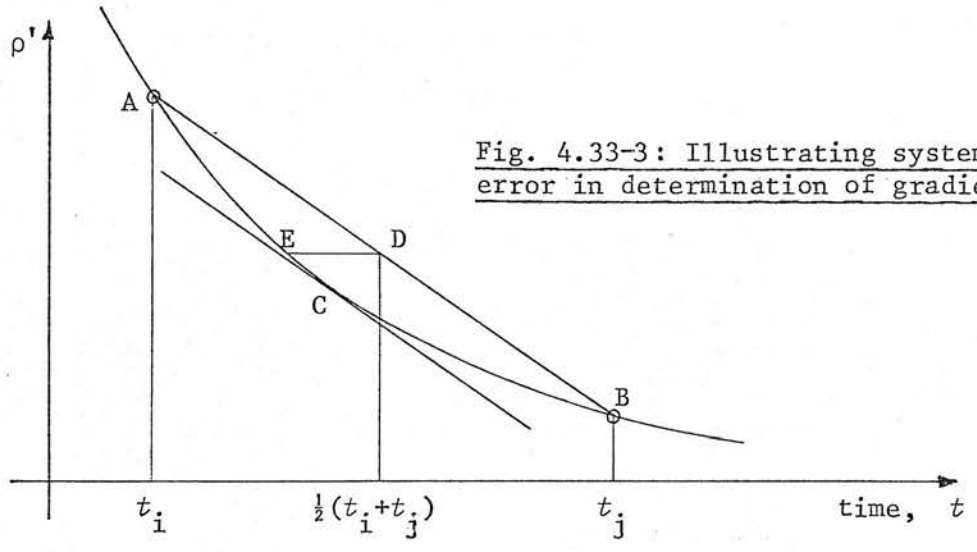

Fig. 4.33-3: Illustrating systematic error in determination of gradient

This error cannot be allowed for without assuming the value of γ, which determines the shape of the curve. For $\gamma = 1$ an estimate of the size of the error may be made as follows:

Assume that the equation of the curve is

$$\rho' = \rho'_0 \exp(-Kt), \text{ where } K = K_0 \exp(-E^m/kT). \qquad (4.33\text{-}1)$$

Then the gradient

$$d\rho'/dt = -K\rho'. \qquad (4.33\text{-}2)$$

If the curve passes through the points (ρ'_i, t_i), (ρ'_j, t_j) the value of K can be found from (4.33-1) as

$$K = \frac{-\ln(\rho'_i/\rho'_j)}{(t_i - t_j)} \qquad (4.33\text{-}3)$$

and the gradient at the point E is then

$$-K\rho'_E = \frac{[\ln(\rho'_i/\rho'_j)]\ \frac{1}{2}(\rho'_i + \rho'_j)}{(t_i - t_j)}$$

(ρ'_E is the value of ρ' at the point E).

Expanding $\ln(\rho'_i/\rho'_j)$ as a power series gives

$$\left(\frac{d\rho'}{dt}\right)_E = -K\rho'_E = \frac{\frac{1}{2}(\rho'_i+\rho'_j)}{(t_i-t_j)}\ 2\left(\frac{\rho'_i-\rho'_j}{\rho'_i+\rho'_j} + \frac{1}{3}\left(\frac{\rho'_i-\rho'_j}{\rho'_i+\rho'_j}\right)^3 + \frac{1}{5}\left(\frac{\rho'_i-\rho'_j}{\rho'_i+\rho'_j}\right)^5 + \ldots\right)$$

$$= \frac{\rho'_i-\rho'_j}{t_i-t_j}\left(1 + \frac{1}{3}\left(\frac{\rho'_i-\rho'_j}{\rho'_i+\rho'_j}\right)^2 + \frac{1}{5}\left(\frac{\rho'_i-\rho'_j}{\rho'_i+\rho'_j}\right)^4 + \ldots\right)$$

where the term outside the brackets is the gradient of the straight line AB. If we put $\rho'_i - \rho'_j = \delta\rho'$, and $t_i - t_j = \delta t$, the first correction term is

$$\frac{1}{12}(\delta\rho'/\rho'_E) \quad \text{since} \quad \rho'_i + \rho'_j = 2\rho'_E.$$

For small values of $\delta\rho'$ this approaches $-\frac{1}{12}(K\delta t)$, from (4.33-2), which equals $\frac{1}{12}[\ln(\rho'_i/\rho'_j)]$ from (4.33-3). Thus the gradient at E differs from the value at C according to the relation

$$(d\rho'/dt)_E = (d\rho'/dt)_C[1 + \frac{1}{12}(\ln\rho'_i - \ln\rho'_j)^2].$$

The value of $(\ln\rho'_i - \ln\rho'_j)$ should be constant for any pair of adjacent points on an isothermal if (4.33-1) holds, and if the points are closely enough spaced the error should be independent of the particular point on the isothermal curve which is being considered. It was found in practice that $(\ln\rho'_i - \ln\rho'_j)$ was less than 0.1, so the error in gradient would be less than 0.001 (0.1%), which is negligible compared with the uncertainty in changes of ρ'. It is also too small to explain the departure from a straight line in Fig. 4.33-2.

The values of gradient obtained from a parabolic rather than a straight line fit would have been subject to a similar error, because

if the three experimental points all lie on an exponential-type curve, and a parabola is constructed to pass through all three of them, it must cross the curve at the middle point and the value of its gradient there will therefore differ from the gradient of the curve. Without knowing the shape of the curve, however, the amount of this difference cannot be determined. There does not appear to be any regular variation in gradient as seen in the graphs of Fig. 4.33-2, alternate points on which were obtained from straight line and parabolic fits.

It appears, therefore, that inadequacies in the gradient determination are not sufficient to explain the points which fall below the line and it is possible that the alternative explanation, non-constant γ, must be used. In that case the theory which has been used as the basis of (4.32-1) is not completely adequate. Variations in γ will be considered further in the following sections.

Variable order of kinetics

If a single process describable by (4.32-1) is taking place at the two temperatures, then the two values of γ should be the same. If they are not, then either the annealing processes are different at the two temperatures or the process is not describable by (4.32-1).

In the latter case, if we can assume that the more general equation (4.31-2) is applicable, we can consider (4.32-1) as an empirical equation which can be adjusted to give a reasonable straight line fit for the purposes of extrapolation. In this case γ has no physical meaning and we need not expect it to be integral, or constant from one set of points to the next. The values of E^m will still be valid, however, since they do not depend on the form of the function $F(\rho')$ in (4.31-2).

If the annealing process changes with temperature, then the effective value of E^m obtained cannot be directly associated with any particular physical process, but has to be interpreted as some kind of mean value. The difficulties of interpreting effective migration energies are discussed in section 5.2.

4.34 Separation of annealing stages due to different defects

A complication which enters into all methods of analysis of annealing data is that the values of resistivity entering into the formulae are properly only the resistivity, ρ', due to the specific type of defect under consideration. If there are contributions from other types of defect which do not anneal in the same temperature range, we can call these contributions ρ'_∞, the resistivity which would remain if the isothermal anneal were continued for a long time. Thus we must identify ρ' with $(\Delta\rho/\rho) - \rho'_\infty$, rather than with $\Delta\rho/\rho$ as suggested in section 4.33. The relationship between ρ', ρ'_∞, and $\Delta\rho/\rho$ is shown in Fig. 4.34-1 for the annealing of a single species of defect. Note that ρ' and ρ'_∞ are expressed as fractions of the fully annealed resistivity ρ, and that ρ' is a function of time, t.

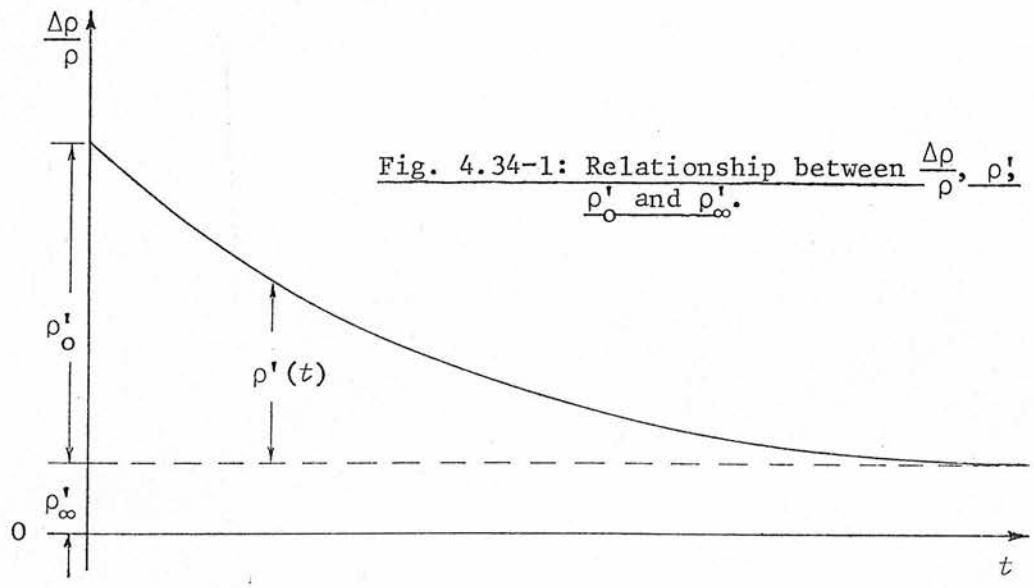

Fig. 4.34-1: Relationship between $\frac{\Delta\rho}{\rho}$, ρ', ρ'_0 and ρ'_∞.

If the isochronal annealing spectrum shows a number of distinct and separate peaks, each due to a single process, then the amount ρ'_∞ to be subtracted at each stage may be determined fairly easily; in the case of a continuous annealing spectrum it is very difficult. In the present work the isochronal spectrum (Fig. 4.21-3) shows changes in the annealing process at 180 K and perhaps at about 140 K, so the analysis could be carried out three times: after subtracting the resistivity remaining at each of these temperatures, and after subtracting the fully annealed resistivity. In fact, since the analysis was done on a computer, it was possible to do it as many times as there were isothermal annealing stages. At each repetition the resistivity at the end of that particular annealing stage was taken as the fully annealed value, and all the preceding stages were analysed with respect to it.

Values of activation energy E^m

The values of activation energy E^m and order of kinetics γ obtained are set out in Table 4.34-1. Two aspects of this table are worthy of note:

a) So long as the annealed value is taken a stage or two further on than the stage being investigated, the value of E^m found from any pair of stages is constant, although the value of γ for each stage changes considerably. This would be expected if (4.31-2) is valid, the value of γ being adjusted as an empirical constant so that ρ'^{γ} fits $F(\rho')$. Values of E^m from Table 4.34-1 are plotted as a function of temperature in Fig. 4.34-2, which also shown points obtained from another specimen.

b) The value of γ increases as the annealed value is taken further away from the end of the stage being investigated. Generally γ for

Table 4.34-1: Values of activation energy and order of kinetics obtained from analysis of data shown in Figs. 4.22-1 and 4.33-2.

Values of γ are shown in elite type; values of E^m are shown in italic type, in positions bridging the temperatures of the two isothermal stages used in their evaluation.

Temperature of the annealing stage after which resistivity is taken as having its fully annealed value, ρ_∞; T/K.	95	104.5	115	126.5	139	153	168.5	185	206.6
95	0.25±0.19								
104.5	1.27±0.88 *0.10±0.03*	0.54±0.20							
115	2.43±1.60 *0.12±0.03*	2.64±0.62 *0.19±0.03*	0.37±0.21						
126.5	4.19±2.63 *0.13±0.03*	5.4 ±1.2 *0.19±0.03*	1.4 ±1.3 *0.09±0.05*	0.09±0.04					
139	7.03±4.13 *0.13±0.03*	9.6 ±2.1 *0.19±0.04*	2.8 ±2.8 *0.09±0.05*	0.61±0.63 *0.13±0.03*	0.68±0.09				
153	10.6±5.8 *0.13±0.03*	14.5±3.1 *0.19±0.04*	4.4 ±4.5 *0.09±0.05*	1.1 ±1.2 *0.17±0.02*	3.3 ±0.3 *0.22±0.02*	0.22±0.09			
168.5	14.4±7.4 *0.14±0.03*	19.1±4.0 *0.19±0.04*	5.9 ±6.1 *0.09±0.05*	1.6 ±1.7 *0.17±0.03*	5.5 ±0.6 *0.26±0.03*	1.7 ±0.4 *0.22±0.03*	1.0±0.2		
185	16.4±8.2 *0.14±0.03*	21.5±4.5 *0.19±0.04*	6.6 ±6.8 *0.09±0.05*	1.8 ±2.0 *0.17±0.03*	6.6 ±0.7 *0.26±0.03*	2.3 ±0.6 *0.26±0.04*	2.6±0.4 *0.10±0.05*	0.1 ±0.12	
206.6	28.7±12.5 *0.14±0.03*	34.8±7.2 *0.19±0.04*	10.6±11.1 *0.09±0.05*	3.0 ±3.5 *0.17±0.03*	12.8±1.5 *0.26±0.03*	5.4 ±1.3 *0.28±0.04*	10.1±2.0 *0.05±0.06*	1.6 ±1.9 *0.66±0.09*	0.02±0.63

Temperature of isothermal annealing stage, T/K.

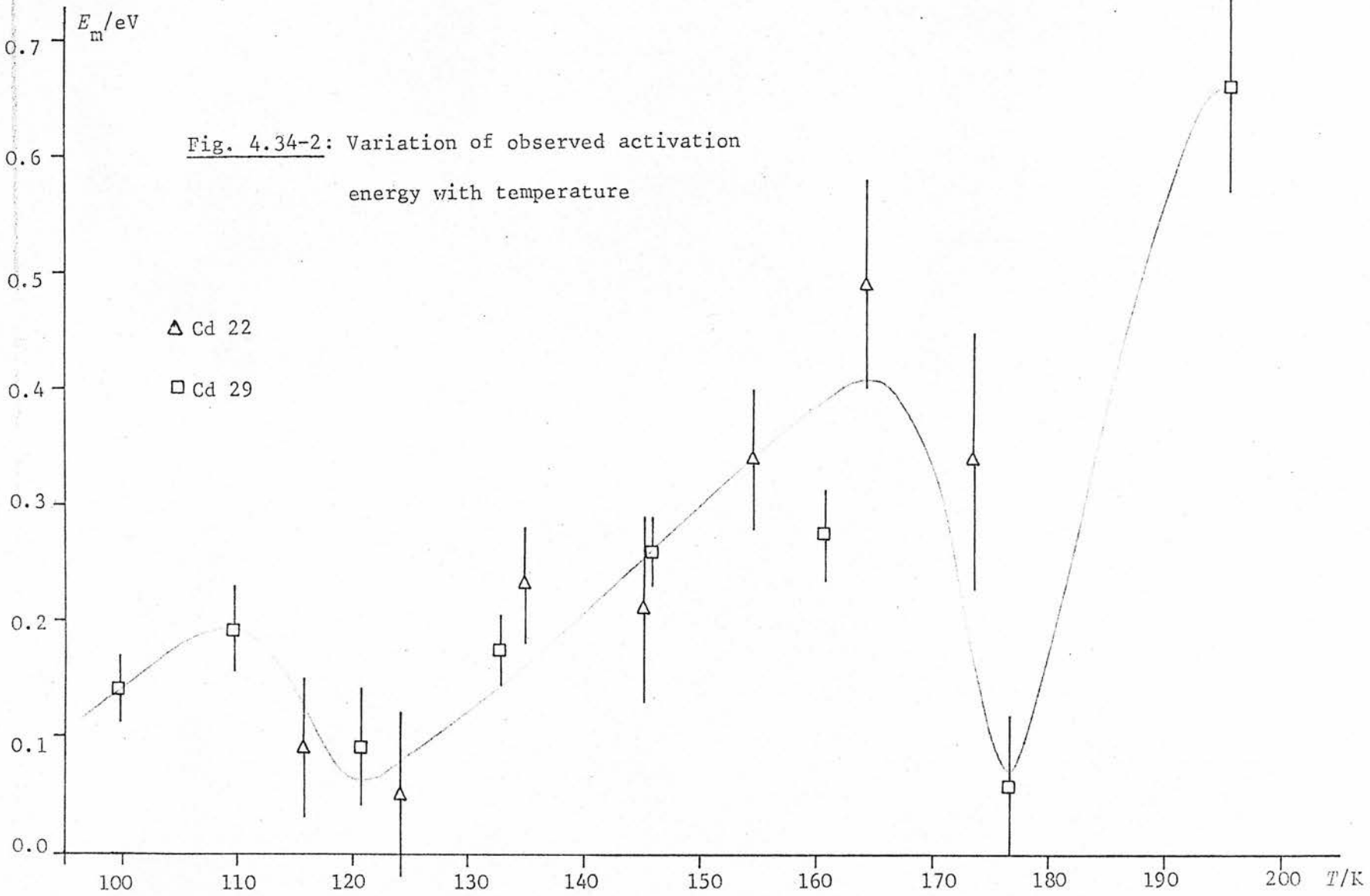

Fig. 4.34-2: Variation of observed activation energy with temperature

any particular stage has a value of less than 1 with respect to the end of that stage and a value greater than 1 with respect to the end of the next and subsequent stages. This suggests that if first order kinetics are obeyed an extrapolation of the annealing graphs for two adjacent stages would look like Fig. 4.34-3 instead of Fig. 4.34-4 which is assumed in the analysis for E^m.

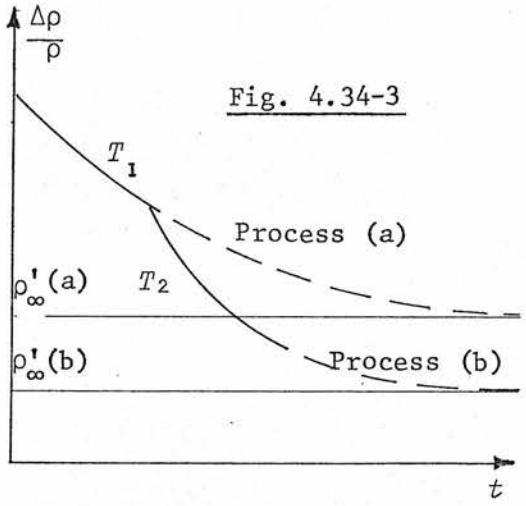

Fig. 4.34-3

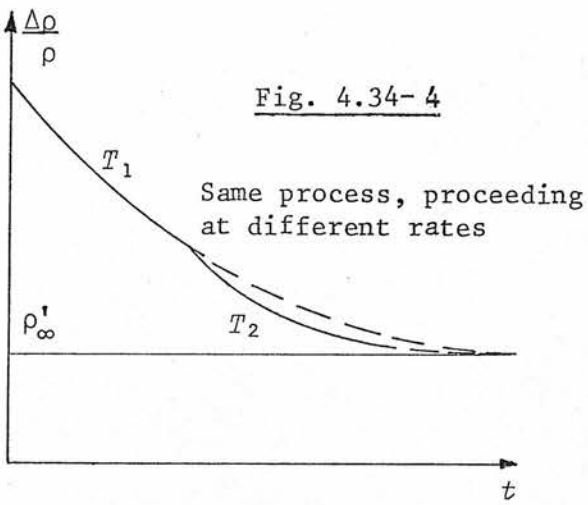

Fig. 4.34-4

This implies that a different process comes into operation each time the temperature is raised, so that the number of defects available for annealing is increased. The interpretation of a distribution of processes of this kind is discussed in section 5.31.

It is seen, therefore, that the value of γ obtained depends on the value which is assumed for ρ'_∞. It is not generally possible to determine both γ and ρ'_∞ independently. A procedure which is often used (e.g. Dworschak et al. 1964) is to assume a value of γ, say 1 or 2, and then by trial and error find a value of ρ'_∞ which makes ρ' fit (4.32-2) or (4.32-3). It is often possible to do this, but as has been shown above the values obtained must be considered to be empirical constants which give a reasonable fit and they cannot be given physical significance.

Lee and Koehler (1968) found a way of avoiding the trial and error fitting of ρ_∞, but their method is applicable only to second order processes ($\gamma = 2$). They plot $(\rho_0' - \rho')^{-1}$ against t^{-1}, and get a straight line; in principle values of ρ_∞ and E^m should be determinable from the slope and intercept, but in practice it is not easy to determine the intercept accurately. A graph of this kind for an isothermal annealing stage was found to fit second order kinetics, giving a value of ρ_∞ below the end of that stage and above the end of the subsequent stage, agreeing with the situation shown in Fig. 4.34-3.

4.35 Analysis of processes distributed in activation energy

There does exist a method of analysis of processes distributed in activation energy, developed by Primak (1955, 1960). By this method it is possible to analyse annealing data to give an "activation energy spectrum" showing the contribution to the total change in the measured property (e.g. resistivity) which is due to defects which would anneal with energies in the range E^m to $E^m + \delta E^m$. This procedure has been used by Stevenson and Peiffer (1964) and by Koehler and co-workers (Magnuson et al. 1958; Dworschak et al. 1964; Lee and Koehler 1968). Before an activation energy spectrum can be determined, however, it is necessary to know the order of the reaction, γ, and Fang (1970) has shown by a mathematical argument that it is impossible to determine both the order of the reaction and the energy spectrum from the analysis of isothermal or isochronal annealing data. Fang concludes that the method used by, e.g. Lee and Koehler, is not self-consistent, and that unless there is other physical evidence there is no mathematical basis for establishing an activation energy spectrum. Since in the present work there is no physical reason for assuming a particular value of γ (and indeed such evidence as there is suggests that γ may not be constant)

it was not thought appropriate to apply Primak's method.

4.36 Number of jumps made by a defect in annealing

If the kinetics can be assumed to be first order, if the activation energy of movement of a defect is known, and if an estimate can be made of the frequency and entropy terms, the number of jumps, n_j, made by a defect in annealing may be calculated from the expression

$$n_j = z\nu t_{1/e} \exp(-E^m/kT) \qquad (4.36\text{-}1)$$

(Sprušil et al. 1970) where z is the coordination number, $t_{1/e}$ is the time taken for the resistivity to fall to 1/e of its value at the beginning of that isothermal stage, and ν combines the atomic vibration frequency ν_o, the activation entropy for migration, S^m, and a geometrical term g in the form $\nu = g\nu_o \exp(-S^m/k)$. Sprušil et al. calculate ν from the expression

$$\nu = \frac{D_0}{b^2 \exp(S^f/kT)}$$

where b is the jump length, S^f is the defect formation entropy, and D_0 is the diffusion coefficient, $D_0 = gb^2\nu_0 \exp[(S^f + S^m)/k]$. D_0, b and S^f can be measured independently, and give ν = (1 to 3) x 10^{13} s^{-1}.

Measured values of $t_{1/e}$, E_m and T in the present work give, from equation (4.36-1), $n_j \sim 3 \times 10^9$ at T = 115 K and $n_j \sim 10^8$ at T = 160 K.

4.4 Effects of anisotropic thermal expansion

One of the major difficulties in carrying out experiments involving temperature changes on anisotropic metals is that of strains introduced by differential thermal expansion. This difficulty has been remarked on by many workers (Lucasson and Walker 1962; Lucasson and Lucasson 1962, 1966; Sharp et al. 1965; Coltman et al. 1967, 1971) but others do not report having had to consider it (Peiffer and Stevenson 1963; Stevenson and Peiffer 1964; Nihoul 1963; Simon and Delaplace 1972).

Sprušil (1965) analyses methods of measuring resistivity changes when extra changes take place during annealing due to causes such as this. He concludes that the best that can be done is to make simultaneous measurements on a dummy which is as nearly identical as possible to the specimen, and to give the dummy all the thermal treatment which the specimen receives before and during annealing except for the process, such as a quench, in which the defects of interest are introduced. It is then hoped that unwanted changes in the resistivity of the specimen will be matched by equal changes in the resistivity of the dummy, and that variations in the ratio of the two resistances will show effects due to defects which are in the specimen alone. This is probably fairly effective in quenching experiments, but when the mechanical properties and dislocation structure of the specimen have been altered by plastic deformation it is no longer quite valid to suppose that the thermoelastic stresses set up or the specimen's response to them will be the same as for an undeformed dummy. The magnitude of resistivity changes due to thermal cycling may be quite large: Levi (1965) found that the resistivity of polycrystalline zinc at 78 K increased by about 3% after 10

cycles between 78 K and 293 K, and changes of a few parts in a thousand were seen after one cycle.

Kuznetsov and Gribanov (1962) found that intense plastic deformation occurred in 1.5 mm polycrystalline wires of cadmium and zinc cycled between room temperature and 88 K. Zinc was made mechanically weaker by the treatment, and its electrical resistivity (presumably at 78 K) increased by over 25% in the first 100 cycles, owing to crack formation. The mechanical properties of cadmium changed in a direction compatible with work-hardening: the flow stress increased from 5.5 kgf/mm^2 to almost 7 kgf/mm^2 (54 MPa to 69 MPa) and the "relative elongation" decreased from 24% to 10% after about 100 cycles. No change in its electrical resistivity was observed, however. Cracks do not occur in cadmium, because plastic flow can relieve the stresses. We can interpret the lack of change in resistivity by assuming that since the specimen was brought to room temperature on each cycle there would be an opportunity for annealing to occur and no cumulative increase in the nunber of defects would result. Thermal cycling at a lower temperature, as is used in pulse annealing experiments, would be expected to increase the resistivity. Boas and Honeycombe (1947) saw two or more sets of slip lines in the same grain in polycrystalline cadmium and zinc cycled between 77 K and room temperature, indicating that secondary slip had occurred.

The effect of thermal cycling on single crystals would be expected to be much smaller than on polycrystals, and in fact Coltman et al. (1971) found no effect upon the residual resistance of monocrystalline ribbons of cadmium 38 μm thick. Some stresses would be expected as a result of misoriented fragments, however, being more serious with larger crystals where the sub-grains could be constrained

on all sides. Postnikov et al. (1967) cycled single crystals of cadmium between a maximum of 260 °C and a minimum of 100 °C and found significant changes in fragment structure, even though the maximum initial disorientation angle was only 16'. They also calculated that the maximum shear stress due to anisotropic thermal expansion was an order of magnitude greater than that due to temperature gradient across the specimen.

Postnikov et al. quote V. A. Likhachev's formula for the maximum shearing stress

$$\tau_{max} = \frac{(\alpha_{\parallel} - \alpha_{\perp})\ \gamma\ \Delta T}{s_{44} + 2s_{13} + 2\sqrt{(s_{11}s_{13})}}$$

into which we can insert the following values for cadmium:

Coefficients of thermal expansion parallel and perpendicular to the c-axis, $\alpha_{\parallel} = 57.6 \times 10^{-6}\ K^{-1}$

$\alpha_{\perp} = 14.0 \times 10^{-6}\ K^{-1}$.

These values are averages of the values quoted by McCammon and White (1965) for 283 K and 75 K.

Maximum disorientation angle, γ, = 16' = 4.7×10^{-3} rad (Postnikov, 1967).

Elastic constants $s_{11} = 1.29 \times 10^{-11}\ Pa^{-1}$

$s_{33} = 3.69 \times 10^{-11}\ Pa^{-1}$

$s_{44} = 6.40 \times 10^{-11}\ Pa^{-1}$

$s_{13} = -0.93 \times 10^{-11}\ Pa^{-1}$

} Room temperature values, from Huntington (1958).

This gives $\tau_{max} \simeq 450$ kPa, which may be compared with the macroscopically measured critical resolved shear stress for basal glide in cadmium of 1000 to 600 kPa (Boček et al. 1964) or 300 to 200 kPa (Krasova and Kratochvíl 1971) at temperatures from 90 to 273 K.

Thus the stress due to anisotropy could easily exceed the critical stress with a disorientation angle, γ, of 16' (0.25°); German (1954)

found angles of 1° to 3° in investigating the perfection of zinc and cadmium single crystals grown in glass tubes, and if my crystals were not much more perfect than his thermal strains would certainly have occurred.

Apart from the effects of anisotropy, stresses also occur because of thermal gradients across the specimen which arise when its temperature is changed. This effect is most important for metals which are being quenched rapidly from high temperatures; it has been investigated for quenched f.c.c. metals by Jackson (1965) and for platinum cycled between room temperature and liquid helium and nitrogen temperatures by Mišek (1972). They both concluded that moving dislocations which were produced were more effective as sinks for vacancies than as sources, having a "sweeping-up" action as they pass through the metal. Postnikov's (1967) conclusion that these strains are an order of magnitude less than the strains due to anisotropy is applicable to the present work, so they will not be considered in more detail here.

In the present experiments a single crystal dummy specimen, initially in an annealed condition, showed variations in resistance which were attributed to these effects, including a decrease in resistance after annealing above 224 K. As annealing in this temperature range is thought to be due to dislocation movement rather than point defects, it appears that the dislocation structure of the dummy had been altered by the thermal cycling. The effect was not investigated in detail, however. To do so would have required a second dummy specimen kept in the cryostat throughout the run while the first one underwent temperature changes.

There seems to be no easy way round these difficulties of unwanted strains. The main steps which have to be taken to alleviate them are:

a) The use of single-crystal specimens which are as near perfect as possible. This has the disadvantage that fewer point defects are produced by a given amount of intentional strain in a perfect crystal, so that they are more difficult to detect; if more strain is used, the crystal becomes less perfect.

b) The use of a dummy which is as nearly identical as possible to the specimen. It might be best to use as a dummy a crystal which was initially the same as the specimen but which had previously been strained and then annealed at about 180 K. Since the recovery stage attributed to dislocation rearrangement lies above 200 K, the orientation and dislocation structure of the dummy should then be similar to that of the strained specimen, only the point defects being absent.

c) Stresses caused by thermal gradients could be reduced by making the changes in temperature occur slowly, but this is incompatible with the need for rectangular temperature-time pulses if the annealing results are to be interpretable.

5. DISCUSSION

5.1 Production of point defects by plastic deformation

In section 4.1 we showed that in polycrystalline cadmium deformed at 78 K the part of the resistivity increment which anneals out at room temperature is proportional to the strain with a coefficient (12.5 ± 0.7) nΩm per unit strain, for strains up to 10%. Simon and Delaplace (1972) find a resistivity increment of 36.6 nΩm per unit strain, but only about 30% of this anneals out at room temperature, that is 11 nΩm compared with my (12.5 ± 0.7) nΩm. We also showed that in single crystal zinc and cadmium strains of 1 to 2% produced resistivity changes of about 0.1 to 0.2%. A linear relationship between resistivity and strain was not established for single crystals, but the figures tend to indicate that if there were such a relationship the coefficient would not be much more than about 1.6 nΩm per unit strain.

We shall now consider possible mechanisms which could account for these increments, to see whether any one gives better agreement than the others. We shall also try to estimate the number of defects which would have been produced, so that we can calculate a value of the resistivity per defect.

The observed resistivity increment will be due to the combined effects of point defects and dislocations. In section 5.2 we attribute the annealing stages observed above 180 K to dislocations, and those below 180 K to point defects, so we can use the isochronal annealing curve Fig. 4.21-1 to find the separate contributions. This shows that 0.46 of the resistivity increment is due to dislocations and 0.54 is due to point defects. The distinction is not really as clear-cut as

this, because the point defects may condense to form loops, which will be bounded by a dislocation (Kratochvíl 1966), thus increasing the dislocation density during the point defect annealing stage, or, alternatively, point defects may allow dislocations to climb, reducing the total length of dislocation line during the point defect annealing stage (Price 1963). Both mechanisms probably operate. However, we can estimate that about half of the resistivity increment is due to point defects, and go on to consider how they may be produced.

The reasons why the rate of production of defects in single crystals is less than that in polycrystals probably include the following:

a) Deformation in single crystals is predominantly on the basal plane, on the (0001)<11$\bar{2}$0> system, so that dislocations are less likely to intersect one another than in polycrystals where in general at least five slip systems have to be operative, or where twinning and grain boundary slip have to occur to avoid discontinuities between grains. (Van Bueren 1961, p. 246).

b) The initial dislocation density in single crystals is likely to be lower than in polycrystals, so that even if the rates of dislocation multiplication are the same the number of additional dislocations produced by a given strain will be less than for polycrystals.

c) The rate of dislocation multiplication in single crystals is likely to be less, since if there are fewer intersections the glide distances are likely to be greater and a dislocation is more likely to escape from the surface than it is to become pinned and form a fresh source (Mott 1952).

Some quantitative estimates may be made of the number of defects produced by a given strain; since the calculations can be made only to an order of magnitude, zinc and cadmium will not be distinguished. Possible defect production mechanisms will be discussed in turn:

5.11 Recombination of parallel dislocations

Lines of point defects may be produced by the combination of parallel dislocations of opposite sign on neighbouring glide planes. This would be thought likely to be an important mechanism in the deformation of zinc and cadmium at low temperatures, where nearly all the mobile dislocations lie on basal planes. Simon and Delaplace (1972) favour this mechanism because it predicts a linear increase in the number of defects with strain, but they do not consider quantitatively the number of defects produced. For this mechanism to give a number of defects proportional to strain we can adopt a "fixed-barrier" model (Van Bueren 1961, pp. 155-159). This assumes that the barriers to dislocation motion confine the loops to a maximum distance L, and that pile-ups occur behind these barriers, eventually stopping the source from operating. According to this model, the number of defects produced per unit strain is l/L^2b^2, where b is the magnitude of the Burgers vector and l is the length of the recombining parts of the dislocations, presumably of the order of magnitude of the source length. To find the maximum number of defects which could reasonably be explained by this mechanism, we can consider the largest likely value of l and the smallest value of L. Suppose that both these values are ~10 μm; this is the average dislocation spacing when the dislocation density is 10^6 cm^{-2}. Then since $b = 3\times10^{-10}$ m, the number of defects produced will be 10^{24} m^{-3} per unit strain, a concentration of 2×10^{-3}% for unit strain. Taking our value of about 6 nΩm per unit strain due to point defects, this gives a resistivity of 3000 nΩm for 1% of defects, compared with theoretical values of around 10 nΩm (section 2.5). Anderson and Brown (1965) calculated a minimum value of 100 nΩm per 1% of vacancies, but this is 30 times less than the value predicted by this mechanism.

It therefore appears that the parallel dislocation recombination mechanism cannot produce a sufficient number of defects to explain the observed resistivity increase in terms of a reasonable value for the resistivity per defect. Even the resistivity increment for single crystals, which is about 10% of that for polycrystals, is too large for this explanation. Van Bueren, presumably using estimates of average values for l and L rather than the extreme values used above, obtains 10^{22} defects per m^3 per unit strain for copper, 100 times less than the value calculated here.

5.12 Movement of jogs

Jogs may be produced by the intersection of two screw dislocations moving on different glide planes, and if such a jog is dragged along by its dislocation it is forced to move non-conservatively and leaves a line of interstitial atoms or vacancies in its wake.

When both dislocations are able to move under the applied stress, it has been shown (Cottrell 1957; Hornstra 1962; Zsoldos 1963) that interstitial-producing jogs are formed when the intersecting dislocations are moving in opposite directions and that vacancy jogs are formed only on a slow-moving dislocation when overtaken by a faster one. Since "overtaking" intersections will be less frequent, more interstitial jogs will be produced than vacancy jogs. This mechanism may play some part in cadmium, where some slip on planes other than the basal plane can take place at low temperatures (this enhances the ductility of cadmium over that of zinc). However, in both metals the main type of dislocation intersection is likely to be between the mobile basal dislocations and the fixed "forest" dislocations. The forest dislocations are as likely to be of one sign as the other, and equal numbers of vacancy and interstitial-producing jogs will therefore be formed. Because the

formation energy of a vacancy is less than the formation energy of an interstitial, however, the vacancy-producing jogs will move more readily under a given stress than the interstitial-producing jogs, and thus more vacancies than interstitials will be formed (Hirth and Lothe 1968, p. 543).

Again we must use a fixed-barrier model to obtain a linear dependence of $\Delta\rho/\rho$ on strain (Van Bueren 1961), and the expression quoted for the number of vacancies per unit volume is $L\Lambda\varepsilon/b^2$. Here Λ, L and b are the dislocation density, the distance between barriers and the length of the Burgers vector respectively, ε being the strain.

Taking the same values as in section 5.11, viz. L = 10 μm, $\Lambda = 10^6$ cm^{-2}, gives a number of defects 10^{24} m^{-3} per unit strain, the same as for the recombination mechanism. However the value of L is now in the numerator, and if we let it take the more realistic value 0.5 mm, which is about the diameter of the grains, the number of defects produced will be about 5×10^{25} m^{-3} per unit strain. This corresponds to a defect concentration of 0.1% per unit strain, and our resistivity change of 6 nΩm per unit strain now leads to a resistivity of 60 nΩm for 1% of defects. This value falls between the theoretical value of 10 nΩm and Anderson and Brown's value of 100 nΩm, and since this is only an approximate order of magnitude calculation it could be compatible with either of them. Gertsriken and Slyusar (1958) found 37 to 55 nΩm.

The dislocation density may be a few orders of magnitude greater than the value of 10^6 assumed above (Kratochvíl and Homola 1966), and this will increase the number of defects produced by the moving-jog model. The effect of a greater dislocation density on the recombination model depends on how it affects the barrier distance L and the recombination length l. Since we have assumed that L is of the order of the dislocation spacing, it would decrease, and l would necessarily do so

too, since it is unlikely that the length over which recombination takes place should be greater than the size of the dislocation loops. The number of point defects produced would increase at the same rate as for the moving-jog model if $l \propto L$.

Boček (1963) has also noted that the number of vacancies produced by recombination is likely to be 3 to 5 orders less than those produced by jog intersection.

Van Bueren (1961) mentions some modifications of these models, such as the use of "growing" rather than "fixed" barriers to dislocation motion; these modified versions no longer predict a linear relationship between strain and the number of defects produced, but they give the same result that the number of defects produced by jog motion is a few orders of magnitude less than the number produced by recombination of edge dislocations.

5.13 Dislocation uncertainty

Kuhlmann-Wilsdorf and Wilsdorf (1962) suggested that thermal vibrations of the lattice might create jogs on dislocations, and the subsequent movement of these jogs could produce point defects. It is difficult to estimate accurately how important this effect would be, but the insertion of a few approximate figures into Kuhlmann-Wilsdorf's expression for the "uncertainty distance", δ, of the position of a dislocation line suggests that it would not play a large part. Taking

$$\delta = \bar{u}(8Gb/2\pi p\tau_{crit})$$

and inserting room temperature values we can put $\bar{u}$ = 5 pm, the mean thermal displacement of the atoms in zinc (Barron and Munn 1967), $p = (\sqrt{3}/2)b$ where p is the periodicity distance of the lattice on the slip plane perpendicular to the dislocation axis and b is the magnitude of the Burgers vector, $\tau_{crit} = G/30$ where τ_{crit} is the largest shear

stress the lattice could stand without dislocations and G is the shear modulus (Cottrell 1953). This gives $\delta \sim 32$ pm or an eighth of the nearest-neighbour atomic spacing, which is 266 pm in zinc. This implies that few jogs are likely to be produced by this mechanism in zinc, although Peiffer (1963) suggested that he had possibly shown that it did operate in copper, in which he found a resistivity increase due to point defects proportional to the resistivity increase due to line defects, as the mechanism predicts. There are other explanations of this proportionality, however, and Peiffer does not discuss the atomic mechanism quantitatively.

5.14 Saada's relation

Saada (1961) has proposed that the concentration of point defects produced by a dislocation-intersection mechanism should be proportional to the work done by the apparatus producing plastic deformation, i.e.

$$C_v \simeq \frac{A}{G}\int_0^{\varepsilon} \sigma d\varepsilon \qquad (5.14\text{-}1)$$

where G is the shear modulus and A is a constant which lies between 0.05 and 0.1 for face-centred cubic metals (van den Beukel 1970). Thus when the stress-strain curve is linear, as it almost is for the plastic deformation of h.c.p. metals (Fig. 3.2-1), C_v should be proportional to ε^2. Experimental results of the present work (section 4.1) and of Simon and Delaplace (1972) are that for cadmium the resistivity increase is proportional to ε up to about 7% deformation, and that Saada's model is therefore apparently not applicable to h.c.p. metals deforming by basal glide. Peiffer (1963a) measured the resistivity increase in cadmium with deformation, but could not fit a uniform power law to his values because they were not reproducible enough. The graph of $\Delta\rho$ vs. ε which he publishes, however, appears fairly linear up to

$\varepsilon = 5\%$.

Because the linearity of the resistance increase with strain has not been established conclusively, however, Saada's relation was applied to the deformation curve shown in Fig.3.2-1. This gave $\int_0^{\varepsilon} \sigma d\varepsilon = 128$ kPa, found by counting squares. The area under the unloading part of the curve was subtracted from the area under the loading part to remove the work done against elastic stresses. With a value of $G = 19.2$ GPa and $A = 0.1$, (5.14-1) predicts a defect concentration of $2.5 \times 10^{-3}\%$. This is the same as was obtained in considering the recombination mechanism, and by the same reasoning it is too small to explain the measured increase in electrical resistivity.

In summary, then, it appears that the non-conservative movement of jogs is the only mechanism which is able to produce sufficient defects to explain the observed resistivity increase, and that an explanation by this mechanism requires a concentration of 1% of defects to change the resistivity by the order of 60 nΩm.

5.2 The annealing of defects in zinc and cadmium

The present results are shown together with results which have been obtained in previous plastic deformation experiments on cadmium in Table 5.2-1 and Fig. 5.2-1. No-one has yet succeeded in producing a recovery spectrum of cold-worked zinc, although there have been other attempts by Sharp et al. (1965), who were not able to detect any change in resistance on annealing single crystals deformed at 90 K. In the present work some annealing was observed in zinc (see section 4.1) but its magnitude was not great enough for separate stages to be resolved satisfactorily.

The various experiments on cadmium have produced a variety of results which reflects the complex nature of the annealing process and its dependence on the state of the material. The annealing in the temperature range 78 to 273 K may be divided into three main ranges, as shown in Fig. 5.2-1. These may also be seen in Fig. 4.21-3, although the broad continuous recovery between 90 and 180 K tends to obscure the lower temperature part of the curve. There is also some indication of more structure, particularly in the curve obtained from specimen Cd 20, which was annealed for the shortest time at each temperature.

The effect of a different annealing programme on revealing fine structure is being investigated by Vostrý and Spružil (private communication, 1973) who obtained the differential isochronal annealing curves shown in Fig. 5.2-2. The curve labelled (1) had anneals of 2 min at temperature steps of 10 K; the curve labelled (2) had anneals of 4 min at temperature steps of 5 K. It appears that more fine structure is revealed when smaller temperature steps are used. From Fig. 4.21-3, however, it also appears that more detail is resolved when the annealing pulse times are short - the peak at 138 K, in particular, moves down in temperature and is

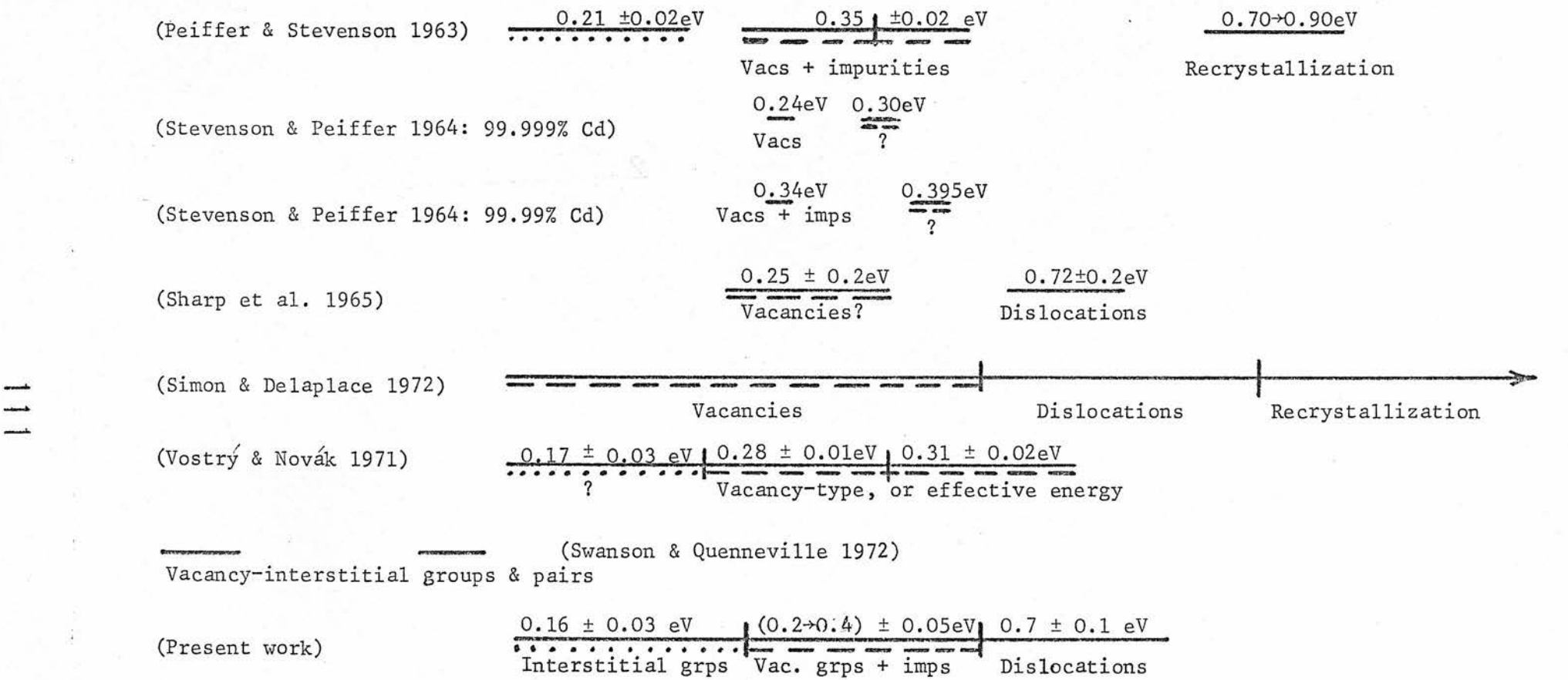

Fig. 5.2-1: Recovery stages in deformed cadmium (c.f. Fig. 2.2-1)

Table 5.2-1: Summary of annealing experiments after plastic deformation

Purity	Activation energy		Temp. range	No. of jumps	Order of kinetics	Interpretation	Investigator
	Method	E^m/eV	T/K				
99.99%	Ratio of slopes	0.21±0.02	78-118	5×10^6	-		Peiffer &
	and		128-158	$\sim10^4$	-	Monovacancies +	Stevenson (1963)
	cross-cuts	0.35±0.02	158-178	$10^5\rightarrow10^7$	-	impurities	
		0.70→0.90	228-258	$10^2\rightarrow10^{-2}$	-	Recrystallization	
99.999%	Ratio of slopes	0.24	138	7×10^6	1	Monovacancies	Stevenson &
		0.30	158	10^7	(assumed)	?	Peiffer (1964)
99.9997%	Cross-cuts	0.25±0.2	125-160	-	-	Vacancies	Sharp et al.
		0.72±0.2	185-210	-	-	Dislocn rearrangement	(1965)
99.9999%	Not determined	-	77-180	-	-	Vacancies?	Simon & Delaplace
		-	180-240	-	-	Dislocn rearrangement / Polygonization	(1972)
			240→	-	-	Recrystallization	
99.998%	Ratio of slopes	0.17±0.03	78-120	-	1	E^m too low for vacs; T too high for interstitials	Vostrý & Novák (1971)
		0.28±0.01	120-160	2×10^6	1	Vacs, divacs, or some	
		0.31±0.02	160-200	5×10^7	1	effective energy	
99.998%	Not determined	-	4.2-10			Vac-interstit groups	Swanson &
			10-20	-	-	and pairs	Quenneville (1972)
			60-75				
99.999%	Logarithmic	0.16±0.03	80-130	3×10^9	Variable	Interstitial groups	Present work
	ratio of slopes	0.2 →0.4	130-180	10^8	Variable	Vacancy groups + imps	
		0.7 ±0.1	180-220	-	-	Dislocn rearrangement	

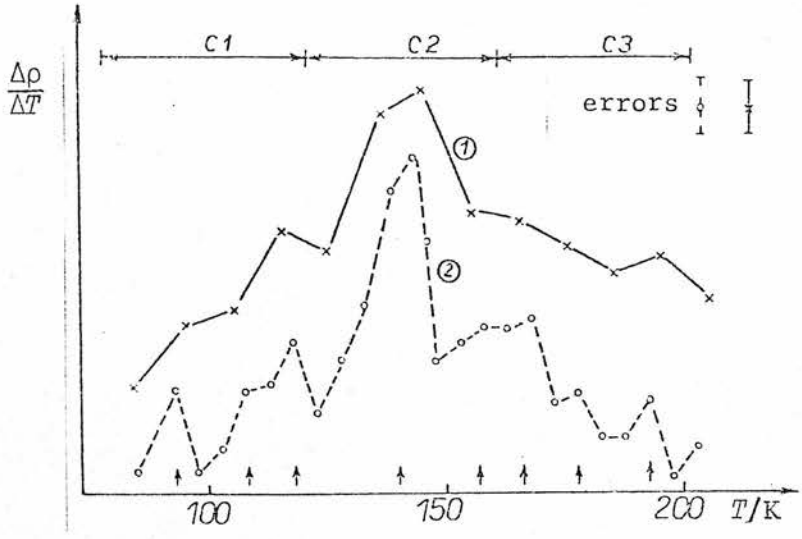

Fig. 5.2-2: Differential annealing curves for 99.998% cadmium deformed by torsion at 78 K. (Sprušil and Novotný, 1973 - private communication from Sprušil and Vostrý)

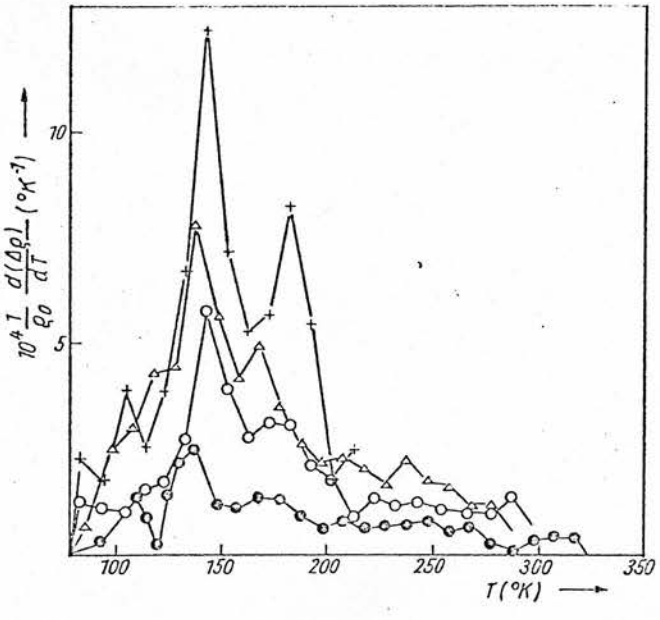

Isochronal differential annealing curves for samples of 99.998 at% Cd deformed by torsion at 78 °K
+ 15 revolutions, △ 12 revolutions, o 10 revolutions, • 8 revolutions

Fig. 5.2-3: Curves published by Vostrý and Novák, 1971

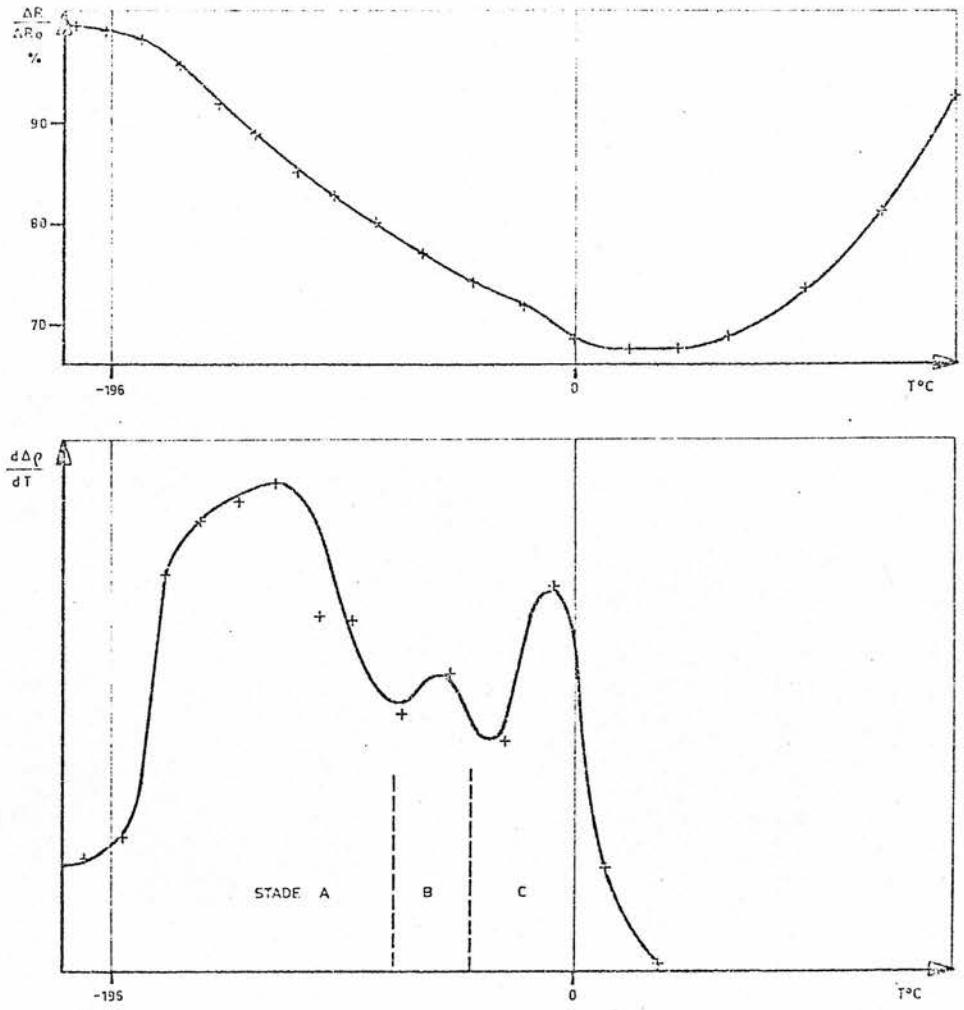

Fig. 5.2-4: Isochronal and differential isochronal annealing curves for a cadmium specimen deformed 8% in tension at 78 K (Simon and Delaplace 1972)

finally lost altogether as the pulse times are increased. Short pulses introduce uncertainties, however, because of the time taken to change temperature at the beginning and end of the pulse. This limits the minimum pulse length which can reasonably be used to about one minute.

The only published differential isochronal annealing spectra of cold-worked cadmium above 78 K are those of Vostrý and Novák (1971) and Simon and Delaplace (1971), reproduced in Figs. 5.2-3 and 5.2-4. Other annealing stages lie at temperatures below 78 K (Swanson and Quenneville 1972) - these were outside the range of the present experiment, but their nature will be considered in attempting to synthesise an overall picture of the annealing processes which occur.

Each of the annealing stages will be discussed in turn, beginning with the highest temperature stages, on which there is most agreement.

5.21 Stage V: dislocation annealing and recrystallization (above 180 K)

It seems to be agreed that recovery above about 180 K is due first to dislocation rearrangement (polygonization) and then, at temperatures above 240 K, to recrystallization. Sharp et al. (1965) and Vostrý and Novák (1971) both observed that above 200 K the diffuse maxima seen in back-reflection X-ray pictures broke up into small groups of sharp spots. In the electron microscope Price (1961) saw rapid recovery by dislocation climb at temperatures above 233 K. Simon and Delaplace (1972) and Sharp et al. (1965) both found a recovery in mechanical properties in an annealing stage between 180 K and 240 K. Simon and Delaplace (1972) and Peiffer and Stevenson (1963) found that the recrystallization tended to increase the proportion of grains having their c-axis parallel to the direction in which the tensile deformation had taken place, with a consequent increase in resistivity in that direction. Because of this, in considering resistivity changes

in a deformed polycrystalline specimen it is not valid to assume that the minimum value of resistivity, with respect to which increments can be measured, will be the value attained after a long anneal at temperatures above 250 K.)

This stage of dislocation recovery is not present in quenched or irradiated specimens, although Sprušil et al. (1970) supposed that a similar mechanism involving the dissolution of some type of vacancy agglomerate was responsible for a stage seen at over 280 K. The activation energy of (0.7 ± 0.1) eV found for this stage (Table 4.34-1) is near the energy of ~ 0.8 eV found by Price (1961) for dislocation climb, which is also about equal to the self-diffusion energy in cadmium which is, on average, 0.82 eV (section 2.14).

5.22 Stage IV: vacancy complexes (130 to 180 K)

The broad peak found at around 150 K, with an energy which increases with temperature from 0.2 to 0.4 eV has also been observed before (Fig. 5.2-1). Stevenson and Peiffer (1964) considered that the energy of 0.24 eV which they found in 99.999% cadmium was the migration energy of monovacancies, and that the higher value, 0.34 eV, which they had previously found in 99.99% cadmium (Peiffer and Stevenson 1963) indicated a binding energy of at least 0.10 eV between vacancies and impurities. Vostrý and Novak (1971), who found a value of 0.28 eV for this peak, thought it too low for E^{m}_{1v}, but suggested that it might be either (a) monovacancy migration in a direction which requires low activation energy, or (b) divacancy migration, or (c) some effective migration energy.

Fig. 4.21-3 shows, for specimen Cd 20, a small sub-stage at about 170 K. A measured value of the energy at this temperature is (0.49 ± 0.09) eV (Fig. 4.34-1). Both the above teams found this peak, at temperatures of 160 K and 180 K

respectively, with energies of 0.4 eV and 0.31 eV, but no specific explanation of it was put forward. It was not observed by Sharp et al., and not mentioned by Simon and Delaplace, although a deviation of their experimental points from the curve which they draw may be evidence for its existence. A corresponding sub-stage with an energy of (0.48 ± 0.05) eV was found in quenched cadmium by Vostrý et al. (1972), who considered that it was caused by the freeing of vacancies from impurity traps. The number of jumps was a few hundred, which was too few for the sub-stage to be entirely due to free vacancy migration to fixed sinks; the annealing kinetics were first order; and the energy was too great (in comparison with estimates from self-diffusion and vacancy formation energies) for single vacancies. They also noticed that the magnitude of this stage saturated, as the quench temperature increased, at a defect concentration of about 10^{-6}, which is the same order as the impurity concentration in their specimens.

The remainder of stage IV is generally attributed to the migration of vacancies or vacancy aggregates. It is difficult to come to more specific conclusions than this. The available information is a mean activation energy of about 0.27 eV, and a number of jumps of about 10^8 (section 4.36). As discussed in sections 4.34 and 4.35, it is not possible to determine a unique value of γ, the order of annealing kinetics, in a broad spectrum of annealing processes, although Vostrý and Novák were able to fit their results in this range to $\gamma = 1$.

Even the activation energy must be interpreted with caution. Johnson (1968) has shown by computer calculations on the annealing of clusters of 2 to 7 vacancies that when two or more types of vacancy cluster are annealing simultaneously anomalous values of activation energy can be obtained, and "even if the results appear to be regular, simple interpretations can be very misleading". When monovacancies

and impurities are included too "in general it will be very difficult to extract meaningful numbers from experimental data". As an example of this, Chick (1970) shows that there are still considerable uncertainties in determining the monovacancy migration energy for a well-investigated face-centred-cubic metal such as gold. At concentrations more than about 10^{-6} atomic fraction of defects the energy measured will be an effective one, and these effective energies have a scatter of at least 0.1 eV, even at a fixed defect concentration. The best values are found to be: for monovacancies, E^{m}_{1v}(Au) = 0.89 eV, and for divacancies, E^{m}_{2v}(Au) = 0.7 eV.

Bearing this caution in mind, we can nevertheless look at the energy values obtained for stage IV to see whether the vacancy interpretation is reasonable. The average self-diffusion energy, E^{sd}, for cadmium is 0.82 eV (Schumacher 1970), and the formation energy, E^{f}_{1v}, is (0.41 ± 0.02) eV (section 2.1). These values lead to

$$E^{m}_{1v} = E^{sd} - E^{f}_{1v} = 0.41 \text{ eV}.$$

For zinc the same sources give E^{f}_{1v} = 0.5 eV and E^{sd} = 1.0 eV, whence E^{m}_{1v} = 0.5 eV. The value of E^{m}_{1v}(Cd) is larger than the energies found experimentally for stage IV annealing, so the mobile defect appears not to be the monovacancy. Sprušil et al. (1970) calculated the divacancy energy E^{m}_{2v} on the assumption that the ratio E^{m}_{1v}/E^{m}_{2v} would be the same for cadmium as for gold. Taking the values for gold quoted above gives E^{m}_{2v}(Cd) = 0.31 eV, in fair agreement with the experimentally determined energy.

A similar calculation was used by Anderson and Brown (1965) in calculating E^{m}_{2v} = 0.32 eV for zinc, this being the activation energy of the defects which they found annealing after deformation jumps at room temperature.

Peiffer and Stevenson (1963) found that the number of jumps taken by defects in this stage was initially ~10^4, but that at later parts of the stage it increased to 10^7. This can be explained if we assume that the defects were vacancies annealing initially to impurity traps - the number of jumps agrees with the impurity concentration of 10^{-4}. When these traps became filled the vacancies would have to go further, presumably to dislocations.

If the number of vacancies produced gave a concentration of 10^{-3} per unit strain, as discussed in section 5.12, Peiffer's 5.8% deformation would have produced a concentration of ~6×10^{-5} defects, compared with an impurity concentration of 10^{-4}. Thus there should have been just about enough defects to fill the available impurity traps, assuming that some of the impurities would be in clusters or segregated to dislocations or grain boundaries where they would not contribute fully as separate traps.

Thus it is reasonable to ascribe stage IV to the annealing of vacancy-type defects, but not to the simple migration of monovacancies. Divacancies and probably other vacancy clusters are likely to be the main mobile defects, but the activation energies and kinetics are complicated by their interactions with each other and with impurities.

5.23 Stage III: interstitials (80 to 130 K)

This is the least well explained stage. It overlaps with stage IV and is not completely resolved in all three curves of Fig. 4.21-3. The activation energy in this stage was found to be (0.16 ± 0.03) eV and the mean number of jumps to destruction was about 10^9.

Peiffer and Stevenson (1963) and Vostrý and Novák (1971) resolved the stage in cold-worked cadmium; Sharp et al. (1965) saw it in single crystals but not in polycrystals, and it was presumably absorbed in

Simon and Delaplace's (1971) very broad stage covering 77 to 180 K (Fig. 5.2-4). The activation energy of around 0.2 eV corresponds to a stage seen between 120 and 200 K in quenched cadmium (Sprusil et al. 1970). Both Vostrý and Spružil dismissed the explanation of this stage in terms of interstitials on the grounds that Coltman et al. (1971) had shown that interstitials produced by irradiation were mobile at below 26 K. Coltman's interpretation has been challenged by Seeger (1970), however, who proposed that interstitials were responsible for Coltman's 120 K annealing stage (see section 2.3). If this is correct, it seems appropriate to interpret stage III in deformed specimens in terms of interstitials too. The fact that it generally occurs at lower temperatures after deformation than after irradiation is probably because of the greater number of dislocation sinks which will be present. The stage attributed to vacancies is also usually at a lower temperature in deformed specimens.

If stage III were due to interstitials, it ought not to have been seen by Spružil et al. (1970) in quenched cadmium. Polycrystalline cadmium was used, however, and as shown in section 4.4 anisotropic thermal expansion would certainly have produced plastic deformation in wires 0.7 mm in diameter when quenched from 503 K to 78 K. It was present, therefore, with an energy (0.19 ± 0.01) eV and 10^{11} jumps to destruction, compared with 3×10^{9} in the present work. Vostry et al. (1972) using 0.25 μm x 1 mm ribbons did not observe the stage, but it may have been obscured by an increase in resistance which took place at that temperature and which was ascribed to "quenching constraints".

Peiffer and Stevenson's calculation of the number of jumps taken by a defect annealing in stage III gave a value of 5×10^{6}. This agrees with the number of up to 10^{7} which they found in the later part of the

0.35 eV annealing stage (stage IV), so the two types of defect could have been annealing to the same dislocation sinks. The impurities which initially trapped vacancies after 10^4 jumps presumably were not effective as traps for interstitials

In the present work about 10^9 jumps were found in stage III, compared with Peiffer's value of 5×10^6. These values correspond to dislocation densities of $\sim 10^{10}$ m^{-2} (10^6 cm^{-2}) and $\sim 5 \times 10^{13}$ m^{-2} (5×10^9 cm^{-2}) respectively. The higher value seems the more reasonable one for polycrystals deformed about 6%. No evidence was seen in the present work of a smaller number of jumps of about 10^5 which would correspond to annealing to impurities, which were present at a concentration of 10^{-5}.

Unfortunately the number of jumps for the stage III peak was not investigated in Stevenson and Peiffer's later experiment (1964) with 99.9999% cadmium, in which the number of jumps of the stage IV defect was found to be $\sim 10^7$. In this case the distance to impurity sinks would have been about the same as the distance to dislocation sinks, so that if stage III was due to interstitials it would have been expected to give a number of jumps of $\sim 10^7$ too.

There are, unfortunately, no theoretical or empirical calculations of the migration energy of interstitials in cadmium with which the observed 0.19 eV can be compared. Van den Beukel (1970) tabulates energies between 0.28 and 0.44 eV which have been found for annealing in the corresponding stage in gold, but there is some disagreement on the nature of the process; Van den Beukel favours the migration or break-up of interstitial agglomerates. If we compare the energy found for this stage for gold with E_{1v}^m for gold and cadmium as we did in section 5.22, we predict that the energy for this stage in cadmium

would be [(0.3 to 0.4) x 0.5/0.9] eV = 1.6 to 2.2 eV, a range which includes the measured value of 0.19 eV. There is therefore some justification for considering that stage III in cadmium is analogous to a stage in gold which has been attributed to the annealing of interstitial-type defects.

5.24 Stages I and II: recombination of close pairs and other groups (<80 K)

The only deformation and recovery experiments in cadmium carried out below 78 K are those of Swanson and Quenneville (1972), who found recovery stages below 60 K similar to those seen by Coltman et al. (1971) in neutron-irradiated material, and attributed to the recombination of Frenkel defects and other vacancy-interstitial groups. Another stage at about 70 K can be seen in Swanson's graphs, which stop at 75 K, and this may well be the beginning of stage III.

5.3 Sinks for defects during annealing

In section 4.36 we calculated that in the present work defects annealed with a mean number of jumps to destruction of about 3×10^9 in stage III and 10^8 in stage IV. The nature of the sinks has been mentioned in sections 5.22 and 5.23. We shall now consider some other possibilities and complications.

The mean number of jumps to destruction is, in the case of point sinks, approximately equal to the reciprocal of the concentration of sinks (Damask and Dienes 1963, pp. 81-84), so if the sinks were impurities their concentration would have to be 10^{-8} to 10^{-9}, values which are much less than the actual impurity concentration of about 10^{-5}. If the sinks are dislocations, the atomic fraction of sites which lie on dislocations is given by the number of dislocation lines cutting unit area, i.e. the dislocation density, Λ, divided by the number of atoms

per unit area, $1/b^2$, where b is the lattice spacing, assuming a cubic lattice. This gives Λb^2 for the effective concentration of point sinks, and $1/\Lambda b^2$ for the mean number of jumps to destruction. This is the expression quoted by Van den Beukel (1970).

With $b = 3 \times 10^{-10}$ m, the experimentally found numbers of jumps then require dislocation densities of 3×10^{9} m^{-2} (3×10^{5} cm^{-2}) at 115 K and 10^{11} m^{-2} (10^{7} cm^{-2}) at 160 K. Both these values seem rather small for the dislocation density in deformed specimens, and it is therefore possible that dislocations are not very effective as sinks for point defects.

Point defects may also anneal to grain boundaries. The mean radius of the grains was ~ 250 μm, and if we assume that they were spherical a solution of the equation for point defect diffusion gives (Damask and Dienes 1963, pp. 79-81) a mean number of jumps to destruction of 7×10^{10}. This is larger than the experimental number of jumps, which therefore lies between the values expected if either dislocations or grain boundaries were acting as traps. If both were effective then this would be reasonable.

However there is also considerable evidence that point defects do not anneal to pre-existing traps at all, but condense to form "platelets" - discs of stacking fault, parallel to the basal plane, bounded by a partial dislocation. Seeger and Trauble (1960) predicted these loops to explain decreases in slip-line length and increases in the work-hardening coefficient which they found after short anneals at room temperature, and they have been seen in the electron microscope by Price (1963) and by Berghezan et al. (1961). This provides another possible reason for the complex annealing kinetics observed, because the resistivity change when point defects condense into loops will depend on the number and size of the loops and the proportion of defects

which create new loops rather than joining pre-existing ones.

These loops may be stable at quite high temperatures, and may even grow as a result of vacancy creation during oxidation of the surface which occurs on exposure to air (Michell and Ogilvie 1966). It has also been suggested (Harris and Masters 1966a, 1966b) that the oxide film may retain supersaturations of vacancies in zinc, magnesium and aluminium at temperatures where they are mobile, by preventing them from condensing at the surface. This effect would be most noticeable in small, perfect single crystals and foils where few traps other than the surface would be available, but in polycrystalline material there would be many other sinks.

6. CONCLUSIONS

6.1 When polycrystalline cadmium is deformed by tensile strains of up to 10% at 78 K the annealable component of the resistivity increment increases linearly with strain, with a coefficient (12.5 ± 0.7) nΩm per unit strain.

6.2 When single crystals of zinc and cadmium are given small tensile strains an annealable component of the resistivity increment is produced. Its magnitude is not very reproducible, but is usually of the order of 0.1% to 0.2% for strains of 1 to 2%.

6.3 The dislocation intersection mechanism with fixed barriers is the most likely means of production of point defects.

6.4 A resistivity of 60 nΩm per atomic percent of point defects in cadmium would be compatible with the results obtained.

6.5 About half of the annealable resistivity increment anneals out at above about 180 K. This stage (stage V) is attributed to dislocation annealing and recrystallization, and occurs with an effective activation energy of (0.7 ± 0.1) eV.

6.6 In the range 130 K - 180 K a broad annealing stage (stage IV) occurs, with an activation energy which increases with temperature from 0.2 to 0.4 eV. A substage at 160 - 180 K, with an energy over 0.4 eV, is probably due to the freeing of vacancies from impurity traps, and the remainder of the stage to the migration of vacancies and complexes of vacancies with other vacancies and with impurities. The stage is clearly not due to a single process, and a unique order of kinetics can therefore not be obtained. The activation energy too should probably not be associated with any specific defect, but Anderson and Brown's (1965) value of (0.32 ± 0.03) eV for the divacancy in zinc falls within the observed range. The number of jumps found was about 10^8,

which would agree with annealing to dislocations at a density of 10^7 cm^{-2}.

6.7 Stage III, at temperatures of 80 K to 130 K, with an activation energy of (0.16 ± 0.03) eV, is probably due to interstitials and their aggregates. The number of jumps was about 3×10^9, so annealing was not to impurity traps but probably to dislocations or grain boundaries.

6.8 Stages I and II, which lie below the range investigated in the present work, are probably due to the recombination of Frenkel defects and other close interstitial-vacancy groups.

7. FUTURE WORK

The available annealing measurements on zinc and cadmium are still not extensive enough for definitive statements to be made about the processes involved. There is no complete set of data from 4.2 K to 300 K for quenched or deformed specimens comparable to the results of Coltman et al. (1971) for irradiated cadmium. The obtaining of such data would not be easy (Coltman's team at Oak Ridge National Laboratory took several years to obtain theirs) but its availability would make the interpretation of the annealing behaviour much more certain. In particular it would be useful to know the annealing behaviour after quenching of high-purity cadmium and zinc in the form of small diameter single crystals of as great a perfection as possible. The contribution of defects other than vacancies should be small in such specimens, so that the stage of vacancy annealing should be identifiable. The use of a second dummy specimen, which remains in the liquid nitrogen bath is to be recommended as a check on the amount of thermal strain introduced during annealing.

The apparatus developed for the present work could be used to obtain more extensive data than is presented here. Some slight modification to the annealing bath is desirable, as mentioned in section 3.45, but then it would be useful to look in more detail at the following:

a) The effect of varying the time and temperature steps in an isochronal annealing programme, to find an optimum combination for revealing details of the annealing spectrum.

b) Isothermal annealing data at various temperatures after various pre-annealing treatments at lower temperatures to try to isolate effects due to individual species of defects.

c) The effect of different structures in the specimen before deformation on both the number of defects produced and their annealing behaviour. The effect of different grain sizes, prior deformation at room temperature, and prior deformation and annealing at low temperature could be investigated, preferably in conjunction with electron-microscope or etch-pit studies of dislocation structure, to clarify the role played by the different defect production mechanisms discussed in section 5.1 and the nature of the traps involved in point defect annealing.

d) The effect of controlled amounts of impurities on the annealing behaviour, to investigate their role as traps for point defects, shown by the effect of the additional binding energy and by the number of jumps taken by a defect in annealing. It would be interesting to look at the different effects of substitutional impurities which were (i) larger than the cadmium atoms, and which would therefore trap vacancies more readily than interstitials, and (ii) smaller than the cadmium atoms and which would therefore trap interstitials more readily.

Much theoretical work in this field still needs to be done too, although some of the problems have remained without a satisfactory solution for so long that they are probably not susceptible to solution by straightforward methods. As mentioned in section 2.5, though, many calculations have been made of the properties of point defects in f.c.c. metals, to the neglect of the hexagonal metals. Some of the techniques developed for the f.c.c's could certainly be applied in this direction. It would be of particular interest to have theoretical values for the formation energy of interstitials in various configurations (e.g. as a crowdion and in the space between adjacent basal planes) and to know with what activation energy, jump frequency and jump vector they migrate.

The present values for the resistivity increment due to vacancies vary widely, and those for interstitials are non-existent, so that theoretical work is also called for on this aspect.

REFERENCES

AFMAN, H.B. (1971) A method for the determination of the activation energy of recovery processes as applied to electron-irradiated molybdenum. *Phys. Stat. Sol. (a)*, 4, 427-433.

ANDERSON, J.M. (1965) A study of point defect production during jump deformation of zinc. Ph.D. thesis, University of Edinburgh.

ANDERSON, J.M. and BROWN, A.F. (1965) Point defect production during jump deformation of zinc. *Phys. Stat. Sol.*, 12, 309-320.

BS 1828:1961 (1961) Reference tables for thermocouples (copper v. constantan). London: British Standards Institution.

BALARIN, M., RATTKE, R. and ZETZSCHE, A. (1967) Zur Auswertung isochroner Ausheilkurven. *Phys. Stat. Sol.*, 22, 123-129.

BALLUFFI, R.W. and SIEGEL, R.W. (1965) On problems associated with the analysis of complex annealing kinetics in quenched metals: annealing model for quenched gold. *In: Lattice defects in quenched metals; an international conference held at the Argonne National Laboratory, 1964. Edited by R.M.J. Cotterill (and others).* New York: Academic Press. pp. 694-712.

BARRON, T.H.K. and MUNN, R.W. (1967) Mean-square atomic displacements in zinc. *Acta Crystallog.*, 22, 170-173.

BERGHEZAN, A., FOURDEUX, A. and AMELINCKX, S. (1961) Transmission electron microscopy studies of dislocations and stacking faults in a hexagonal metal: zinc. *Acta Metall.*, 9, 464-490.

BELL, F. and SIZMANN, R. (1966) Determination of activation energy from step annealing. *Phys. Stat. Sol.*, 15, 369-376.

BLEWITT, T.H., COLTMAN, R.R., HOLMES, D.K. and NOGGLE, T.S. (1957) Mechanism of annealing in neutron irradiated metals. *In: Creep and recovery: a seminar on creep and recovery of metals held during the thirty-eighth National Metal Congress and Exposition, Cleveland, 1956.* Cleveland: Amer. Soc. for Metals.

BOAS, W. and HONEYCOMBE, R.W.K. (1947) The anisotropy of thermal expansion as a cause of deformation in metals and alloys. *Proc. Roy. Soc., A*, 188, 427-439.

BOČEK, M. (1963) Zusammenfassende Darstellung der Gleitverformung in Metallen mit dichtest gepackter Strucktur. *Phys. Stat. Sol.*, 3, 2169-2214.

BOČEK, M., LUKÁČ, P., SMOLA, B. and SVÁBOVÁ, M. (1964) Die Temperaturabhängigkeit der Verfestigungskenngrößen von Kadmiumeinkristallen. *Phys. Stat. Sol.*, 7, 173-188.

BRINKWORTH, B.J. (1968) An introduction to experimentation. London: English U.P.

CHALMERS, B. (1935) The twinning of single crystals of tin. *Proc. Phys. Soc.*, 47, 733-746.

CHICK, K.P. (1970) Annealing and clustering of quenched-in vacancies in f.c.c. metals. *In: Vacancies and interstitials in metals; proceedings of the International Conference held at Jülich, Germany, 1968. Editors A. Seeger (and others).* Amsterdam: North-Holland. pp. 183-212.

COLTMAN, R.R., KLABUNDE, C.E. and REDMAN, J.K. (1967) Survey of thermal-neutron damage in pure metals. *Phys. Rev.*, 156, 715-734.

COLTMAN, R.R., KLABUNDE, C.E., REDMAN, J.K. and SOUTHERN, A.L. (1971) Thermal neutron damage in cadmium. *Radiation Effects*, 7, 235-262.

CONNORS, D.C., CRISP, V.H.C. and WEST, R.N. (1971) The effects of vacancies on positron annihilation in cadmium. *J. Phys., F*, 1, 355-362.

COTTERILL, R.M.J. (1965) Lattice defects in quenched metals; an international conference held at the Argonne National Laboratory, 1964. Edited by R.M.J. Cotterill (and others). New York: Academic Press.

COTTRELL, A.H. (1953) Dislocations and plastic flow in crystals. Oxford: Oxford U.P.

COTTRELL, A.H. (1957) The intersection of gliding screw dislocations. *In: Dislocations and mechanical properties of crystals. An international conference held at Lake Placid, 1956. Editors J.C. Fisher (and others).* New York: Wiley; London: Chapman & Hall.

DAMASK, A.C. and DIENES, G.J. (1963) Point defects in metals. New York: Gordon & Breach.

DIMITROV, O. (1968) Méthodes expérimentales de mesure de la résistivité résiduelle. *Mem. Sci. Rev. Métall.*, 65, 469-475.

DUGDALE, R.A. (1952) The extra electrical resistance due to cold work and neutron irradiation of platinum. *Phil. Mag.*, 43, 912-914.

DWORSCHAK, F., HERSCHBACH, K. and KOEHLER, J.S. (1964) Experiments on stage III annealing in the noble metals. *Phys. Rev.*, 133, A293-A303.

FANG, P.H. (1970) Reaction-rate kinetics and distribution of activation energies. *Phys. Rev., B*, 1, 932-933.

FEDER, R. and NOWICK, A.S. (1972) Dilatometric and X-ray thermal expansion in noncubic crystals. II. Experiments on cadmium. *Phys. Rev, B*, 5, 1244-1253.

FISCHER, O. (1969) Method of least squares. Fitting curves to empirical data. Elements of the calculus of observations. *In: Survey of applicable mathematics, edited by K. Rektorys.* London: Iliffe. Chapter 35, pp. 1285-1321.

FUJITA, F.E. and DAMASK, A.C. (1964) Kinetics of carbon precipitation in irradiate iron. II. Electrical resistivity measurements. *Acta Metall.*, 12, 331-339.

GERMAN, S. (1954) Crystallographic lattice defects in zinc and cadmium single crystals. *Z. Metallkunde*, 45, 674-676.

GERRITSEN, A.N. (1956) Metallic conductivity, experimental part. *In: Encyclopedia of physics (Handbuch der Physik) edited by S. Flügge. Vol. 19: Electrical conductivity I.* Berlin: Springer. pp. 137-226.

GERTSRIKEN, S.D. and SLYUSAR, B.F. (1958) On the determination of the energy of vacancy formation and their number in pure metals. *Phys. Metals Metallogr.*, 6, 103-111.

GEVERS, R., NIHOUL, J. and STALS, L. (1968) On the analysis of experimental data on point defect recovery. *Phys. Stat. Sol.*, 15, 701-716.

GILDER, H.M. and WALLMARK, G.N. (1969) Thermal-expansion measurements of vacancy formation parameters in zinc single crystals. *Phys. Rev.*, 182, 771-777.

GILMAN, J.J. (1956) Etch pits and dislocations in zinc monocrystals. *J. Metals (Trans. AIME)*, 206, 998-1004.

GOSS, A.J. (1953) An optical goniometer for the examination of long metal single crystals. *J. Sci. Instrum.*, 30, 283-285.

HARRIS, J.E. and MASTERS, B.C. (1966a) The effect of a surface oxide film on the lifetime of vacancies in quenched specimens. *Phil. Mag.*, 13, 963-969.

HARRIS, J.E. and MASTERS, B.C. (1966b) The annealing of faulted loops in magnesium and zinc. *Proc. Roy. Soc., A*, 292, 240-263.

HARRISON, W.A. (1963) Electronic structure and the properties of metals. I: Formulation. II: Application to zinc. *Phys. Rev.*, 129, 2305-2311, 2512-2524.

HILLAIRET, J., MARTINET, B. and SCHUMACHER, D. (1969) Etude des lacunes dans le cadmium. *Phys. Stat. Sol.*, 34, 797-803.

HIRTH, J.P. and LOTHE, J. (1968) Theory of dislocations. New York: McGraw-Hill.

HOCH, M. (1970) Equilibrium measurements in high melting point materials. *In: Vacancies and interstitials in metals; proceedings of the International Conference held at Jülich, Germany, 1968. Editors A. Seeger (and others).* Amsterdam: North-Holland. pp. 81-90.

HORNSTRA, J. (1962) On the type of point defects formed after crossing of dislocations. *Acta Metall.*, 10, 987-988.

HUBER, J.C. (1969) Gas flow temperature controller. *J. Sci. Instrum., Series 2*, 2, 294-296.

HUNTINGTON, H.B. (1958) The elastic constants of crystals. *In: Solid state physics; advances in research and applications. Editors F. Seitz and D. Turnbull.* New York: Academic Press. Vol. 7, pp. 213-351.

JACKSON, J.J. (1965) Strains in quenched metals. *In: Lattice defects in quenched metals; an international conference held at the Argonne National Laboratory, 1964. Edited by R.M.J. Cotterill (and others).* New York: Academic Press. pp. 479-520.

JANOT, C. and GEORGE, B. (1971) Dilatometric observation of vacancies in cadmium. (In French). *In: French Soc. Metallurgy autumn meeting, Paris, 27 Sep - 1 Oct 1971. Abstracts.* Paris: Fr. Soc. Metall. 2pp.

JOHNSON, R.A. (1968) Kinetic study of vacancy clustering and annealing in metals. *Phys. Rev.*, 174, 684-690.

JOHNSON, R.A. (1973) Empirical potentials and their use in the calculation of energies of point defects in metals. *J. Phys., F*, 3, 295-321.

KANOLT, C.W. (1926) Nonflammable liquids for cryostats. *Bur. Stand. Sci. Pap.*, 520, 619-633.

KRASOVA, J. and KRATOCHVÍL, P. (1971) Temperature dependence of the flow stress in secondary glide planes of cadmium single crystals. *Phys. Stat. Sol., (a)*, 7, 255-261.

KRATOCHVÍL, P. (1966) On the dislocation arrangement in deformed crystals of zinc. *Phil. Mag.*, 13, 267-274.

KRATOCHVÍL, P. and HOMOLA, J. (1966) On dislocations etched in deformed cadmium single crystals. *Acta Metall.*, 14, 1757-1764.

KUHLMANN-WILSDORF, D. and RAGHAVAN, K.S. (1962) New tensile testing machine for thin specimens. *Rev. Sci. Instrum.*, 33, 930-933.

KUHLMANN-WILSDORF, D. and WILSDORF, H.G.F. (1962) Production of point defects and jogs through dislocation uncertainty. *Acta Metall.*, 10, 584-586.

KURIBAYASHI, K., TANIGAWA, S. NANAO, S. and DOYAMA, M. (1973) Evaluation of the formation entropy of a single vacancy by means of positron annihilation. *Solid State Commun.*, 12, 1179-1182.

KUZNETSOV, V.D. and GRIBANOV, S.A. (1962) Low-temperature cyclic heat treatment of metals with hexagonal structure. *Sov. Phys. Doklady*, 7, 558-560.

LEE, C. and KOEHLER, J.S. (1968) Stage 3 annealing in gold after electron irradiation. *Phys. Rev.*, 176, 813-826.

LEVI, F.A. (1965) Resistivity changes caused by low-temperature thermal expansion. *Nuov. Chim. Suppl.*, 3, 1255-1257.

LUCASSON, A. and LUCASSON, P. (1966) Experimental results obtained in low temperature electron irradiation of Pd, Mo, Zn and α-U. *J. Phys. Chem. Solids*, 27, 1423-1429.

LUCASSON, P.G. and WALKER, R.M. (1962) Production and recovery of electron-induced radiation damage in a number of metals. *Phys. Rev.*, 127, 485-500.

McCAMMON, R.D. and WHITE, G.K. (1965) Thermal expansion at low temperatures of hexagonal metals: Mg, Zn and Cd. *Phil. Mag.*, 11, 1125-1134.

McKEE, B.T.A., TRIDTSHÄUSER, W. and STEWART, A.T. (1972) Vacancy-formation energies in metals from positron annihilation. *Phys. Rev. Lett.*, 28, 358-360.

MAGNUSON, G.D., PALMER, W. and KOEHLER, J.S. (1958) Isothermal annealing below 60 ^{o}K of deuteron irradiated noble metals. *Phys. Rev.*, 109, 1990-2002.

MARCH, N.H. (1973) Displaced charge and formation energies of point defects in metals. *J. Phys., F*, 3, 233-247.

MAURY, F., LUCASSON, A. and LUCASSON, P. (1969) On the behaviour of low temperature irradiated cadmium. *Radiation Effects*, 1, 241-248.

MAURY, F., LUCASSON, A. and LUCASSON, P. (1971a) Damage production and recovery in low temperature irradiated zinc. *Crystal Lattice Defects*, 2, 47-54.

MAURY, F., VAJDA, P., LUCASSON, A. and LUCASSON, P. (1971b) Subthreshold events and atomic displacements in electron-irradiated cadmium. *Radiation Effects*, 10, 239-245.

MÍŠEK, K. (1970) Deviations from the Matthiessen rule in gold. *Crystal Lattice Defects*, 1, 223-227.

MÍŠEK, K. (1971) Measuring the changes of the resistivity of metals. (In Czech.) *Cesk. Cas. Fis., A*, 21, 143-151.

MÍŠEK, K. (1972) Thermal shock during immersion in cryogenic liquids. *Crystal Lattice Defects*, 3, 175-176.

MICHELL, D. and OGILVIE, G.J. (1966) The effect of exposure to air on dislocations in zinc and cadmium crystals. *Phys. Stat. Sol.*, 15, 83-94.

MOTT, N.F. (1952) Theory of work-hardening of metal crystals. *Phil. Mag.*, 43, 1151-1178.

MUKHERJEE, K. (1965) Monovacancy formation energy and Debye temperature of close-packed metals. *Phil. Mag.*, 12, 915-918.

NEUMANN, G.M. (1967) Beziehungen zwischen der Leerstellenbildungs- und -wanderungsenergie sowie der Aktivierungsenergie der Diffusion und der Debye-Temperatur von Metallen. *Z. Phys. Chem.*, 56, 342-351.

NIHOUL, J. (1963) The recovery of neutron-irradiated zinc. *Phys. Stat. Sol.*, 3, 2061-2068.

NOGGLE, T.S. (1953) A "soft" mold technique for growing single crystals of aluminium. *Rev. Sci. Instrum.*, 24, 184-185.

OSIPOV, K.A. (1971) On values of activation energy for migration of single vacancies in metals. *Phil. Mag.*, 23, 167-174.

OVERHAUSER, A.W. (1953) Isothermal annealing effects in irradiated copper. *Phys. Rev.*, 90, 393-400.

PEIFFER, H.R. (1963) A possible verification of dislocation uncertainty as applied to point defect production. *Acta Metall.*, 11, 435-438.

PEIFFER, H.R. (1963a) The effect of deformation and recovery on the subsequent resistivity increase in cold-worked cadmium. Baltimore: RIAS [i.e. Res. Inst. Adv. Stud., Martin Co.]. Office of Naval Research technical report no. 7, contract Nonr-3707(00). US Government report no. AD-435840.

PEIFFER, H.R. and STEVENSON, F.R. (1963) Recovery of defects from 78 ^{o} to 300 ^{o}K in cadmium elongated at 78 ^{o}K. *J. Appl. Phys.*, 34, 2804-2809.

POSTNIKOV, V.S., BELIKOV, A.M. and ZOLOTUKHIN, I.V. (1967) Influence of the heating and cooling cycles on the fragment structure of single crystals of aluminium and cadmium. *Phys. Metals Metallogr.*, 23(1), 177-180.

PRICE, P.B. (1961) Non-basal glide in dislocation-free cadmium crystals. II: The $(11\bar{2}2)[\bar{1}123]$ system. *J. Appl. Phys.*, 32, 1750-1757.

PRICE, P.B. (1963) Direct observations of glide, climb, and twinning in hexagonal metal crystals. *In: Electron microscopy and strength of crystals: proceedings of the First Berkeley International Materials Conference ... University of California, Berkeley, 1961. Edited by G. Thomas and J. Washburn.* New York: Interscience. Chapter 2, pp. 41-130.

PRIMAK, W. (1955) Kinetics of processes distributed in activation energy. *Phys. Rev.*, 100, 1677-1689.

PRIMAK, W. (1960) Large temperature range annealing. *J. Appl. Phys.*, 31, 1524-1533.

REALE, C. (1962) Electrical resistivity by lattice vacancies in multivalent non-transition metals. *Phys. Lett.*, 2, 268-270.

RIDER, J.G. and FOXON, C.T.B. (1966) An experimental determination of electrical resistivity of dislocations in aluminium. *Phil. Mag.*, 13, 289-303.

SAADA, G. (1961) Interaction des dislocations, écrouissage et production de défauts ponctuels dans les métaux c.f.c. *Acta Metall.*, 9 166-168.

SAADA, G. (1961) Sur la nature des défauts ponctuels créés par le croisement des dislocations. *Acta Metall.*, 9, 965-966.

SAVITSKIY, A.P. and SAVITSKAYA, L.K. (1964) Formation of pores in cadmium as a result of repeated quenching. *Phys. Metals Metallogr.*, 17, 86-91.

SCHUMACHER, D. (1970) Vacancies and interstitials in hexagonal close-packed metals. *In: Vacancies and interstitials in metals; proceedings of the International Conference held at Jülich, Germany, 1968. Editors A. Seeger (and others).* Amsterdam: North-Holland. pp. 889-931.

SCOTT, R.B. (1941) The calibration of thermocouples at low temperatures. *In: Temperature, its measurement and control in science and industry; papers presented at a symposium held in New York city, 1939.* New York: Reinhold. pp. 206-218.

SEEGER, A. (1970) Vacancies and interstitials in metals; proceedings of the International Conference held at Jülich, Germany, 1968. Editors A. Seeger (and others). Amsterdam: North-Holland.

SEEGER, A. (1973) Investigation of point defects in equilibrium concentrations with particular reference to positron annihilation techniques. *J. Phys., F,* 3, 248-294.

SEEGER, A. and MEHRER, H. (1970) Analysis of self-diffusion and equilibrium measurements. *In: Vacancies and interstitials in metals; proceedings of the International Conference held at Julich, Germany, 1968. Editors A. Seeger (and others).* Amsterdam: North-Holland. pp. 1-58

SEEGER, A. and TRAUBLE, H. (1960) Die plastische Verformung von Zink-einkristallen. *Z. Metallkunde,* 51, 436-456.

SHARP, J.V., MITCHELL, A. and CHRISTIAN, J.W. (1965) The recovery of deformed cadmium, magnesium, zinc and cobalt. *Acta Metall.*, 13, 965-971.

SIMON, J.P. and DELAPLACE, J. (1972) Etude des défauts créés dans le magnésium et le cadmium par écrouissage à bass temperature. *J. Nucl. Mater.*, 42, 161-179.

SIMON, J.P. and MINIER, C. (1972) Low temperature electron radiation damage and recovery in cadmium. *Radiation Effects,* 13, 137-142.

SPRUŠIL, B. (1963) An estimation of the activation energies for the formation and movement of vacancies in zinc. *Phys. Stat. Sol.*, 3, K86-K88.

SPRUŠIL, B. (1965) On the evaluation of measurements of small changes in electrical resistance. (In German). *Czech. J. Phys., B,* 15, 287-298.

SPRUŠIL, B., VOSTRÝ, P. and PAMĚTNICKÁ, I. (1970) Resistivity changes in quenched Cd. *Phys. Stat. Sol.*, 41, 425-430.

STEVENSON, F.R. and PEIFFER, H.R. (1964) Recovery of defects following deformation of high purity Cd at 78 °K. *Phys. Stat. Sol.*, 4, 411-418.

STRONG, J. (1938) Modern physical laboratory practice. London: Blackie. p. 582.

SVECHKAREV, I.V. and SOLIYSHKIN, D.D. (1971) Effect of vacancies on the temperature dependence of the lattice parameters of zinc. *Fiz. Metal. Metallov.*, 32(1), 164-165.

SWANSON, M.L. and QUENNEVILLE, A.F. (1972) Low temperature recovery of plastically deformed cadmium, indium, tin and lead. *Phys. Stat. Sol., (a),* 9, 135-143.

TEWARY, V.K. (1973) On a relation between the monovacancy formation energy and the Debye temperature for metals. *J. Phys., F,* 3, 704-708.

VAN BUEREN, H.G. (1961) Imperfections in crystals. Amsterdam: North-Holland.

VAN DEN BEUKEL, A. (1970) Point defects in cold worked f.c.c. metals. *In: Vacancies and interstitials in metals; proceedings of the International Conference held at Jülich, Germany, 1968. Editors A. Seeger (and others).* Amsterdam: North-Holland. pp. 427-481.

VOSTRÝ, P. and NOVÁK, V. (1971) Resistivity changes in cold-worked Cd. *Phys. Stat. Sol., (a),* 4, K203-K206.

VOSTRÝ, P., SIMON, J.P. and HILLAIRET, J. (1972) Formation et mobilité des lacunes dans le cadmium. *Phys. Stat. Sol., (b),* 50, K75-K79.

WESSEL, E.T. (1957) Refrigeration techniques and apparatus for very low temperatures (to 4.2 K). *Refrig. Engng.*, 65(10), 37-45.

YAMAMOTO, M. and WATANABE, J. (1950) *Sci. Rep. Res. Inst. Tôhoku Univ.*, 2. Light figures of zinc crystals, pp. 81-95; Orientation determination of zinc crystals by the light-figure method, pp. 270-279.

YAMAMOTO, M. and WATANABE, J. (1955) Light figure phenomena revealed, and single crystal planes developed by chemical etching in zinc single crystals. *Sci. Rep. Res. Inst. Tôhoku Univ.*, 7, 329-337.

ZEN, K.R., WANG, S.S. and WANG, Y.C. (1965) Measurement of formation energy of vacancy in cadmium. (In Chinese). *Acta Physica Sinica*, 21, 2033-2036. [Cited by Schumacher (1970)].

ZSOLDOS, L. (1963) On the type of jogs on intersecting screw dislocations. *Phys. Stat. Sol.*, 3, 2127-2131.